MSc thesis in Civil Engineering

Assessing the cooling potential of (modified) ground coverage on the drinking water temperature

Lisanne Sophie Middelbeek

2024

Gemeente Rotterdam

TU Delft Delft University of Technology

Lisanne Sophie Middelbeek: *Assessing the cooling potential of (modified) ground coverage on the drinking water temperature* (2024)

The work in this thesis was carried out in collaboration with:

Supervisors: Dr.ir. A.M. (Arjan) Droste
Dr.ir. E.J.M. (Mirjam) Blokker
ir. G.A. (Gijs) Vis
ir. T.A. (Tara) van Iersel (Gemeente Rotterdam)

Preface

A thesis submitted to the Delft University of Technology (TU Delft) is partial fulfillment of the requirements for the degree of Master of Science in Civil Engineering. The research for this master's thesis was conducted from April to December 2023. The research topic falls within the domain of the Water Management department, specifically Water Resources Engineering. The topic is relevant to society as it focuses on mitigating the adverse effects of climate change on drinking water quality. The research has been set up in collaboration with the municipality of Rotterdam, who raised the issue of rising drinking water temperatures, impacting the drinking water quality. Other parties which contributed generously to the research are The Green Village (TGV) and KWR Water Research Institute (KWR). I am pleased to have attended a workshop day at KWR and to have acquired the soil temperature model. Thanks to TGV, I was able to test all the measures I devised, including those that would have been impractical to test in an urban area. I am grateful for the opportunities provided in this innovative fieldlab and for the assistance in placing sensors. Additionally, I would like to express my gratitude to the drinking water companies Dunea and Evides. Dunea, for lending me sensors and loggers, and for their presence on the day I organized in TGV. Evides, also for their participation on that day and for other updates regarding their current status of the research topic. Thanks to all these parties, I was able to gather a lot of information, knowledge, data, and contacts.

My sincere thanks go especially to my supervisors: Martine Rutten, for her guidance during the initial months of my research; Arjan Droste, who flexibly took over the weekly supervision; Mirjam Blokker, whose expertise in this topic significantly contributed to my research; and Gijs Vis, the expert in Distributed Temperature Sensing (DTS). Also, I extend my gratitude to Tara van Iersel for her supervision on behalf of the municipality and for introducing me to other employees of the municipality. Thanks to all their expertise and guidance, I was able to successfully execute my research.

Lisanne Middelbeek
Rotterdam, February 29, 2024

Abstract

This research addresses the issue of rising soil temperatures, driven by climate change. As the Drinking Water Distribution System (DWDS) is located in the sub-surface, the drinking water temperature in the distribution mains attains this rising soil temperature. Because the temperature of drinking water is an important determinant of water quality, Dutch law mandates that drinking water temperature may not exceed 25 °C. This study assesses several measures, including their quantitative impact on soil temperature reduction, and consequently on drinking water temperature reduction. These measures center on modifying the ground coverage, as this measure can be implemented without excavation and disrupting existing infrastructure in the sub-surface. This includes different types of ground coverage (e.g. changing concrete tiles, which are the existing top layer type, to vegetation), and creating temporary shade or applying white paint to the existing coverage type. The effect of (re)locating pipes to a deeper level or in the shade are also considered. The effect at the depth of a distribution main is analysed, which is shallow (0.7 m) in Rotterdam, and 1 m depth in general in the Netherlands.

Measurements confirm the significant influence of the ground coverage, mainly impacting the soil temperature in vertical (in-depth) direction. A detailed analysis reveals the quantitative effectiveness of the considered measures, indicating substantial cooling potential by modifying the ground coverage. Replacing concrete tiles with vegetation (in sandy soil) results in the most cooling effect of all analysed measures. White paint on concrete tiles emerges as particularly effective in reducing the soil temperature at the current depth in Rotterdam (0.7 m), and is considered an easily executable measure to prevent exceedances of the 25 °C threshold, mainly in case of urgency. In general, modifying the top layer as measure is considered feasible. This is because it avoids the need for excavation, in contrast to the alternative measures of relocation to a deeper level or in the shade. Additionally, the study quantifies soil temperature through simulations. A comparative analysis between simulations conducted by the soil temperature model and measurements facilitates an examination of the anticipated progression and the predicted effect of measures by the model, allowing for the formulation of recommendations to enhance the model.

As the results indicate that modifications to the ground coverage can significantly contribute to cooling the soil, this can mitigate potential threats to drinking water quality. Collaboration is crucial for the proper implementation of measures, as drinking water companies are responsible for maintaining drinking water quality, while the municipality oversees the ground coverage necessary for applying these measures. Therefore, the study advocates an integrated approach to decision-making, which includes collaboration with research institutes. This cooperative effort is essential for identifying and implementing the most suitable and effective measures to safeguard high-quality drinking water, both now and in the future.

Acronyms

TGV The Green Village iii
KWR KWR Water Research Institute iii
DTS Distributed Temperature Sensing iii
DWDS Drinking Water Distribution System iv
SSUHI Sub-Surface Urban Heat Island 1
KNMI Royal Netherlands Meteorological Institute 8
UHI Urban Heat Island 6
SUHI Surface Urban Heat Island 6
RL Roughness Layer 73
SS Soil Surface 73
LAF Length Along Fiber 12

Contents

1. Introduction

1.1. Rising drinking water temperature

Drinking water is a basic need for human survival and well-being. In 2010, the United Nations General Assembly explicitly recognized the human right to safe drinking water. Access to clean and safe drinking water is fundamental for maintaining health and preventing waterborne diseases (United Nations, 2010). One important determinant of water quality is the water temperature, since it affects physical, chemical, and biological processes such as adsorption of chemicals (Agudelo-Vera et al., 2017), contaminants, and pathogens (Uber and Boxall, 2010). Therefore, the Netherlands has set a legal norm for the drinking water temperature of maximally 25 °C (Overheid Wettenbank, 2023). This drinking water temperature is affected by external factors, with the soil temperature playing a crucial role. This is because the Drinking Water Distribution System (DWDS), which is in many countries the way how the drinking water is transported, is located in the sub-surface. In the Netherlands, the depth of the distribution mains is generally 1 m. The drinking water temperature in the pipe attains the surrounding soil temperature, as the time that the water is located in the distribution mains (the residence time) is longer than the time required for the water to reach the soil temperature (the heating time) (Blokker and Pieterse-Quirijns, 2013). This heating of the drinking water in the DWDS is more elaborated in Chapter 2, Section 2.7.1. As a result of climate change, air temperatures and high temperature extremes increase (Lee et al., 2022). This results in higher soil temperatures. The phenomenon Sub-Surface Urban Heat Island (SSUHI) also contributes to higher soil temperatures in urban areas specifically. SSUHI refers to warmer soil temperatures within urban settlements compared to the soil temperature at the surrounding rural areas (Agudelo-Vera and Blokker, 2017). The higher soil temperatures as a result of these factors can pose a threat to delivering water of proper quality. Sections 2.2 and 2.3 in Chapter 2 elaborate on the effect of climate change and SSUHI, and the (current and predicted) number of exceedances of the 25 °C threshold. While the current risk in exceeding this threshold is deemed low, it is crucial to anticipate and to search for effective measures to reduce the chance of, or to completely avoid, exceeding the drinking water temperature of 25 °C.

1.2. Influences on the soil temperature

Due to the strong relation between the soil temperature and the drinking water temperature, a possible solution in reducing the drinking water temperature can be found in reducing the soil temperature. The study of Blokker and Pieterse-Quirijns (2012) already found that the greatest effectiveness in reducing the drinking water temperature can be achieved by cooling the soil in the entire network. To advocate possible measures, it is important to consider the aspects that influence the reaching of the threshold temperature in the soil. Agudelo-Vera et al. (2017) have provided an overview of the urban characterization and possible heat sources that influence the soil temperature, as can be seen in Table 1.1. It must be noted that this table focuses on the urban aspects and human activity, so on aspects that can be influenced ('engineered') by humans. Other influential aspects on the soil temperature, like water content, soil type, and (historical) weather conditions, are not included in this table. Since they also affect the soil temperature, these aspects are also taken into account in this research and are addressed throughout the report.

As shown in Table 1.1, the top layer influences the soil temperature. This indicates the potential of reducing the soil temperature by modifying the top layer. This report also refers to the top layer as 'ground coverage'. Both terms refer to the material serving as the covering for the soil,

positioned immediately above the soil. The top layer can be modified by completely altering the type or by applying measures to the existing top layer. Both can either be implemented when (new) pipes are replaced or installed, but the main advantage is that the top layer can also be modified without changing the existing DWDS. The DWDS network should preferably be designed for a lifespan of at least 50 years according to the standard NEN-EN 805 (Meerkerk and Beuken, 2020). The NEN promotes the development of standards for products, services, and processes and can be interpreted as guidelines. In practice, the lifespan set in this norm is generously exceeded. As the DWDS network is meant to be stationed in the ground for years, it is not desirable to replace pipes before their lifespan is reached. Therefore, modifying the top layer, which does not require replacing or rerouting of the pipes, might be considered as a feasible measure to avoid exceedances of 25 °C. Temporary implementation of measures can also be useful, especially for areas which do not experience heating often, so it might be undesirable to implement a permanent solution. These temporary measures can be applied in the event of extremely hot days, for example creation of shade.

Table 1.1.: Overview of the urban characterisation and heat sources that influence the soil temperature (Agudelo-Vera et al., 2017).

Characteristics		**Examples**					
Shade condition		No shade		Partial shade		Shade	
Urban type		Industrial		Residential	Urban square	Park	
Top layer		Concrete paving slabs			Grass		
Anthropogenic sources	*Above ground*	Hospital	Laundry facilities	Reflection of buildings	Swimming pool	High density of buildings	Electrical distribution substations
	Under ground	Metro	High-power cables	ATES	Parking	District heating systems	

1.3. Quantification of the soil temperature

The soil temperature can be quantified by measuring and modelling. Modelling can be preferred over measuring because the in-situ measurements of soil temperature at various depths are spatially and temporally limited (Mihalakakou, 2002), and because of limitations by practical consideration of positioning sensors in urban areas (Gentine et al., 2012). Therefore, modelling is considered as less labor intensive and as a more flexible approach to complement and validate on-site measurements. Moreover, modelling allows a better understanding of the influence of different parameters, as one can easily adjust a parameter and analyse the difference it causes (Agudelo-Vera et al., 2015). Currently, research mainly uses models to predict the soil temperature and consequently the drinking water temperature at the tap. Sections 2.5 and 2.6 discuss these researches, which predict the number of exceedances of the 25 °C threshold with a soil temperature model. These simulations consider three urban types: peri-urban, urban, and hotspot, depending on the level of urbanization. Studies also use this model to predict the effect of measures on reduction of the soil temperature. These studies are addressed in Section 2.10. The drinking water company in Rotterdam, Evides, currently also uses this model in its business operation, to predict the number of exceedances of the threshold of 25 °C in the future. The soil temperature model which is used in the mentionned studies and by Evides is based on the characteristics presented in Table 1.1.

Another way of quantifying the soil temperature is through measuring. The study by Van Vossen et al. (2019) researched the effect of vegetation on the soil temperature, and stated that measurements to validate the simulated temperature effect of vegetation are limited and not always representative for the Netherlands and the specific case, nor do they always include monitoring throughout the entire day. Therefore, the study recommends conducting more field measurements. Measuring can be done by point temperature sensors, but also by more advanced techniques like Distributed Temperature Sensing (DTS). Of both measurement techniques, the technique of DTS has a high spatial and temporal resolution and is able to provide an even richer

data set than could be obtained from point temperature sensors (Bense et al., 2016). The DTS technique has not been used for understanding the SSUHI before, neither for determining the effect of the top layer.

1.4. Objectives and research questions

Because of the influence of the top layer on the soil temperature, and because the top layer can be modified without need of interfering with the current underground infrastructure, the research for this thesis focuses on quantifying the effect of the (modified) top layer. The results can show whether and which adjustments to the top layer can be recommended to lower the soil, and therefore the drinking water temperature.

The effect of measures on the soil temperature is quantified by both modelling and measuring in this thesis research. Although modelling can ease the quantification, modelled situations are not exactly similar to the reality. Routine water quality samples at the tap in urban areas have already indicated locations with relatively high tap temperatures, and thus soil temperatures, compared to the expected modelled soil temperatures (Agudelo-Vera and Blokker, 2016). Therefore, and in line with recommendations from other studies to conduct more field measurements (Van Vossen et al., 2019), this thesis research focuses primarily on a quantification of the effect of the top layer based on measurements. This is achieved by using point temperature sensors and DTS. Because of its high resolution, the DTS technique can provide detailed information about the effect of top layer types, and to which horizontal extent it affects the soil temperature. Also, as sensors can be located underneath all types of ground coverages, measurements enable to analyse the effect of more different types of top layer and (temporary) measures, and in more dimensions, compared to the soil temperature model which makes a distinction between only concrete paving slabs and grass as top layer (Table 1.1). Still, as Evides and previous studies regarding this research topic use the soil temperature model, this model is also included in this thesis research. By comparing the measurements to the simulations, this can provide insights in whether they align in the progression of soil temperature in time and in the predicted effect of measures. This can also help determine whether the current approach of categorizing locations into three urban types based on their level of urbanization, as used for the simulation, is appropriate. As modelling remains important for large scale projects, to predict the magnitude of the issue in the future and effect of possible measures, these insights can help to properly interpret the results of modelling and to provide preliminary recommendations about improvement of the current soil temperature model.

These objectives lead to the following main research question: *How do ground coverage types or modifications to ground coverage quantitatively influence soil temperature at the depth of distribution mains?*

This main question can be divided into three different sub-questions:

1. What is the quantified soil temperature at 0.7 and 1 m depth, measured beneath various types of (modified) ground coverage?
2. How do the measurements compare to the outcome of the soil temperature model, and how can the model be improved and used?
3. Is modifying the ground coverage a feasible mitigation measure to prevent the temperature of drinking water from exceeding 25 °C?

1.5. Structure of the report

To find answers to this main research question and its sub-questions, Chapter 2 first provides relevant background information. It discusses the causes and vulnerability for the rising drinking water temperature, the current state of this research topic and of (heating in) the DWDS in Rotterdam. Besides, the functioning of the soil temperature model is explained, and the expected effect on the soil temperature as a result of adjustments to the top layer is discussed. Chapter 3 then discusses the method, including a description of the field sites, the materials, and relevant specifics detailing how the procedure was executed. The results in Chapter 4 provide the outcome of the measurements, including the comparison to the outcome of the soil temperature model. The results are utilized for the discussion presented in Chapter 5, which examines the interpretation of the results for each measure, their effectiveness and limitations, and the potential implementation. Additionally, the chapter provides recommendations for enhancing the soil temperature model and its utilization. Furthermore, the chapter addresses the limitations of the research. Lastly, Chapter 6 provides conclusions of the research, and recommendations for future research.

2. Theoretical Framework

2.1. Chapter outline

This chapter furnishes relevant background information for the research. First, this chapter elaborates on the driving forces for the problem: climate change and the SSUHI. These phenomena highlight the causes of the problem and the vulnerability of urban areas. Besides, the relation of drinking water temperature to water quality is explained. Then, previous research about the current state and predictions of the exceedances of the 25 °C threshold is provided. This chapter then provides information that is crucial for comprehending the selected measurement depths, measures and other methodological aspects of this research. This incorporates a description of the Drinking Water Distribution System (DWDS) in the Netherlands, including the depth and diameters and where heating of the drinking water occurs. The vertical and horizontal location of the DWDS network is discussed for Rotterdam specifically. This location determines the current type of top layer. Then, the functioning of the soil temperature model is provided, including the input for each urban type. The last section describes possible adjustments to the top layer which can influence the soil temperature and could therefore function as mitigation measure. A lot of previous research about this topic has been performed by KWR and important outcomes of these studies were used as foundation for this research.

2.2. High temperature extremes

Due to climate change, the global mean air temperature rises and extreme weather events are becoming more extreme, including high temperature extremes. It is virtually certain (meaning a 99-100 % probability, according to the Intergovernmental Panel on Climate Change) that globally hot extremes have already become more frequent and more intense across most land regions since the 1950s (Lee et al., 2022). Moreover, with every additional increment of global warming, changes in extremes continue to increase (Lee et al., 2022).

Besides climate change, urbanization is another driving force causing an increase in hot extremes in urban areas specifically, including heatwaves (Lee et al., 2022). Urbanization alters albedo and geometry compared to rural surfaces. The albedo of a surface determines how much radiation is reflected. Besides, urbanization reduces vegetation cover and increases impervious surfaces. This reduces the amount of evapotranspiration and latent heat flux, partitioning more energy into sensible heat which results in higher temperatures (Oke, 1982). Besides this change in land use, urbanization also involves an increase in human activities, such as energy consumption, and buildings store heat. These anthropogenic emissions and heat storage in buildings are released into the atmosphere, also contributing to higher temperatures. In the Netherlands, as of 2022, 93 % of the total population already lives in urban areas (The World Bank, 2022). This means that a large part of the population is exposed to these higher temperatures as a result of urbanization. With the continuing growth of urban areas, the number of people exposed to hot extremes is expected to increase (Lee et al., 2022).

There has been little focus on the interaction between the two driving forces urbanization and climate change and their combined impact on heat stress. Chapman et al. (2017) conducted a literature study and found eight studies that examined the combination of both factors. Although few, these studies all found temperatures increased more than when the effect of either climate change or urbanization was considered independently (Chapman et al., 2017).

2.3. Sub-Surface Urban Heat Island

Consequently, as climate change and urbanization result in higher temperatures, and even higher temperatures when the combination of factors is considered, the combination of climate change and urbanization put pressure on the Urban Heat Island (UHI). The UHI refers to the higher temperatures within urban settlements compared to the temperatures in the surrounding rural areas (Oke, 1976). This effect can occur in different types of temperatures: the temperature of the air, the temperature of the surface (Surface Urban Heat Island (SUHI)), and of the sub-surface (SSUHI). The research of the UHI first focused primarily on air temperature and later on surface temperature (Klok et al., 2012). The first study in the Netherlands on the presence of the Urban Heat Island effect on the soil temperature was published by Agudelo-Vera et al. (2015), and it demonstrated the appearance with a case-study in Rotterdam: the soil temperatures in urban areas were higher compared to the soil temperature in surrounding rural areas, as simplified visualised in Figure 2.1.

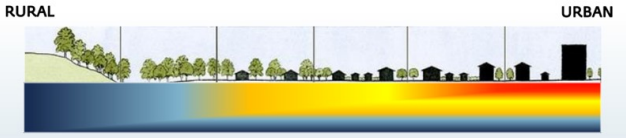

Figure 2.1.: A visualisation of the SSUHI effect (Agudelo-Vera and Blokker, 2014).

With regard to the soil temperature, urban areas are more vulnerable than rural areas because the upper soil level has often been modified by adding sand as soil improvement (Agudelo-Vera et al., 2015). The main thermal properties of a soil are thermal conductivity (λ [W/m/K]) and volumetric heat capacity (C_p [J/m^3/K]). The ratio between these two properties determines the thermal diffusivity (α [m^2/s]). In general, the bigger the thermal diffusivity (α), the faster the heating. The thermal properties depend on the soil type and moisture content of the soil. Given the same amount of water content, sand has a higher thermal conductivity compared to peat and clay (Agudelo-Vera et al., 2015). Of all thermal properties, mainly this thermal conductivity is known to have a significant impact on the resulting soil temperature (Blokker and Pieterse-Quirijns, 2013). The soil thermal properties of sand cause that sand generally transfers heat easily. Compared to peat, for example, the temperature of the soil shows a maximum difference of 6–9°C in sand compared with peat at 1 m depth under the same weather conditions (Blokker and Pieterse-Quirijns, 2013).

Hence, the existence of SSUHI and the presence of sandy soils in urban areas show the vulnerability of an urban area to high soil temperatures. Not every area within a city experiences the same risk. The results presented in Agudelo-Vera et al. (2015) presented higher soil temperatures in urban areas compared to in surrounding rural areas, but it also indicated that the SSUHI exhibits variation within an urban area itself. As the soil temperature was found to differ within an urban area, three different urban types were defined for simulations, to simulate the variation range in urban soil temperatures. The three defined urban types are: peri-urban (neighbourhoods at outer areas of the city), urban (average city), and hot-spots. The three urban types decide the input of the soil temperature model which is related to characteristics of an urban area which influence the soil temperature, e.g. the amount of heat storage. The specific input per urban type is provided in Section 2.9.3. Of the three types, hot-spots are areas which are most prone to the SSUHI, due to for example high (in)direct solar radiation, anthropogenic heat sources, and heat storage. The observation of soil temperature variation within an urban area was further substantiated by the findings of Agudelo-Vera et al. (2017), as their research revealed a significant spread in soil temperatures through measurements conducted at 44 distinct locations within the urban area Rotterdam. The measurements have been used to validate the soil temperature model for an urban area. The three urban types were also used in studies mentioned in Sections 2.5 and 2.6, by Evides, and thus by this thesis research.

2.4. Drinking water quality

The high soil temperatures as a result of climate change and urbanization, pressurizing SSUHI, form an issue because they cause increased drinking water temperature. This can present a hazard to water quality, especially because this can lead to increased microbial activity. A recent study in 2020 has shown that an elevated drinking water temperature increases the risk of growth of opportunistic pathogens in the distribution system. Opportunistic pathogens are pathogens that increase health risk for people with weakened immune systems (Van der Wielen, 2020). Van der Kooij et al. (2009) have shown that a temperature above 25 °C leads to more exceedances of the legal standard for the micro-organisms Aeromonas and Legionella. Legionella is a common waterborne pathogen and this has the highest priority to avoid in order to protect public health. The most dangerous type, Legionella pneumophila, grows between 25-45 °C in practice. Between 25-30 °C, the expression of virulence factors is the highest, making the bacterium the most contagious (Agudelo-Vera et al., 2020). Because of these risks, the Dutch regulation 'Drinkwaterregeling' requires Legionella prevention and mandates that the drinking water at the customer´s tap may not exceed 25 °C (Overheid Wettenbank, 2023). This maximum is set as a legal norm because drinking water in the Netherlands is distributed without an additional residual disinfectant like chlorine. The World Health Organization (WHO) also recommends that whenever possible, water temperatures should be kept outside the range of 25-50 °C and preferably even 20-50 °C (World Health Organization, 2022), to limit regrowth of Legionella. Hence, this threshold of 25 °C is of importance to prevent a health risk for residents.

2.5. Measurements and simulations of the drinking water temperature: current state

The legal norm of 25 °C is sometimes already exceeded. In 2006, 0.1 % of almost 22,000 samples of the distribution system (at the tap) exceeded this threshold of 25 °C (Versteegh and Dik, 2007). These measurements are performed by drinking water companies at the tap, where the measurement of the temperature is performed once the temperature is stabilized after letting the water run for a few minutes. This stabilized temperature is recorded which represents the temperature of the water in the distribution mains (Agudelo-Vera et al., 2020). The most recent study of the year 2021 showed an exceeding percentage of 0.01 %, based on approximately 53,000 samples (Inspectie Leefomgeving en Transport, 2022). This decreased percentage seems to suggest that the situation has improved. However, since these percentages are the outcome of random sampling monitoring, this conclusion cannot be made. This random sampling monitoring provides just one snapshot (in location and time) which does not aim at the hottest days. Hence, these percentages demonstrate that there are occurrences of exceedances within a year, but they do not provide a precise count of the total number of exceedances in that year.

Mapping the complete number of exceedances would require measuring the temperature with inclusion of all critical days with elevated air temperatures, and at all taps in urban areas, This would necessitate taking numerous measurements, which is simply not feasible. Therefore, previous research has used the soil temperature model with the three urban types. As the drinking water attains the surrounding soil temperature, the simulated soil temperature can be used to indicate the drinking water temperature and thus the total number of exceedances of the 25 °C threshold. For each of the three defined urban types (peri-urban, urban, and hot-spot), the number of exceedances can be determined. So, depending on which of these three urban types a location is assigned to, the number of exceedances for a location can be estimated.

The research of Agudelo-Vera et al. (2017) used this soil temperature model for the city of Rotterdam. It showed exceedances for the summer months for the period 2000-2016 in eight of the sixteen simulated years, accounting for locations which are assigned to be hot-spots. For these

hot-spots, the threshold was exceeded 75 days in total in 16 years (Agudelo-Vera et al., 2017). So, this simulation showed that the city, and especially the designated areas identified as hot-spots, are areas of concern. These areas are vulnerable to rising soil and thus drinking water temperatures during the summer months, already posing a threat to poor water quality.

2.6. Simulations of the drinking water temperature: predictions

Simulations also enable to predict what happens when circumstances change, for instance, climate change. Agudelo-Vera et al. (2015) included the effect of climate change by considering several climate scenarios of the Royal Netherlands Meteorological Institute (KNMI), which predict the temperature rise. This research used the warm summer of 2012 as reference. Simulations showed that the threshold of 25 °C was exceeded 9 days for hot-spots in this reference year. The outcome of the simulation is provided in Table 2.1, which shows that this number is expected to increase to 55 days in 2030 and up to 83 days in 2050 for hot-spots. These numbers of exceedances are the result of a simulation which considers the most extreme climate scenario of KNMI, W+, originating from the scenarios made in 2006. This 2006 W+ scenario takes into account a global mean temperature rise of 2 °C in 2050 and a change in mean temperature in the summer time of +2.8 °C relative to 1990 (Agudelo-Vera et al., 2015). However, it must be noted that the scenarios for 2050 were revised in 2014 where the most extreme scenario projects a mean temperature rise of +2.3 °C in the summer time (with reference period 1981-2010) (Klein Tank et al., 2015), and later in 2023 the revision showed the most extreme scenario for 2050 projects a mean temperature rise of +2.1 °C in the summer time (with reference period 1991-2020) (Bessembinder et al., 2023). Both mean temperature rises for the summer period are slightly less than the used 2.8 °C. Still, this study illustrates the pressure of climate change, which especially forms a high risk for the hot-spots (Agudelo-Vera and Blokker, 2016). Moreover, the study illustrates that exceedances already occurred in the reference year. Given that the year 2021 was warmer than the reference year of 2012, this suggests that the number of exceedances in 2021 would surpass the number observed when using 2012 as the reference year. This highlights that the present issue is larger than one would derive from Table 2.1. Therefore, it is crucial to proactively anticipate the (already) increasing soil water temperatures by exploring potential measures, to guarantee that the temperature of drinking water remains below 25 °C, also in the future. As stated in Chapter 1, the soil temperature can potentially be reduced via the top layer, and quantifying this effect is the objective of the research for this thesis. In order to devise effective alterations to the top layer, it is crucial to comprehend the locations and conditions where heating of the drinking water occurs.

Table 2.1.: Overview of the number days in a year in which drinking water temperature will exceed 25 °C and 28 °C for 2012 (warm summer) and for a warm summer in the future climate scenario W+ for 2030 and 2050 (Agudelo-Vera et al., 2015).

	Number of days per year with drinking water temperature 25 °C			**Number of days per year with drinking water temperature 28 °C**		
	2012	**2030 (W+)**	**2050 (W+)**	**2012**	**2030 (W+)**	**2050 (W+)**
Peri-urban neighbourhoods	0	0	0	0	0	0
Average city	0	0	7	0	0	0
Hot-spots	9	55	83	0	2	22

2.7. Drinking Water Distribution System in the Netherlands and in Rotterdam

2.7.1. Heating in the Drinking Water Distribution System

In the Netherlands, the drinking water is transported via a Drinking Water Distribution System (DWDS) and the drinking water remains in the DWDS network for 24 hours up to 5 days. After leaving the pumping station at the drinking water treatment plant, the drinking water first enters the transport mains. These pipes have a large diameter (around 300 mm or larger), are typically situated at a depth of 1.20 m, and contain relatively fast flowing water. Then, the water enters the distribution mains. These pipes are smaller in size, with generally a diameter of 100 mm and they are located less deep, at a depth of generally 1 m. Lastly, the water enters the connection lines, where the drinking water eventually enters a building. These pipes have a diameter of only 25 mm at a depth of 0.8 m to ground level (Blokker et al., 2017).

Whether drinking water within the pipes actually heat up, depends on the residence time (the time the water is in the pipeline) and the heating time (the required time to heat up). When the residence time is longer than the heating time, the drinking water will adopt the temperature of the surrounding soil when this soil temperature is higher.

A lower flow velocity means a longer residence time, which provides more time to reach the, in case of heating, higher soil temperature as final temperature. The heating time depends on the material of the pipe, which can be insulating or conductive. For conductive materials (like cast iron), the conduction through the wall occurs faster than the heating of the water through convection. The heating time is then closely related to the flow velocity. The higher the flow velocity, the faster the heating occurs, so the shorter the heating time for drinking water in a conductive material. The flow velocity is less important for insulating materials (like PVC). For these materials the diameter is the most influential aspect. For both conductive and insulating material accounts that the smaller the diameter, the faster the heating occurs (shorter heating time) for drinking water (Blokker and Pieterse-Quirijns, 2010).

This seems to imply that the heating of drinking water can be affected by the material of the pipe and the diameter. However, adjusting the material of the pipe at most slows down the process of heating, and enlarging the diameter leads to a larger heating time but also proportionally increases the residence time. Therefore, these adjustments are not efficient to prevent heating of drinking water (Blokker and Pieterse-Quirijns, 2010). For this reason, these aspects are not further taken into account in this research.

In practice, when considering the three different sections in the DWDS, only minor heating occurs in the transport mains because of the larger diameters, relatively high flow velocities (thus a limited residence time), and deeper location (generally a lower soil temperature, Figure 2.3). Since the connection lines have a small diameter and are located less deep, heating occurs here. However, the residence time is small here and also after a longer residence time during the night where the water remains stagnant (when there is no water demand within the building), the heated water is flushed away when there is a substantial demand, so for example after the first toilet flush in the morning (Blokker and Pieterse-Quirijns, 2010).

The most critical location where the drinking water temperature can heat up is in the distribution mains, where the diameters are relatively small (Blokker and Pieterse-Quirijns, 2010). During the night, the water is practically stagnant and during the day it moves back and forth in these pipes, with a higher water flow during the peak demand in the morning. In this distribution network, there is enough time for heat transfer from the surrounding soil to the drinking water in the pipeline (Blokker et al., 2017) since generally, the residence time in the distribution mains is longer than 12 hours (Blokker and Pieterse-Quirijns, 2010). Consequently, the water in the distribution mains attain the same temperature as the surrounding soil (Blokker and Pieterse-Quirijns, 2013), regardless of the material of the pipes and the temperature at the pumping station where

the water has been treated (Blokker and Pieterse-Quirijns, 2010). So, the soil temperature is considered as the biggest influence on the drinking water temperature in the distribution mains and at the tap (Blokker et al., 2017).

2.7.2. Location of the Drinking Water Distribution System

In the Netherlands, the use of underground space, including location of the cables and pipes, is regulated via the manual 'Handboek Kabels en Leidingen 2018'. The horizontal and vertical location of cables and pipes is determined beforehand. With regard to the horizontal location, the cables and pipeline route is generally and preferably situated underneath the sidewalk. With regard to the vertical location, the manual has as guiding principle to locate transport mains deeper than distribution mains (Overheid Lokale wet- en regelgeving, n.d.). Generally, the distribution mains of the DWDS are located at a depth of 1 m in the Netherlands (Blokker and Pieterse-Quirijns, 2013).

For the city Rotterdam, the municipality has its own manual 'Handboek Beheer Ondergrond' (Manual Subsoil Management). The manual contains appendices, of which one has incorporated a standardized road layout. The horizontal location is in line with the Dutch regulation: the standard road layout localizes the drinking water pipes below the sidewalk on each predetermined layout (Gemeente Rotterdam, 2009). An example for the standard road layout in an urban area is presented in Figure 2.2.

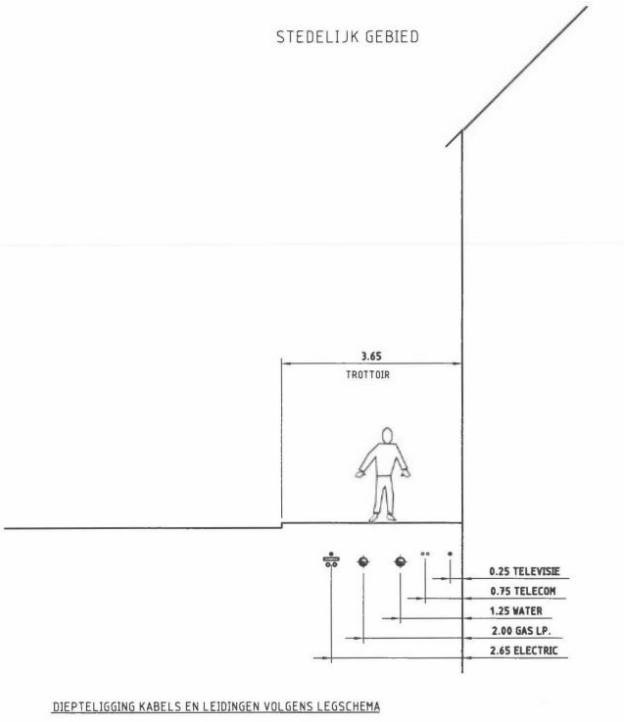

Figure 2.2.: Standard road layout urban area (Gemeente Rotterdam, 2009).

The depth of the cables and pipes is determined in the 'Legschema Leidingen', of which the full scheme is presented in Appendix D.2, Figure D.5. As visible in this figure, the depth for connection lines must be 0.8 m. For the other drinking water pipes, it states that for pipes with a diameter $\leq$ 250 mm, the coverage depth must be 0.7 m, and for pipes diameter $>$ 250 mm, the coverage depth must be 1 m (Gemeente Rotterdam, 2022). The distribution mains generally have a diameter of 60 - 200 mm (Agudelo-Vera et al., 2017). Also in Rotterdam, the distribution mains have a diameter smaller than 250 mm, meaning that the coverage depth is 70 cm. This means

the distribution mains are located less deep in Rotterdam compared to the average depth in the Netherlands.

The coverage depth is of importance because it influences the soil temperature. Figure 2.3 shows that the annual mean maximum temperature decreases with depth, using 27 year soil temperature records (Agudelo-Vera et al., 2015). This means a deeper location of the distribution mains generally results in less high temperatures of the surrounding soil and thus lower drinking water temperatures. The reason is that a deeper level means less dependency of short time weather changes. This reflects standard behaviour where the amplitude of diurnal variability is dampened in the soil, and a delay of peak values occurs (Bense et al., 2016).

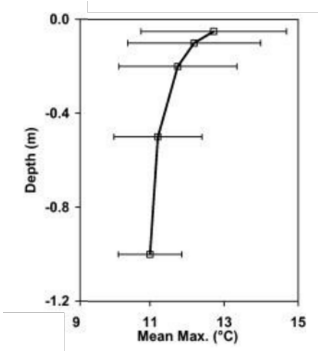

Figure 2.3.: Annual mean maximum temperatures (of 27 year soil temperature records) in a soil in a grassland in the Netherlands (Agudelo-Vera et al., 2015).

According to the municipality of Rotterdam, the reason for this positioning relatively close to the surface is because it requires less excavation. In the municipality of Rotterdam, 1 of 18 digging movements results in damage to a pipeline. Resultingly, a more shallow localization of the mains means less digging movements and thus supposedly ensures a smaller chance of damage. Besides, the inconvenience of excavation for local residents has increased and therefore this is kept to a minimum by less digging. According to the municipality, the difference between the coverage depth per size of diameter (larger or smaller than 250 mm) is allocated to the fact that a smaller diameter means a faster flow velocity, so a lower residence time. This should reduce the heating in these pipes, so pipes with a smaller diameter can be stationed nearer to the surface (Gemeente Rotterdam, personal communication, June 6, 2023). However, as discussed in 2.7.1, this influence of the diameter depends on the material of the pipes. For conductive materials, a faster flow velocity also means a shorter heating time, so the heating occurs faster. Additionally, considering the long residence time of drinking water in the distribution mains, especially during the night, there is sufficient time for the water to heat up. As these arguments are disputable, the increased pressure of elevated soil temperatures, attributable to climate change and urbanization, is likely to alter the equilibrium between advantages and disadvantages of the current depth choice. This can possibly lead to a reconsideration of the depth.

Either way, this depth is currently in line with the NEN7171. The standard NEN7171 provides criteria for the proper organization of underground utility networks in public areas during new construction. One of the five working groups of the norm committee currently explicitly focuses on the heating of the soil and drinking water (NEN, 2023), which may lead to revised guidelines for the coverage depth for new construction. Because in this thesis research the quantification of soil temperature is performed at various depths, the results can also be utilized to provide recommendations regarding the depth of the pipes. This can be useful for pipelines that are planned to be installed in the future, since it can help in decision making of the coverage depth incorporated in the newest NEN7171.

In the 'Legschema Leidingen', the vertical position of other types of pipes is also predetermined. Besides, the scheme determines the vertical position of specific pipes with respect to other pipes, as shown on the right-hand side of the table in Figure D.5 in Appendix D.2. This scheme includes the location of the district heating system, which is a heat source for the soil temperature (Table 1.1). With regard to the vertical position of this system, the drinking water pipes $\leq$ 250 mm (i.e. for the distribution mains) are predetermined above the connecting lines and transport pipes

of the district heating system, and below the distribution pipes of the district heating system (Gemeente Rotterdam, 2022). With respect to the horizontal distance between the DWDS and the district heating system, the standard road layout locates the district heating below the road, whereas the DWDS is located below the sidewalk (Gemeente Rotterdam, 2009). Therefore, the distance between them is assumed to be sufficient for the current system in Rotterdam, and the influence of the district heating system on the soil temperature is thus not explicitly analysed for this research.

2.8. Measuring with Distributed Temperature Sensing

Understanding the heating within the DWDS has highlighted the influence of soil temperature and clarified that the relevant depths for analysing soil temperature are at 0.7 m and 1 m, which correspond to the depth of the distribution mains. This thesis research uses point temperature sensors and DTS to measure the soil temperature. The DTS technology uses fiber-optic cables to monitor spatial and temporal variations in the soil temperature. The temperature along the cable path is obtained by sending a laser pulse of one constant wavelength into the core of the optical fiber. A small part (around one billionth) of the pulse is backscattered due to the disordered (noncrystalline) structure of glass (Selker et al., 2006). The Raman backscattering is detected, which is an inelastic backscattering. This means that the wavelength of the incoming laser pulse is slightly shifted thus the scattering emits a different wavelength, either with decreased or increased energy of the molecule (des Tombe et al., 2020). A portion of the backscattered photons return at frequencies higher (corresponding to shorter wavelengths) than the primary laser light, while others return at lower frequencies (corresponding to larger wavelengths). These phenomena are respectively termed anti-Stokes and Stokes intensities, and they are measured by the detectors of a DTS system. The anti-Stokes intensity is more strongly affected by the temperature. Therefore, the ratio of anti-Stokes and Stokes intensities can provide the temperature (Bense et al., 2016). The principle of DTS deploys the equations 2.1 and 2.2 (des Tombe et al., 2020).

$$T(x,t) = \frac{\gamma}{I(x,t) + C(t) + \int_0^x \Delta\alpha(x')\,dx'} \tag{2.1}$$

Where the intensity, I, is given by equation 2.2.

$$I(x,t) = \ln\left(\frac{P_+(x,t)}{P_-(x,t)}\right) \tag{2.2}$$

In these equations, T is the temperature [K], at a specific Length Along Fiber (LAF) (x) and time (t). The constant γ is the sensitivity of the Stokes and anti-Stokes scattering to temperature in Kelvin [K] and depends on the fiber material. The intensity (I) depends on the power of the Stokes (P_+) and the power of the anti-Stokes (P_-), measured at the detector(s) in a DTS system. C(t) depends on the device itself: how much backscattering is detected. This is time-dependent. Furthermore, $\Delta\alpha$ [m^{-1}] is the differential attenuation. The specifications of the used DTS technology for this thesis research specifically are elaborated in Section 3.2. This section also provides specifications of the other measurement method: point temperature sensors.

2.9. Soil temperature model

2.9.1. General information and input

For the research of this thesis, the measurements were compared to the outcomes of the soil temperature model used in previous research (e.g., by Agudelo-Vera et al. (2015)) and currently in operation by Evides. Through this comparative analysis, the objective of providing a more accurate interpretation of the simulations and offering preliminary recommendations for improving the model can be achieved. This implies that the model is utilized in a similar manner to how it was used in previous research and by Evides. Therefore, default settings are applied, and the input of specific parameters depends on the defined urban types (peri-urban/urban/hot-spot). The model has already been validated for the three urban types. For the urban and hot-spot scenario, Rotterdam has been used to calibrate the model, for the summer condition. For the peri-urban scenario, historic KNMI soil temperature records of the Bilt have been used to validate the model (Agudelo-Vera et al., 2015). The Bilt is an area in the centre of the Netherlands were the main weather station of the KNMI is located. The soil temperature model runs on MATLAB®. The parameters constituting inputs for the soil temperature model are as follows:

- meteorological data (air temperature [°C], average wind speed [m/s], cloud cover [in eighths], global radiation [W/m^2], wind direction [degrees: N=360, E=90, S=180, W= 270], relative humidity [%], and precipitation [mm] time series)
- the initial soil temperature (T_{soil}) [°C] (for each depth)
- thermal conductivity of the soil (λ_{soil}) [W/m/K]
- soil density (ρ_{soil}) [kg/m^3]
- soil heat capacity (Cp_{soil}) [J/kg/K]
- soil surface albedo (a_{SS}) [-]
- anthropogenic heat emission (QF) [W/m^2]
- empirical value to estimate heat storage (a3) [W/m^2]
- presence of grass [0 or 1]
- presence of shade [0, 0.5, or 1]
- scenario name ['name']

The input parameters which depend on the urban type are provided in Section 2.9.3. To enable provision of preliminary recommendations to improve the model, the model was extensively analysed to understand its functioning, set input parameters, and assumptions. Appendix A describes the general functioning of the model and the simulated processes, including the heat transfer and considered energy balances. This appendix also elaborates on aspects related to this heat transfer, describing net radiation, albedo, urban evapotranspiration, heat storage, and anthropogenic heat emissions. All specific equations which are used in the model are provided in Appendix B. The heat transfer between the atmosphere and through the soil which is calculated by the model eventually results in equation 2.3. This ΔT_{soil} updates the temperature of the soil layer for each time step dt, which initially started at 4 °C. This is more elaborated in Appendix B.

$$\Delta T_{\text{soil}} = \frac{dt}{dz_{\text{soil}} \cdot \rho_{\text{soil}} \cdot Cp_{\text{soil}}} \cdot (G + \text{Isfc} \cdot (-H_{\text{soil}\rightarrow\text{RL}} + R_{\text{net}} - \text{LvET} + QF - dQs)) \tag{2.3}$$

All parameters of the equations mentioned in Appendices A and B, including their units, are provided in Appendix C. When the model uses a constant (fixed) value, the value is also provided in this appendix. These appendices show that the thermal conductivity is expressed via the ground heat flux G, equation 2.4:

$$G = \lambda_{soil} \cdot -1 \cdot \text{temperature gradient soil} \tag{2.4}$$

2.9.2. Soil thermal properties

The model assumes a homogeneous soil profile, whereas in reality soil is heterogeneous. The exact properties of a soil are hard to determine. For urban areas, sandy soils are assumed since this is often used as soil improvement in urban areas in the Netherlands. This soil type determines the thermal properties. The thermal properties of a soil depend on the soil water content, which is affected by factors such as the water table level. The research for this thesis focuses on the summer condition, because of the vulnerability for high soil and thus drinking water temperature in this period. It is assumed for this summer condition, and especially for hot summers, that the water table level and therefore the soil water content can be assumed as a fixed value. This fixed moisture content in the soil is implicitly taken into account in the soil temperature model, expressed via the spatially constant thermal properties (Agudelo-Vera et al., 2017).

For urban areas specifically, the influence of the groundwater table on the moisture content is especially large since urban areas mostly consist of impermeable cover. This impermeable cover limits infiltration and evapotranspiration, which disrupts the natural water balance, thereby enlarging the influence of the groundwater level. Agudelo-Vera et al. (2015) have interpolated the ground water levels in Rotterdam and found ground water levels vary from -1.0 m to -2.0 m from surface level in August 2013. The moisture level is expected to be between 100% (for the water table at 1 m depth) and 50% (for the water table at 2 m depth). The thermal properties can be derived from Table 2.2, using this expected fixed moisture level between 50 % and 100 %. This means ρ is 1.83 - 2.0 x 10^3 kg/m^3, Cp is 1.11 - 1.37 x 10^3 J/kg/K, and λ is 0.7 - 14 W/m/K.

Table 2.2.: Thermal properties for sand and clay for different moisture content (Agudelo-Vera et al., 2015).

Soil type	Condition	θ	ρ [10^3 kg m^{-3}]	Cp [10^3 J kg^{-1} K^{-1}]	ρCp [10^6 J m^{-3} K^{-1}]	λ (min - max) [W m^{-1} K^{-1}]	α [m^2 s^{-1}]
Sand	Dry	0.0	1.66	0.81	1.34	0.17 - 0.25	0.13 - 0.19
	50% saturation	0.5	1.83	1.11	2.03	0.7 - 5.0	0.94 - 2.46
	Saturated	1.0	2.0	1.37	2.74	2.6 - 14	0.95 - 5.11
Clay	Dry	0.0	1.47	0.82	1.21	0.17 - 0.30	0.14 - 0.25
	50% saturation	0.5	1.69	1.25	2.11	0.17 - 1.35	0.08 - 0.64
	Saturated	1.0	1.91	1.6	3.06	1.3 - 6.7	0.43 - 2.19

It should be noted that estimating soil thermal properties show large uncertainty. This is because soil type, which is often a mix of types, determines these properties, and in addition to being contingent on moisture content, they also vary based on compaction. Thus, in reality, the properties vary spatially, and in case of the moisture content also temporally. A sensitivity analysis has shown that the most relevant parameters in determining the soil temperature in an urban area are the thermal properties of the soil, and especially the thermal conductivity (λ) (Agudelo-Vera et al., 2015). Therefore, when interpreting the results, it must be taken into consideration that this assumption of a homogeneous soil with constant thermal properties differs from reality and influences the outcome.

The model has been calibrated for the summer condition in Rotterdam. The final soil thermal properties assume sandy soil and were determined to be as follows:

- the thermal conductivity (λ) = 1 for peri-urban, 1.2 for urban, and 2.6 W/m/K for hot-spot

- the density of the soil (ρ) = 2000 kg/m^3
- the soil heat capacity (Cp) = 1000 J/kg/K

Since the model was calibrated for summer conditions in Rotterdam and since the model does not account for phase change during winter freezing of the soil, the model runs most accurately for summer conditions. Because this is the period of interest, this will not provide any issues for the analyses in this research.

2.9.3. Urban types

Agudelo-Vera et al. (2015) have defined three urban types, based on the level of urbanization and SSUHI: peri-urban, urban, and hot-spots. Peri-urban areas refer to the transition zone or interface between a city or urban area and its surrounding rural or non-urban areas. Urban and rural characteristics and land uses often mix or coexist here. Urban areas typically have a higher population density, (even) more paved infrastructure, and higher buildings. Hot-spots mainly occur due to a combination of high (in)direct solar radiation (no shade), dry sandy soil, tiles as ground cover, and presence of anthropogenic heat sources and heat storage (Agudelo-Vera, 2018). This combination of factors results in hot-spots experiencing a high SSUHI and being vulnerable to high soil temperatures (Agudelo-Vera et al., 2017).
These urban types determine some of the input parameters of the model. The following apply for each scenario:

1. Peri-urban: λ = 1 W/m/K, QF = 50 W/m^2, a3 = -50 W/m^2
2. Urban: λ = 1.2 W/m/K, QF = 100 W/m^2, a3 = -100 W/m^2
3. Hot-spot: λ = 2.6 W/m/K, QF = 150 W/m^2, a3 = -120 W/m^2

In summary, the parameters which are included in the processes of the soil temperature model are provided in the overview in Figure 2.4. Although most is adopted from the original soil temperature model, also some changes have been made to the model for this thesis research specifically. These changes are addressed in Chapter 3, Section 3.2.5.

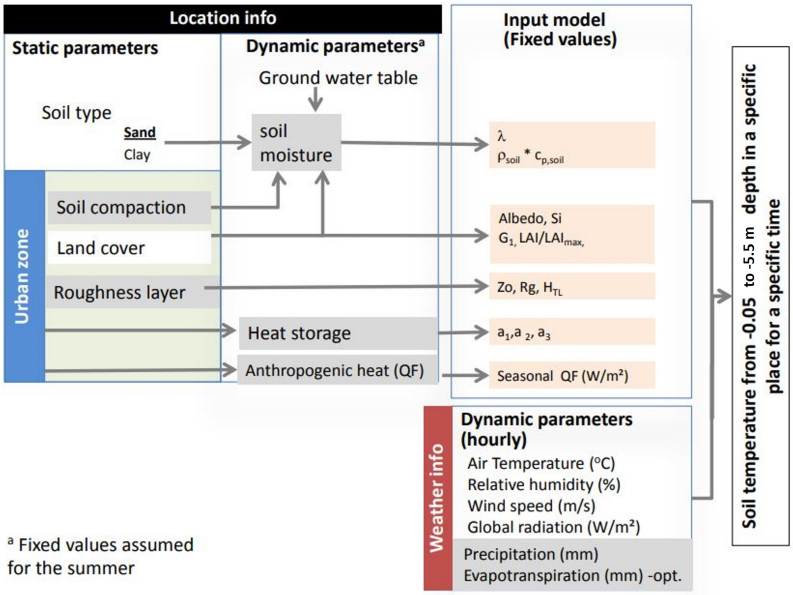

Figure 2.4.: Overview of variables included in the study (Agudelo-Vera et al., 2015).

2.10. Possible mitigation measures to reduce the soil temperature via the top layer

2.10.1. Mitigation measures

Modifying the top layer is one way to lower the soil temperature in the entire network, which has the greatest effectiveness in reducing the drinking water temperature (Blokker and Pieterse-Quirijns, 2012). Another possibility for cooling of the soil is by avoiding sand, because of its soil thermal properties which lead to the most heating in a sandy soil. The study of Blokker and Pieterse-Quirijns (2012) showed that even when 50 % is replaced with clay or peat, exceedances of the threshold occur. Because avoiding sand is considered not explicitly as an effective solution, and it requires excavation, this measure is not considered in the research for this thesis. Besides, avoiding sand is not desirable as sand is constructive, forming a better foundation for a pipeline compared to other soil types.

To lower the soil temperature in the entire network, deeper installation of the pipes is also a possibility. However, this is costly and the effect on the (duration of) exceedances of the temperature threshold is small (Blokker et al., 2014). The study of Blokker and Pieterse-Quirijns (2012) used the soil temperature model to predict the temperature as a result of deeper installation. This showed that for a 100 % sandy soil, the standard of maximum 25 °C is only met when the pipes are located deeper than 1.75 m, which is more than twice the current depth of 0.7 m for Rotterdam. Although this does not look promising, a more recent study of Van Vossen et al. (2019) shows that increasing the depth from 1 to 1.5 m results in a decrease in soil temperature of 1-2.5 °C. As the effectiveness differs in studies, the research for this thesis does include this measure in the analysis to gain more insight in the effect. This can help in decision making for the new standard NEN7171.

2.10.2. Current top layer

The top layer can be modified by completely altering the type or by applying measures to the existing top layer. To propose measures to implement to the existing top layer, it is important to know what the current top layer type of the distribution mains is. As discussed in Section 2.7, the distribution mains are located beneath the sidewalk on every predetermined layout of Rotterdam. The 'Handboek Rotterdamse Stijl' determines which types of pavement are approved as sidewalk. In most cases, the sidewalk contains grey concrete tiles as top layer, visible in Figure 2.5 (Gemeente Rotterdam, 2020). This tile is preferred because of the limited thickness, which is desirable for the environment. However, these tiles make the soil vulnerable to high temperatures. Reduction in soil temperature can possibly be achieved by modifying the albedo of these concrete tiles, or by creating shade on the tiles. Changing the concrete tiles to vegetation or other types of ground coverage is also possible. The following section provides information about why these measures would work and what the expected effect is, where references are made to studies which all use the soil temperature model to determine the effect of these modifications. As these predicted effects are based on simulations, although measurements have been used to validate the model, this can differ from reality. Therefore, this thesis research complemented information about the effect of the top layer primarily with measurements, performed for a longer period of time. In the following chapter, Chapter 3, detailed information is provided about how the effect of (modified) top layer was quantified for this thesis research specifically.

Figure 2.5.: Concrete tile 'Rotterdam' (Gemeente Rotterdam, 2020).

2.10.3. Possible effects of modification of the top layer

Shade

A measure which can lower the soil temperature is creation of shade. This lowers the direct incoming shortwave radiation, as can be derived from equation B.2 and B.3 in Appendix B. This lower shortwave radiation lowers Rnet (equation B.18). A lower Rnet in equation 2.3 results in a smaller ΔT_{soil}. As shade causes less heating of the soil, this also means that the temperature of the surface of the soil is less, which reduces the outgoing longwave radiation (equation B.5), resulting in less cooling of the soil. However, overall, shade generally causes less heating of the soil and thus lower soil temperature. The degree of shading (light transmittance and heat resistance) depends on the way how the shade is created. For example, when textile is used as canopy, the shading depends on the type of the textile (e.g. the weave density) and the color.

Simulations by Van Vossen et al. (2019) have shown that the creation of shade can clearly reduce the temperature with a cooling effect of 1 - 3.5 °C at 1 m depth. However, when shade is created temporarily during a heatwave, the peak temperature can already be reached before the period of shade creation. Then, the shade has little influence on the maximum temperature at a depth of 1 m.

Albedo

The albedo determines the temperature of the (sub-)surface as it influences the reflection of the solar irradiation. The net radiation (Rnet) in equation 2.3 decreases for a higher albedo, because the shortwave radiation decreases as albedo increases (equation B.3 and equation B.18 in Appendix B). This smaller Rnet leads to a smaller ΔT_{soil}, so less heating of the soil. The albedo depends on several factors, mostly on surface roughness and surface color. Rough surfaces tend to scatter sunlight, leading to lower albedos, while smooth surfaces allow for more direct reflection and higher albedos (Oguntunde et al., 2006). With regard to surface color, white is known to have a higher albedo (as described in Appendix A). Stache et al. (2022) have measured the albedo for different materials. When considering HPL white, which is most commonly used as a light-colored facade, the determined albedo in the study was 0.35. The investigation of this HPL white demonstrated that reflection is an efficient means for reducing absorbed solar energy, thereby reducing the UHI. Although this conclusion is based on materials for facades, the same is expected for reduction in the SSUHI by ground coverages with a high albedo. The albedo of concrete tiles (grey) was determined to be 0.13 in the study of Stache et al. (2022).

Blokker and Pieterse-Quirijns (2012) have already shown with simulations that a high albedo is

favorable to prevent excessive heating of the soil. When considering a depth of 1 m, the temperature will remain below the 25 °C threshold when the albedo is greater than 0.45. For a smaller coverage depth, the albedo needs to be higher to prevent heating above the threshold. For a depth of 0.75 m, the albedo must be at least 0.58.

Vegetation

Vegetation as coverage of the soil surface leads to less and slower heating of the soil. This is because plants evaporate water and this requires energy. The phase change of liquid water into water vapour by vegetation ensures that a substantial part of absorbed radiative energy is channeled into latent heat (27-50%). As evaporation is the result of the phase change of water, it underscores the importance of having an adequate water availability to achieve the cooling effect. The channeling into latent heat consequently leaves less available energy to heat the soil. This can be derived from equation 2.3: LvET increases, leading to a lower ΔT_{soil}. As a result, the soil will reach lower temperatures.

The simulation of Blokker and Pieterse-Quirijns (2012) showed that changing the top layer to vegetation assures the most cooling of the soil temperature at 1 m depth, resulting in no exceedances of the 25 °C threshold (compared to 44 exceedances initially). However, a more recent study indicates less effect of vegetation compared to other measures (Agudelo-Vera et al., 2020). This is based on the outcome of a research of Van Vossen et al. (2019) for which measurements were performed. It showed that vegetation cools the soil at 1 m depth with 1.5 °C. So, the cooling effect of vegetation is clear, but the effectiveness of vegetation differs per study. Additionally, although vegetation cools down the soil, it remains unclear how close the vegetation should be to the pipeline in order to sufficiently lower the soil temperature around it (Blokker et al., 2014).

The height of vegetation matters in the warming of the soil, as the height clearly influences the diurnal signal. For taller vegetation (50-90 cm), diurnal ground surface temperature (GST) and ground heat flux (Gsub) variations are significantly smaller indicating that the air temperature fluctuations are more effectively dampened by thicker canopy. This results in temperatures that are higher during the night underneath taller vegetation. During daytime, the temperatures are relatively cool underneath taller vegetation, compared to areas with the lowest canopy height ($< 5cm$) (Bense et al., 2016). The height of vegetation also matters because of the creation of shade. Higher plants or trees create more shade which cools down the surface temperature and the sub-surface temperature. Besides the height, the size of the leaves and the density of the leaves also contribute to shade creation and thus the cooling effect. The degree of shading also depends on the time of year and the time of day. Another contributing factor to the cooling effect of vegetation is the higher albedo of vegetation compared to concrete tiles (as later presented in Chapter 3, Table 3.2).

3. Method

3.1. Field sites

For this research, data of the soil temperature was gathered. These measurements were performed in The Green Village in Delft and at six locations in Rotterdam. Both Delft and Rotterdam are located in the Netherlands (Europe), with Delft on the north-west side of Rotterdam. The straight-line distance between Delft and Rotterdam is approximately 12.5 kilometers. Rotterdam is the second largest and most populated city in the Netherlands, known for containing the largest port of Europe. It has an area of 324 km^2 and a population of 663,900 people in 2023. Delft is a smaller urban area, of 24 km^2, and with a population size of 106,086 in 2023 (Centraal Bureau voor de Statistiek, 2023). Both urban areas have the same temperate maritime climate. The summer period takes place during June, July, and August. When taking into account the period 1991-2020, the summer period shows average temperatures ranging from a mean minimum of 12.6 °C to a mean maximum of 22 °C (KNMI, 2023a).

3.1.1. The Green Village (TGV), Delft

TGV is located at Van Den Broekweg 4, 2628 CR Delft, with coordinates 51°59'48.3"N 4°22'39.2"E. The village contains an area of approximately 130 x 90 m. TGV is a fieldlab for sustainable innovations and it provides various insights to enhance climate adaptation. With this knowledge, cities are empowered in finding suitable solutions that enhance resilience and improve the quality of living in the city. Appendix D.1 provides a simplistic map of the whole area.

TGV contains a HeatSquare, with an area of approximately 30 x 15 m. Until recently, the HeatSquare consisted of Stelcon plates, at which measurements have been performed as reference (Mao, 2022). However, these measurements were not performed for the temperature in the soil. During spring in 2023, the square was renovated, and various types of ground coverages were installed. The aim of this renovated square was to provide insights into the heat effect and possible reduction of heat by the design/set-up of the renovated square, so cities can adapt to climate change in an efficient way. For the research of this thesis no specific adjustments were made to the original design, of which a visual impression is presented in Figure 3.1a, as the execution of the renovation had already started. Still, this design enables to quantify the effect of the different types of ground coverages on the soil temperature. A map of the renovated HeatSquare is provided in Appendix D.1.

Besides this HeatSquare, another square within TGV was involved and prepared for measurements for this thesis research specifically. This square is referred to as the Hydrogen Square, and it has a dimension of approximately 6 x 7 m. Most part of the field is located in the sun for the whole day, just like the HeatSquare. The straight-line distance between the centre of the HeatSquare and the Hydrogen Square is around 60 m. This square contains a type of ground coverage which is not present on the HeatSquare, namely grey concrete tiles. These are similar to concrete tile 'Rotterdam', which is the current top layer of the distribution mains in Rotterdam. Therefore, the Hydrogen Square is suitable to test (temporary) measures which could potentially be implemented on the existing top layer in Rotterdam. The location of the Hydrogen Square within TGV can be found in Appendix D.1, Figure D.1. Figure 3.1b presents a picture of the Hydrogen Square.

The soils present in TGV are area specific soil combined with sand. On two plots on the HeatSquare, roof substrate ('daksubstraat') is present on the upper 40 centimeters. The vegetation

grows in this roof substrate. Below this 40 cm roof substrate, again area specific soil with sand is present. In this thesis research, a 'plot' refers to a square-shaped area on the HeatSquare with vegetation as top layer, either in roof substrate or sandy soil. The plots are labeled in Section 3.2.2.

(a) Render of the renovated HeatSquare in The Green Village.

(b) The Hydrogen Square in The Green Village.

Figure 3.1.: The squares in The Green Village where measurements are performed.

3.1.2. Rotterdam

Within the city Rotterdam there are six locations where the soil temperature is monitored. At each location, the soil temperature is measured at eight different depths. Information about the exact locations is provided in Table 3.1. The coordinates are in RD (EPSG 28992). So for example, for L1 X=89422.592 meter, Y=436888.158 meter, Z=-1.252 m NAP. These locations were selected by the municipality, and they have installed the sensors. Although the sensors were installed by the municipality for a different research purpose, this urban soil temperature data was also found to be relevant for the analyses conducted in this thesis research. The six locations in Rotterdam where the soil temperature is measured are pointed out on the map in Appendix D.2, Figure D.6, with locations L1-L6. The map shows that there are two pairs of locations where the locations are near each other: L2 & L3 and L5 & L6. Appendix D.2 provides more detailed maps of, and information about, the six locations. The maps of all locations are provided in Figures D.7-D.10. The measurements at locations L1 and L4 are performed on a square, so not below the sidewalk. Pictures of the ground coverages at the locations are presented in Figure D.11 and D.12. Most locations (L2, L3, L4, L5, and L6) have the standard concrete tile 'Rotterdam' as ground coverage (as presented in Figure 2.5). Only location L1 has a different ground coverage as can be seen in Figure D.11a, namely bricks.

Table 3.1.: The six locations in Rotterdam.

Name	Number in ElliTrack	Location	Coordinates ground level, in RD (EPSG 28992)
L1	22032208	Bellamyplein	89422.592, 436888.158, -1.252
L2	22032204	Hofplein	92470.466, 437778.203, -0.143
L3	22032206	Hofplein	92520.567, 437714.373, -0.105
L4	22032205	Frederiksplein	93241.547, 438586.300, -1.297
L5	22032207	Rozenlaan	92159.066, 439967.249, -1.682
L6	22032209	Rozenlaan	92208.772, 439990.276, -1.356

No drilling profiles of the soil have been recorded at the exact location of the temperature sensors. However, there were some drilling profiles recorded at representative locations nearby. These profiles show that each location contains moderately fine sand, and all are either moderately or weakly silty and weakly humic (Gemeente Rotterdam, 2023). An example of such drilling profile representative for Hofplein (so L2 and L3) is visible in Appendix D.2, Figure D.15. The drilling profiles of all locations confirm the assumption of sand in the soil temperature model.

3.2. Materials

3.2.1. Distributed Temperature Sensing (DTS)

In TGV, DTS was used to measure the soil temperature at the renovated HeatSquare. The design was made such that the DTS cable loops around the HeatSquare at two depths depths. One of these depths is as shallow as possible, and the deep depth was chosen with the aim to remove the effect of the diurnal cycle. The shallow depth is located at 0.3 or 0.1 m and the deep depth is at 0.6 m. The path of the cable is presented in Figure 3.2. Appendix D.1, Figure D.2, provides the full version of this map. Sometimes, a loop of DTS cables was installed. These loops are visible in the separate maps of the deep and shallow cable configuration: Figure D.3 and D.4 in Appendix D.1. It must be noted that when the cable loops underneath paved area, the cable at shallow depth is located in red casing, to protect the cable during the construction of the square. These locations are visible in Figure D.3. Since there is air present within the casing and the cable is not surrounded by soil, the DTS measurements do not provide the soil temperature at these locations, and only the depth of 0.6 m can provide information about the soil temperature there.

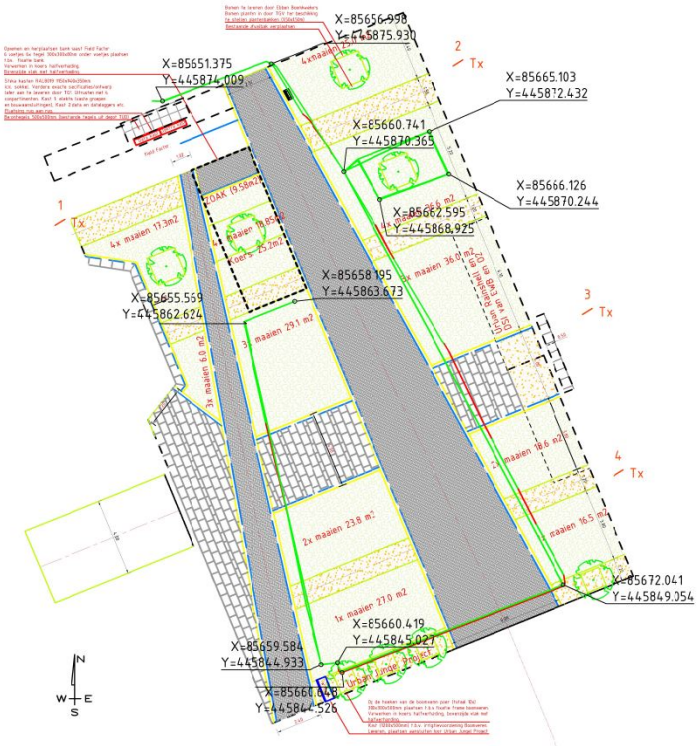

Figure 3.2.: The path of the DTS cable on the HeatSquare.

The measurement design was already finalized before the research for this thesis started. The concept behind the DTS setup was to provide data for a research study of one's choice, allowing researchers the flexibility to determine the focus of their analysis with the obtained data. So, help was given to the installation of the cable, but no specific adjustments with regard to the

path or depth were made for this research specifically. Therefore, the DTS cables are not present specifically at the depth of the distribution mains (0.7 or 1 m depth). The depth of 0.6 m is used for analysis as this is the closest to 0.7 m depth.

The installation of the cables was performed at the end of February 2023 (deep cable) and in the beginning of March 2023 (shallow cable). The optical fiber which loops underneath the ground coverages on the HeatSquare has a diameter of 150 μm. The principle of DTS which is used on the HeatSquare in TGV uses multimode as type of light guiding and the type of setup is double-ended, meaning that the fiber is connected to an interrogator on two sides, so as a loop. Therefore, the information at every point along the length is sent in two directions and measurements are carried out from both ends of the fiber which must be combined. In this way, there is differentiation between the effect of temperature and local attenuation (assuming attenuation is symmetrical) (des Tombe et al., 2020).

Splicing was performed to connect two fibers to each other and to connect the fiber to the connector to plug it into the computer. To enable splicing, there were several steps carried out: stripping, cleaning, cleaving, and using the fusion splicer. The cable was then connected to a computer of Silixa (ULTIMA-M) located in the Control Room next to the HeatSquare, where the data can be read from the screen. Connectors were used to connect the optical fiber to the DTS machine. The type is E2000/APC. Before use, these connectors were cleaned with 'one-click' cleaners.

Temperature along the fiber is estimated from the measured intensities of the Stokes and anti-Stokes scatter by calibrating to reference sections with a known temperature (des Tombe et al., 2020). To do so, a calibration bath was set in the Control Room and used as reference sections to calibrate the data, such that the right absolute temperature could be gained. Around 10 meter of the cable was laid down in the bath. To keep the temperature of the water in the bath homogeneous, a mechanical agitation (a water pump) was used for mixing of the water. To measure this reference temperature, a PT100 probe was used.

The DTS was installed such that it provides temperature measurements along the fiber-optic cable at spatial intervals of 25.4 centimeters and temporal intervals of 30 seconds. Each 2 minutes, a XML-file is saved on the Silixa computer. With these XML-files, a .nc structure can be created by using Spyder (Python 3.11, 'DTS_HeatSquare_processing.py', written by Gijs Vis). This script imports the open-source Python package 'dtscalibration', for calibration of the data. This imports the raw data and executes an extensive calibration and provides confidence intervals (des Tombe et al., 2020). The .nc structure provides the LAF in meters [m], the temperature in degrees Celsius [°C], and the time in UTC (Coordinated Universal Time) [hh:mm]. As the time is provided in UTC, it must be taken into account that for observing the middle of the day and night (15:00 and 03:00), 15:00 is 13:00 UTC and 03:00 is 01:00 UTC in the data set during summer time. The research for this thesis used this script in Spyder, and another Python script was written for this research specifically to read the .nc files and to transfer this data into graphs providing the soil temperature along the length of the cable. The LAF was translated to physical coordinates of the HeatSquare (this is called fiber mapping) with this written Python script. Analysing the soil temperature along the fiber's length on a random day and time has enabled the derivation of the LAF where the cable enters the HeatSquare at 0.6 m depth. This conclusion is drawn from observing elevated temperatures (air temperatures) when the cable is still above ground. This LAF where the cable enters the HeatSquare was set at LAF=114 m. The LAF at the transition to a new ground coverage was determined based on the documented LAF during installation of the DTS cables and based on the dimensions of the plots (Figure D.2 in Appendix D.1).

The output of the written Python script is a horizontal temperature profile. This can illustrate the effect (at the transition) of a ground coverage type.

The top layers where the DTS cable loops underneath, and which are included in the analysis, are:

- Pavement, dark (black)
- Pavement, light (light grey)
- Semi-pavement ('Halfverharding Koers')
- Three modular urban trees ('Urban Jungle Project')
- Vegetation in sandy soil
- Vegetation in 40 cm roof substrate

The vegetation grows in two types of substrates: completely local sandy soil (mixed with tree soil) or local sandy soil with 40 cm roof (garden) substrate on top. Roof (garden) substrate ensures good infiltration of rainwater and retains a lot of moisture. This substrate is used on roofs or roof gardens. The 'vegetation' in 40 cm roof substrate represents an indigenous herbal mixture. All species in this mixture stay low. The mixture exists of around 20 species, predominantly clover species. The 'vegetation' in local sandy soil also represents several species, e.g. Jerusalem artichoke. The vegetation species in the sandy soil have a greater height compared to the ones in 40 cm roof substrate. Figure 3.3 shows both types of vegetation.

(a) Vegetation in 40 cm roof substrate. (b) Vegetation in sandy soil.

Figure 3.3.: Vegetation types on the HeatSquare in TGV.

3.2.2. Point temperature sensors

Temperature sensors in The Green Village

HeatSquare

Besides using DTS at the HeatSquare to measure the soil temperature, this square also contains point temperature sensors in five of the plots with vegetation. Each of these five plots contains six sensors arranged at various depths below, or nearly below, each other, connected to a logger with six ports. A simplified map of the HeatSquare can be seen in Figure 3.4, indicating in which plots sensors are present. This figure includes the Device Serial Number of each logger. The configuration of sensors connected to the ports in a logger are similar in each logger. This configuration of ports P1 - P6 is also presented in the figure. This shows that, in each logger, port P1 is connected to a Tensiometer, which measures soil moisture tension or suction, and port P5 is connected to an anemometer which measures the wind speed. Ports P2, P3, P4, and P6 measure

the soil temperature at the depths 0.05, 0.10, 0.3, and 1 m respectively. The measurement data of sensor P6 at 1 m depth is used for analyses in this research. These sensors were installed for this research specifically, because this is the general depth of distribution mains in the Netherlands. The sensors had to be placed in manually drilled boreholes. Since the sensors at this depth were installed after the construction of the HeatSquare and paving, this was only possible at locations with vegetation as ground coverage type.

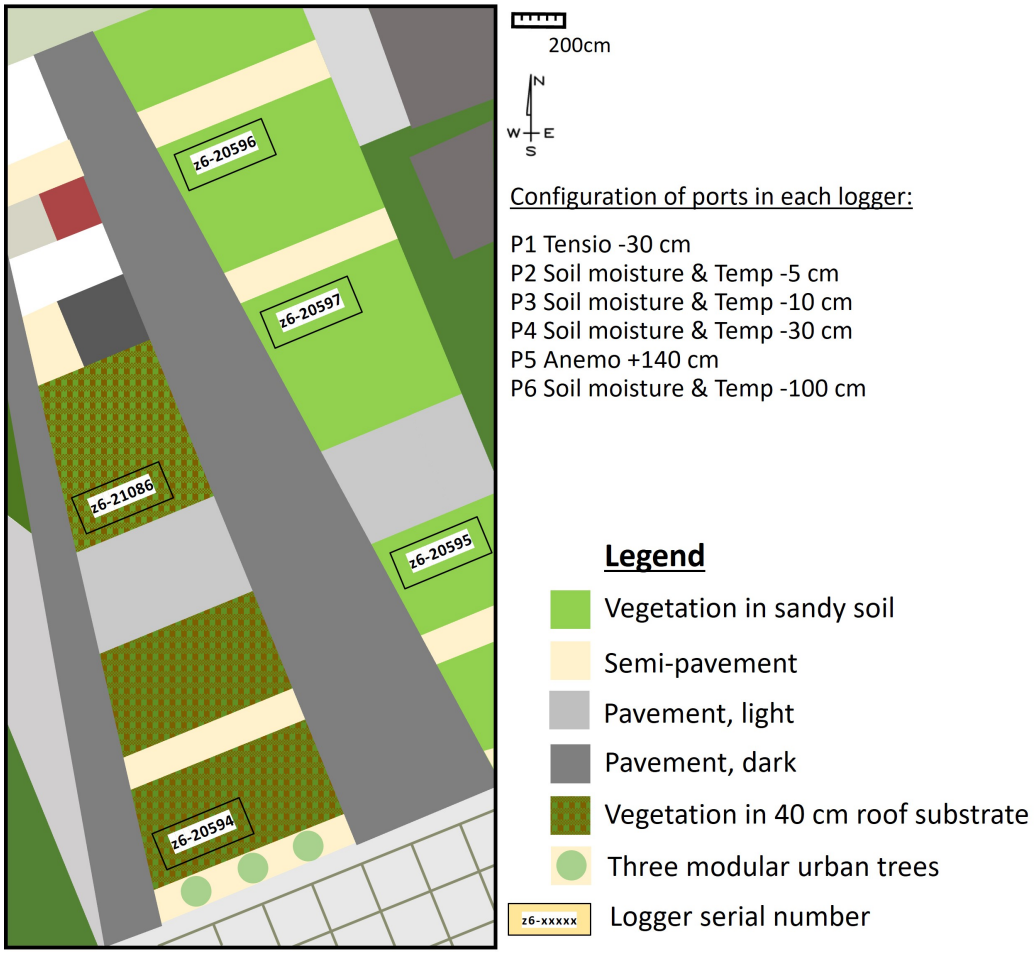

Figure 3.4.: Simplistic map of the HeatSquare with device serial number of the loggers. Each logger contains six ports, at which sensors are connected, all with the same configuration.

The sensors are either TEROS 11 or TEROS 12 and measure both the temperature and the soil moisture. TEROS 12 also measures the EC (Electrical Conductivity). The accuracy of the TEROS 11 and 12 sensor is ± 0.5 °C. The loggers are ZL6 UMTS 3G GSM Cellular from METER Group and have a log frequency of 5 or 15 minutes and the data of soil temperature is stored in ZENTRA Cloud, which is accessible with an account via the website:
https://zentracloud.com/accounts/login/.
As the sensors connected to ports P2, P3, and P4 were installed on April 12 2023, the soil temperature data is stored since this day for these depths. The installation of the sensor at 1 m depth (connected to port P6) has been performed on May 17 2023, so data was collected since then. Because this was executed in the beginning, there was enough time for the vegetation to regrow before the measurements were analysed. For analyses, the measurement data of logger z6-20597 were used to represent vegetation in sandy soil, and the measurement data of logger z6-21086 to represent vegetation in 40 cm roof substrate. The logger z6-20597 has a measurement interval of 15 minutes, and logger z6-21086 of 5 minutes.

Hydrogen Square

As the Hydrogen Square in TGV was involved for this research specifically, sensors needed to be installed here. The sensors were installed during the research (July 12 2023) but in time before the occurrence of warm periods (mid August and begin September). In total, four temperature sensors were installed below the concrete tiles. An overview of the location of the sensors is presented in Figure 3.5. The location of the sensors was chosen such that they minimally fall in the shade of the outdoor electric or gas boxes. The sensor at location A is therefore located in a corner, and the sensor at location B is located in the middle of the tile. At each location (A and B), two sensors were installed on top of each other: one at 0.7 m depth and at 1 m depth. The 0.7 m was chosen because this is the depth of the distribution mains in Rotterdam, and 1 m depth because this is the general depth of distribution mains in the Netherlands.

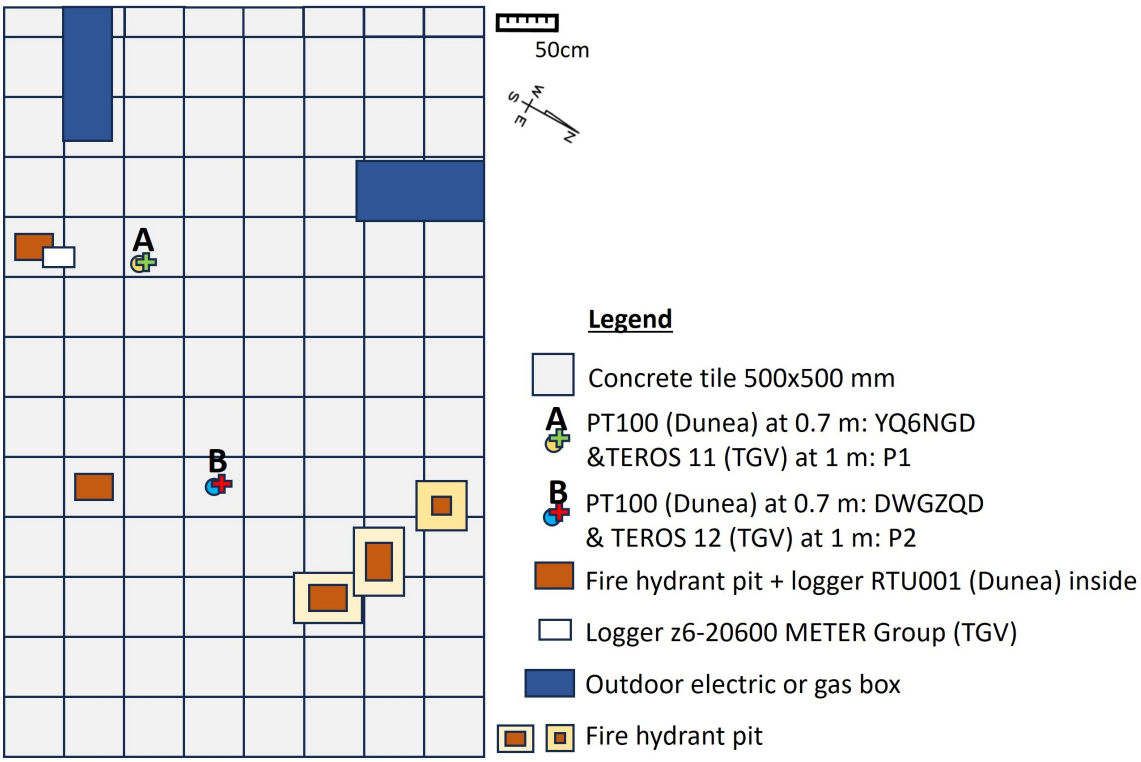

Figure 3.5.: Map of the Hydrogen Square and the locations and serial numbers of the sensors.

At 1 m depth, the same sensor type (TEROS 11/12) as present on the HeatSquare at 1 m depth (but then below vegetation) was installed. The sensors are connected to port P1 and P2 on the same type of logger as on the HeatSqaure (ZL6). As the device types are similar at 1 m depth, this enables a proper comparison between concrete tiles and vegetation as ground coverage type, without influence of sensor dependent accuracy.

At 0.7 m depth, sensors which were borrowed from Dunea (a Dutch drinking water company) were installed. Two ports are available on this type of logger, but due to the cable connected to the sensors being of limited length, two loggers were necessary. This is because the sensors could not be positioned in close proximity to each other, as one of them serves as a reference and the reference should not be influenced by the modifications to the top layer at the other location. The sensor types of Dunea are PT100 and they only measure the temperature. PT100 sensors generally have an accuracy in the order of 0.1 °C. These sensors are connected to loggers RTU001 NB-IoT RTU, of the brand Crest. The soil temperature data at 0.7 m depth below concrete tiles was used to analyse the effect of measures which are applied to the concrete tiles.

Figure 3.5 contains the serial numbers of the loggers of Dunea, and for sensors TEROS 11/12 to which port they are connected in the logger. In this way, the location of the measurement data can

be derived from the websites. The data from the sensors at 1 m depth can again be obtained from the ZENTRA Cloud, with a log frequency of 15 minutes. The data of the sensors of Dunea are registered every 10 minutes and can be obtained via an account in WithTheGrid, via the website: https://app.withthegrid.com/#/e/myg2nd
All four sensors on the Hydrogen Square were operational from the day of installation, so July 12 2023. There were sometimes outliers measured by the PT100 sensors, which were clearly visible on the website WithTheGrid, as the website provides graphs and sometimes contained steep peaks or troughs. The date and times when these peaks and troughs occurred were manually searched for in the downloaded dataset. The outliers were just one value each time there was one, so this value was replaced by linearly interpolating the value.

It must be taken into account that, although the shade was considered beforehand of the installation, the sensor on location A was still prone to the influence of shade of the electric boxes, resulting in systematic biases of the sensors. When looking at the time before (temporary) measures were applied on the tiles, i.e. from the installation on July 12 to August 21 2023, the soil temperature at 1 m depth shows the same progression for temperature, but the soil temperature at location A is consistently lower than at location B. Figure 3.6 shows the progression of the soil temperature at 1 m depth for both locations for this period. The soil temperature of location B can be up to 1.5 °C higher than at location A. The shade could be one reason for the steadily lower soil temperature of location A.

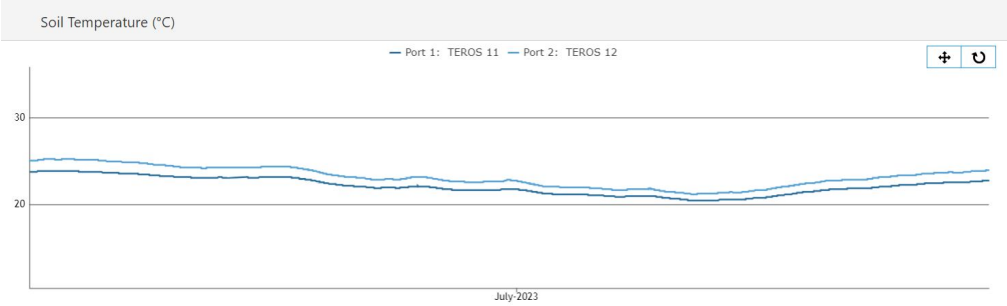

Figure 3.6.: The soil temperature [°C] at 1 m depth of location A (port 1, dark blue) and B (port 2, light blue) on the Hydrogen Square.

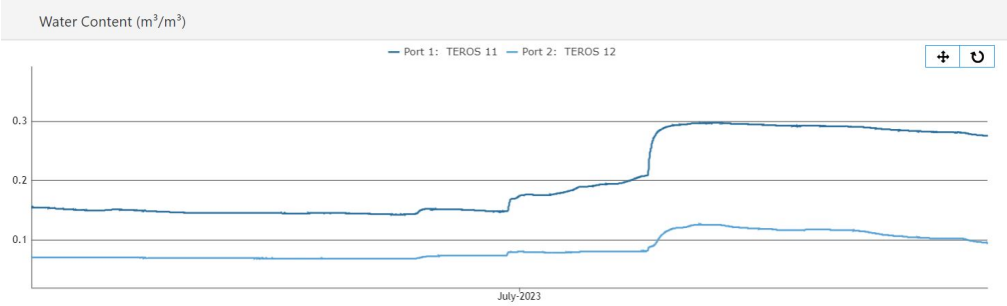

Figure 3.7.: The water content [m^3/m^3] at 1 m depth of location A (port 1, dark blue) and B (port 2, light blue) on the Hydrogen Square.

Another reason could be the difference in moisture content of location A and B. At 1 m depth, the moisture content is measured by the TEROS 11 and 12 sensors. Figure 3.7 shows the moisture content of both locations. This figure shows that the water content follows the same progression at both locations, but the water content at location A (the reference) is consistently higher (0.075 - 0.184 m^3/m^3 higher) than the moisture content at location B. A higher soil moisture content increases the heat capacity of the soil (C_p [J/m^3/K]) and the thermal conductivity (λ [W/m/K])

(see Table 2.2). As the ratio between these two properties determines the thermal diffusivity (α [m^2/s]), this means α is also higher for a higher soil moisture content. A higher heat capacity means that it can absorb more heat energy without a substantial increase in temperature: a larger C_p in the denominator of Equation 2.3 lowers ΔT_{soil} at location A. A higher thermal conductivity can lead to more effective heat transfer, leading to lower soil temperatures.

Temperature sensors in Rotterdam

At the six locations in Rotterdam, which were addressed in Section 3.1.2, temperature sensors were installed at eight different depths at each location (locations L1-L6 in Table 3.1). The eight depths are ground level, 0.2 m, 0.4 m, 0.8 m, 1 m, 1.2 m, 2 m, and 3m. The sensors at these depths only measure temperature. The serial numbers for each location are presented in Table 3.1. The measurements in Rotterdam are not performed at the depth of the distribution mains specifically (0.7 m). The closest depth to the depth of the distribution mains is 0.8 m. So 0.8 m (T5) depth was analysed, and 1 m depth (T4), because this is the average depth of distribution mains in the Netherlands.

The soil temperature measurements are registered every hour. The data is stored in ElliTrack and can be obtained via an account on the website: https://www.ellitrack.nl/auth/login.
The data was stored since April 2023. In the downloaded temperature dataset, the temperature is presented as minimum, average, and maximum measured temperature for each sensor. The average value is used for this research.

Some locations were chosen by the municipality such that a pair is located near each other, of which only one is located in the shade and one is not. This is the case for locations L2 and L3 at Hofplein. In Tygron, maps of the shade were made for one day of each summer month: June 15 14:00, July 15 14:00, and August 15 14:00. These were made for the year 2013, because this is set as standard year in Tygron. Figure 3.8 shows one of these maps. This shows that location L2 is located in the sun and location L3 in the shade of the buildings. The other shade maps are presented in Appendix D.2, Figure D.13 and D.14.

Figure 3.8.: Shade map of Hofplein in Rotterdam, July 15 2013 14:00, made in Tygron. 'L2' and 'L3' mark the locations where, at both locations, eight sensors are present. Table 3.1 and Appendix D.2 provide more detailed information about the exact locations.

3.2.3. Albedo measurements

The albedo of a material is quantified by dividing outgoing shortwave- by incoming shortwave radiation. This can be measured with respectively downward- and upward facing pyranometers. The albedo of materials can also be derived from literature (e.g. the study of Stache et al. (2022)). However, in the context of this thesis research, direct measurements of albedo were conducted. This methodology was essential for more accurately examining the possible impact of albedo on soil temperature, given the absence of precise albedo values in literature for the specific ground coverages within the TGV. A NR01 radiometer was used to measure the albedo. The NR01 is a 4-Component Net Radiometer, manufactured by Hukseflux. It measures the energy balance between incoming short-wave and long-wave infrared radiation versus surface-reflected short-wave and outgoing long-wave infrared radiation. The measured radiation was logged by a Campbell CR1000X and the LoggerNet application was used to read the measured albedo. Figure 3.9 shows the measurement set-up for this research. The height of the radiometers was set at approximately 1.5 m and the equipment was stationed in the middle of each field for a minimum of 10 minutes and a maximum of 60 minutes. LoggerNet was set such that it displayed the albedo each 2 seconds, and the average of the measured albedo in 10 minutes was saved in a file. For certainty, it was tested with a white material whether the device functioned properly. The values went up to higher values immediately (approaching 0.7) as it should for brighter materials, so the device functioned well. Table 3.2 presents the albedo values along with the days and times when the albedo was measured for the relevant ground coverages. The values for concrete tiles align with the measurements performed in the study of Stache et al. (2022). The values for the albedo of vegetation in soil in the table are higher than what was measured in the same study (0.09), but they still align with albedos found in the literature (0.16-0.26 or 0.05-0.40) (Stache et al., 2022).

Figure 3.9.: Measurement set-up to measure the albedo of different ground coverages on the Heat-Square.

Table 3.2.: Measured albedo values in The Green Village.

Date [dd-mm-yyyy]	Time [hh:mm]	Ground coverage	Albedo [-]
30-06-2023	12:50-13:08	Semi-pavement	0.23
30-06-2023	13:14-14:24	Vegetation in sandy soil (z6-20597)	0.19
30-06-2023	13:29-14:50	Pavement, light	0.21
30-06-2023	15:55-15:15	Pavement, dark	0.13
30-06-2023	15:20-15:30	Roof substrate, no vegetation yet (z6-21086)	0.12
30-06-2023	15:32-15:44	Artificial grass	0.09
30-06-2023	16:15-16:30	Concrete tile (Hydrogen Square)	0.14
23-08-2023	15:47-16:03	Vegetation in sandy soil (z6-20597)	0.20
23-08-2023	16:11-16:22	Vegetation in 40 cm roof substrate (z6-21086)	0.19
23-08-2023	16:44-17:01	Concrete tiles (Hydrogen Square)	0.14
23-08-2023	17:06-17:16	White paint on concrete tile (Hydrogen Square)	0.85

3.2.4. Meteorological data

The input of the soil temperature model is meteorological data. For TGV, there is a weather station present in TGV itself, on the Officelab. For Rotterdam, weather station 344 of KNMI can be used. This station is located on the north west side of the city, near Rotterdam The Hague Airport. The straight-line maximum distance between this station and a measurement location in Rotterdam (location L1) is 5.2 km. This is less than the distance to TGV (12.5 km), making it more accurate to use the KNMI station for the comparative analysis between the simulation and the measurements in Rotterdam. An explanation about the exact locations of the weather stations and about how the weather data can be downloaded and transferred to the right format (in case of weather data from TGV) is explained in Appendix E. This appendix also elaborates on how the files are transferred to proper input files for the soil temperature model in MATLAB®.

Figure D.16 in Appendix D shows the air temperature measured by KNMI and the Officelab in one graph. Figure D.17 shows the measured solar radiation at both locations. As both show similar air temperatures and solar radiation for TGV and Rotterdam, this indicates that possible differences in measured soil temperature between the two locations cannot be contributed to differences in air temperature or solar radiation.

3.2.5. Adjustments to the soil temperature model

The soil temperature model runs on MATLAB®, and it generates an output of soil temperature for depths per hour. The results can for example be used for a graphic representation by plotting the soil temperature versus depth for a particular time or to plot the soil temperature at a particular depth for a certain period.

The MATLAB® script was fully analysed for this research to clearly describe the functioning. Information has been provided in Section 2.9, and Appendices A, B, and C. The information for the description of the model mainly originates from research of Agudelo-Vera et al. (2015). After this analysis, some changes have been made to the original model. The equations B.17 and B.28 were initially provided differently in the soil temperature model in MATLAB®. These two equations were originating from Grimmond and Oke (1991) but were wrongly coded in MATLAB®. The equations which were originally present in the MATLAB® code are provided at the end of the Appendix C.

Another change which was made is that a_veg was originally hard-coded to be 0.19. This was changed to a_veg = a_{SS}, where a_{SS} is the albedo of the ground coverage (SS = Soil Surface). By making it a variable parameter, the albedo can be changed according to the measured value. Apart from these changes, the model was used in its original state.

3.3. Description of methodology

3.3.1. Analysed influences and time frames

The research for this thesis analyses the effect of several measures which potentially influence the soil temperature. Table 3.3 summarizes all influences and possible measures which were analysed for this research. In general, the collection of soil temperature data stopped at October 1 2023 at last. By this time, the summer had ended and the air temperatures, and thus soil temperatures, were already reducing. The exact time frame of each analysis depended on the purpose of the analysis. Table 3.3 summarizes the time frame of each analysis and its reason. When an influential factor or measure contains a '*', this means that also simulations were performed of this effect, to compare to the measurements.

Table 3.3.: Overview of the aspects of which their influence on the soil temperature is analysed in this thesis research, including their time frame and reason for this time frame.
*: these effects are also simulated for similar time frames as the measurements, to see whether the measured effect is similar to what can be expected with the soil temperature model. Section 3.3.3 describes how.

Location	Effect on soil temperature of:	Time frame (in 2023)	Reason
TGV	Ground coverage type: horizontal/vertical	Sept 5 and 10 (day and night) Aug 28 (day and night)	Begin and end warm period. And reference day: humid day with clouds.
Rotterdam & TGV	Level of urbanization*: six locations Rotterdam vs location A and B TGV	July 12 - Oct 1 Location B to August 21	Concrete tiles without modifications.
Rotterdam	Depth 0.8 m vs 1 m* : six locations	May 1 - Oct 1	Includes all summer months and extends to some surrounding months to enable a comprehensive analysis of the full progression.
TGV	Depth 0.7 m vs 1 m*: location A and B	July 12 - Aug 21	Installation sensors Hydrogen Square July 12, to analyse temperature difference below concrete tiles at location A and B before any measures were applied.
TGV	Concrete tiles vs Vegetation*	Aug 1 - Oct 1 Warm period: Aug 30 - Sept 17	At this time the vegetation in 40 cm roof substrate had grown (as presented in Figure 3.3a). Warm period to see delay in heating and difference during vulnerable days.
TGV	Bare substrate (no cooling effect due to evapotranspiration). 40 cm Roof substrate vs Sandy soil	May 18 - June 1	May 18 installation sensors. There was no vegetation present till June, only some in sandy soil (Figure 3.10).
TGV	Growth vegetation	June 1 - Aug 1	Further progression till vegetation in both substrates grew fully.
TGV	Temporary shade	Aug 14 - Aug 23	Temporary shade was created on Aug 21 and 22. Days before to see regular progression.
Rotterdam	Permanent shade*	May 1 - Oct 1 Warm period: Aug 30 - Sept 17	Full period to analyse difference shade and no shade. Warm period to analyse whether effect shade increases or decreases during vulnerable days.
TGV	White paint*	Aug 23 - Oct 1	White paint was applied at location B on August 23.

Figure 3.10.: The plot 'Vegetation in sandy soil', z6-20597. Photo taken on June 1 2023.

As stated in Table 3.3, the time frame of the effect of vegetation versus concrete tiles depended on the growth of vegetation. The vegetation did not grow immediately. Figure 3.11 shows a picture made with a drone in June. This shows that the vegetation was not grown yet (there were only some sprouts) in the plots with 40 cm roof substrate (z6-20594 and z6-21086 in Figure 3.4). For this reason, the first relevant (warm) period in 2023, June, could not be used for analysis of the effect of vegetation. Figure 3.11 also shows that the plot z6-20595 has occasionally been opened up, regularly resulting in bare substrate. This is because of the presence of the innovation 'Urban Rainshell' below ground level, which stores and treats rainwater with natural and renewable materials: shells and minerals. Adjustments were sometimes performed and for this reason the ground was sometimes excavated. As also visible in Figure 3.11, above the 'Pavement, light' as ground coverage, picnic tables were present (on the right-side of the picture). This creates shade on this type of ground coverage. Besides these seats, a party tent was also installed here most of the time during the summer months, creating extra shade.

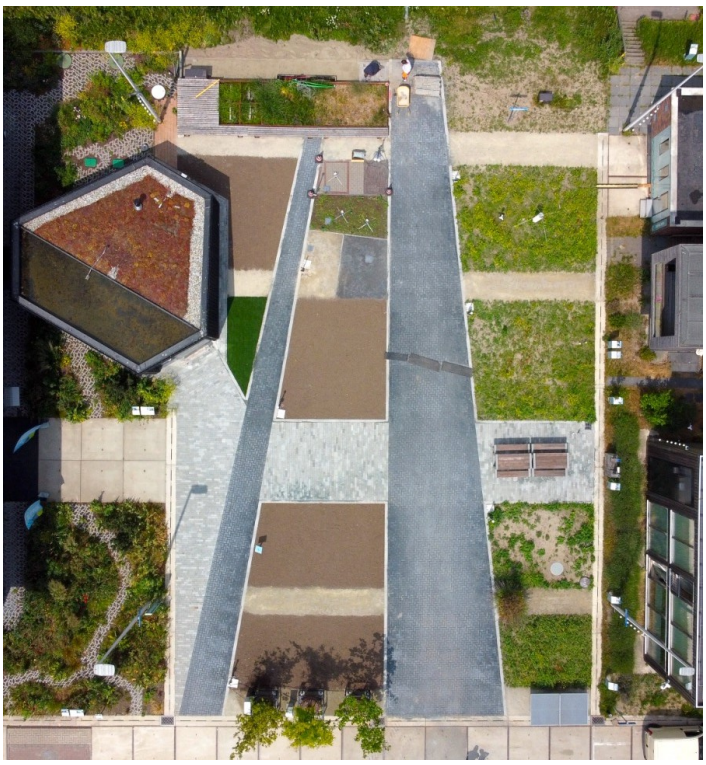

Figure 3.11.: Picture of the renovated HeatSquare in The Green Village, made with a drone in June.

3.3.2. Measuring

The installation of the sensors at all locations in TGV and Rotterdam has been addressed in Section 3.2. As the measurement data originated from various websites, data has been transformed to ensure similar formats for each analysis. These sensors enabled to provide data for the analyses as presented in Table 3.3. To determine the effect of permanent shade at 0.8 and 1 m depth, the measurement locations L2 and L3 in Rotterdam (at Hofplein) were used. Location L2 is located in the sun during every day of the summer, and location L3 is located in the shade, see Figure 3.8. Since the locations are very near each other (Figure D.8, Appendix D.2), other influential aspects like soil type could be assumed to be similar, both represented by the drilling profile presented in Figure D.15 in the same appendix.

The Hydrogen Square, Figure 3.5, was used to execute modifications to the top layer, to enable an analysis of the effect of temporary shade and white paint on concrete tiles. Above the sensors on location A, none of the two measures were applied. These measured soil temperatures were used as reference, to compare the effect of measures to a situation where the top layer has remained unchanged. During the first warm days around mid August no measures were applied, to allow heating of the soil. This serves as reference: warm days without any modifications to the top layer. The measures were applied on the following days:

- August 21 11:00 - August 23 10:00: temporary shade
- August 23 11:00 - September 5 12:00: white paint, 30 cm
- September 5 12:00 onwards: white paint, broadened to 150 cm

Temporary shade

When the warm, sunny period occurred around mid August, creating shade above the surface was performed first. This was done on two consecutive days (August 21 and 22), so temporary, with no cloud cover, and an air temperature of around 25 °C. The shade was created with a

partytent (Figure 3.12). The partytent was moved several times during the day, because of the change of position of the sun, which changed the location where shade was created. The shade was kept mostly as presented in Figure 3.12, so in the middle between location A and B.

Figure 3.12.: Measurement set-up to analyse the effect of temporary shade.

White paint

After two days of shade creation, the concrete tiles at the Hydrogen Square were painted white on August 23 2023 with the paint: 'Drost Devetaal Supreme Grondlak'. The coating was applied above the sensors at location B, which is located in the centre of the 500x500 mm tile, as presented in Figure 3.13a. The paint was applied with two layers on the tiles with a width of 30 cm, because this is the width of the standard concrete tile Rotterdam (Figure 2.5). Because it was considered possible that the surrounding, still grey, concrete tiles affected the soil temperature measured by the sensor at location B, the white coating was widened to 150 cm on September 5 2023 (Figure 3.13b), with the sensor located in the centre. This was done to assure that the effect of white paint dominated.

(a) 30 cm white paint

(b) 150 cm white paint

Figure 3.13.: Measurement set-up to analyse the effect of white paint on concrete tiles.

3.3.3. Simulating

The measurements were compared to the outcome of the soil temperature model to observe whether the progression of the soil temperature in time is simulated well, and whether a distinction in three urban types is appropriate to represent different measurement locations. For simulations of the soil temperature, weather data of the two measurement locations (TGV and Rotterdam) were available, as described in Section 3.2.4 and Appendix E. To simulate the soil temperature in TGV most accurately, the meteorological data of TGV was used as input. To simulate the soil temperature in Rotterdam, the meteorological data of KNMI, station 344, was used as input. The meteorological dataset for both TGV and Rotterdam ran from December 24 2021 to October 1 2023.

Furthermore, as the albedo in the model has been made variable instead of hard-coded for this thesis research, the input of a_{SS} depends on the measurement location. For simulating the soil temperature in TGV, the input of the albedo (a_{SS}) was adopted from the measured albedos: Table 3.2. For Rotterdam, the albedo which was already set in the model was used: a_{SS}=0.12.

Other input for the model was subtracted from Section 2.9.3, depending on the urban type. TGV can be expected to be peri-urban based on the definition of this type, but urban and hot-spot scenarios were also considered. For the simulations of Rotterdam, all three urban types were considered.

The soil temperature model is also used to see whether the model predicts similar effects of measures to what is measured as a result of these measures. So, situations (i.e. particular modifications to the top layer) which are measured are simulated by changing the relevant parameters in the model.

Simulating vegetation

In the comparative analysis of the effect of vegetation, only Location A was chosen to represent the measurements below concrete tiles, because no measures were applied on this location. For the measurements below vegetation, vegetation in sandy soil was used, as this is more common than vegetation in roof substrate. Measurement data of logger z6-20597 was used (Figure 3.4). For simulations, the peri-urban scenario was used. For simulating concrete tiles, no specific adjustments were made to what was described in the beginning of this section. To simulate vegetation as ground coverage, the input of grass was set to 1. Besides, a_{SS} was set to the measured albedo for vegetation in sandy soil, so 0.20 (see Table 3.2).

Simulating shade

To analyse the difference between the expected (simulated) and observed (measured) soil temperature as a result of the effect of shade, the measurements of location L2 and L3 in Rotterdam were compared to the outcome of the model. In the soil temperature model, the urban scenario was used, and shade is an input which can be set to 0 or 1. Shade=1 simulates shade (comparable to location L3) and shade=0 simulates no shade (comparable to location L2).

Simulating white paint

The conditions for which measurement data was available, were replicated with simulations, for the urban scenario. The effect of white paint on concrete tiles at location B was simulated by altering the albedo on the day that the white paint was applied, so on August 23 2023 11:00, The model was set such that it first ran until August 23 2023 11:00 with the initial albedo of the concrete tiles, so a_{SS}=0.14. Then, the outcome of this simulation was used as initial T_soil for the run from August 23 2023 to October 1. This run was performed with the albedo of white paint on concrete tiles, so with an albedo of a_{SS}=0.85. To simulate the conditions of location A, which remained unmodified concrete tiles, a_{SS} was set to 0.14 in the full run. The situation in which concrete tiles were consistently painted white was also simulated. In this simulation, the parameter a_{SS} was set to 0.85 for the entire run. This functions as check, to determine whether the simulation performs well in taking the right initial conditions on August 23 2023 11:00. Although

no measurements were performed below consistently white-painted tiles, this simulation offers insight into the duration required to achieve the full potential impact of white paint on concrete tiles. Specifically, it determines the time it takes for the simulation with a change in albedo to diverge from an a_{SS} value of 0.14 to reach the same soil temperature as under consistently white-painted tiles (an a_{SS} value of 0.85).

It is important to highlight that the simulations to compare to the measured soil temperature were also made for other urban types (peri-urban /urban/ hot-spot) than the one mentioned. However, these other types were found to show similar outcomes in soil temperature differences (between e.g. concrete tiles and vegetation), and therefore only one urban type is presented to demonstrate the difference.

4. Results

4.1. Measurements

This chapter provides the results of the analyses presented in Table 3.3, so the effect on the soil temperature of the following aspects.

4.1.1. Ground coverage type: horizontal/vertical

The results of the horizontal temperature profiles of the HeatSquare in TGV, at the beginning and at the end of six consecutive warm days, are provided in Figure 4.1 and 4.2. August 28 2023 was analysed as reference. This graph is included in Appendix F, Figure F.1. The soil temperature in the middle of the day (15:00) and in the middle of the following night (03:00) are displayed in the same graph. The type of ground coverage is indicated on the top of the graph.

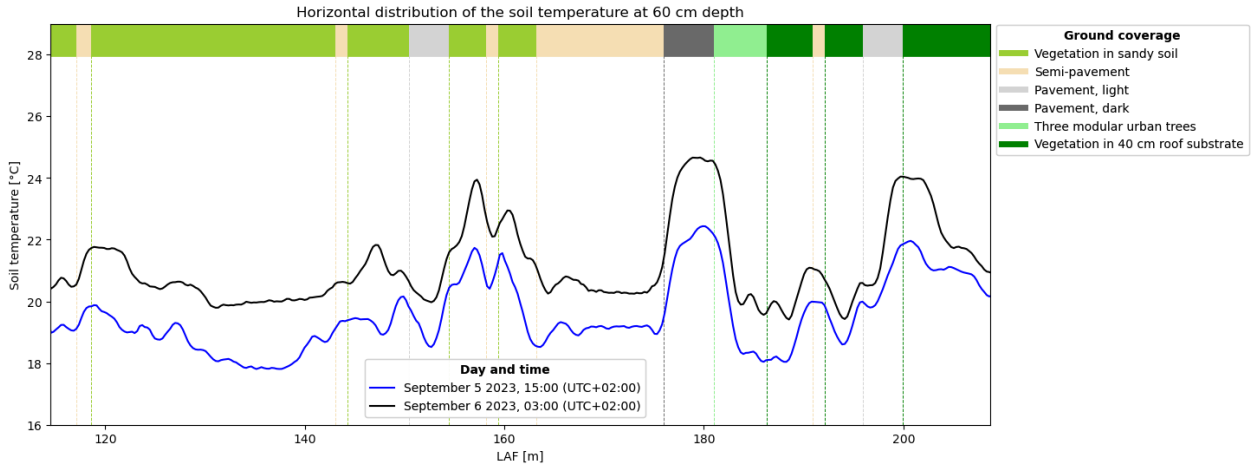

Figure 4.1.: Horizontal temperature profile of the HeatSquare in The Green Village, made with DTS at 60 cm depth for September 5 2023, day and night.

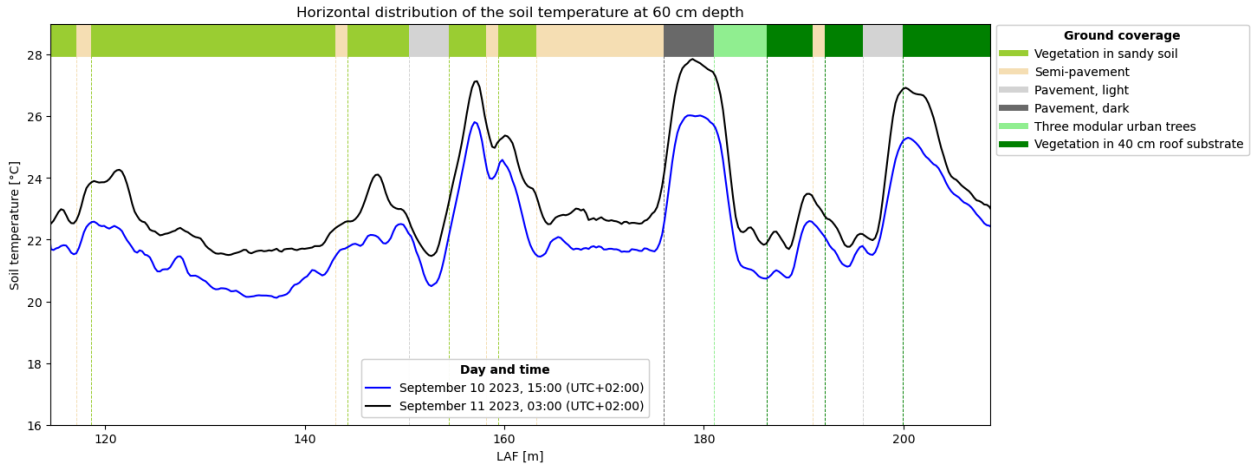

Figure 4.2.: Horizontal temperature profile of the HeatSquare in The Green Village, made with DTS at 60 cm depth, for September 10 2023, day and night.

As the y-limits are similar on all graphs, they clearly show an uplifted soil temperature at the end of the warm period compared to the beginning. This heating is up to 3.2 °C below dark pavement. Additionally, the soil temperature is higher during the night. The temperature difference between night and day decreases as the soil becomes more heated (at the end of a warm period: Figure 4.2). The maximum difference between day and night soil temperature is 2.8 °C at the beginning of the warm period, and 2.0 °C at the end. On the reference day, which had cloud cover and moisture, the difference between day and night soil temperature was smaller, maximally 1.4 °C (Figure F.1). At each analysed day, the highest temperatures can be found below 'Pavement, dark', at the transition of 'Pavement, light' to 'Vegetation in 40 cm roof substrate', and below the fourth 'Vegetation in sandy soil'. The lowest temperatures can be found below the second 'Vegetation in sandy soil', the first 'Vegetation in 40 cm roof substrate', and the first 'Pavement, light'.

Although the magnitude changes while looping below the ground coverage types on the Heat-Square, the progression of the soil temperature shows a similar trend beneath the entire Heat-Square in each graph. The horizontal soil temperature profiles for an individual day and time (e.g. considering only September 5 15:00: blue line in Figure 4.1), show that while external circumstances are the same (e.g. the weather conditions at 15:00), the soil temperature at 60 cm depth clearly exhibits a change when looping beneath different ground coverage types. Even for other weather conditions, when comparing day and night on an individual day (e.g. considering only September 5, blue and black lines in Figure 4.1), or comparing to other individual days (e.g. comparing September 5, Figure F.1, to September 10, Figure 4.2), the progression of the soil temperature follows the same pattern. The peaks and troughs (although differing in magnitude) frequently coincide with the same locations along the length of the cable (LAF), so below the same type of ground coverage. Also, the loops are clearly visible in the graphs. The constant temperatures along the length of the loops, which are stationed below one ground coverage type, also indicate the influence of the ground coverage type. As for all individual days (including different weather conditions), the magnitude changes at the LAF of a transition to a different type, the effect of the ground coverage type mainly seems to influence the temperature in vertical (in-depth) direction. As this transition is gradually, this indicates that ground coverages also affect the soil temperature laterally.

Upon examining a specific day and time, it becomes evident that the soil temperature does not consistently exhibit identical (constant) soil temperature (patterns) each time below the same type of ground coverage. This shows that other local factors, beyond ground coverage type alone, also contribute to the change in the soil temperature, e.g. local variation in soil type. Also within one plot, with one ground coverage type, this is evident from the erratic trajectory of the graph along the length of the cable in that plot. As heat dispersion and damping occur in all directions, not just vertically downward, soil temperature can vary horizontally depending on the distance from the local heat or cooling sources. However, the change in soil temperature that can arise when comparing two different ground coverage types is larger compared to the changes in temperature which occur below a single plot with one ground coverage type (caused by other local influences). For instance, on September 10 2023 15:00, the difference between the minimum and maximum soil temperature experienced below only ´Semi-pavement' is 0.7 °C (the one before 'Pavement, dark'), whereas the difference between two different ground coverage types is larger: for this same 'Semi-pavement' and the subsequent 'Pavement, dark', this difference is 4.6 °C. This indicates that the type of top layer can be considered to have a significant influence on the soil temperature. In general, the results show that soil below ground coverage types with vegetation and/or a high albedo experience the lowest temperature. The difference in soil temperature experienced between individual types of top layer increases in times of elevated air temperatures.

4.1.2. Level of urbanization

The measurements of the soil temperature in Rotterdam are provided in Figure 4.3 for 0.8 m depth and in Figure 4.4 for 1 m depth. The sensor at 1 m depth at location L4 (Frederiksplein) showed a constant temperature of 325 °C, which is not realistic and because of this malfunctioning the measurement data from this sensor was excluded from the analysis. The sensor at 0.8 m depth at this location L4 did function properly, so for the analysis of this depth (Figure 4.3) this location was included. When two locations are near each other (L2 and L3, and L5 and L6), the lines are displayed in the same color but either solid or dotted.

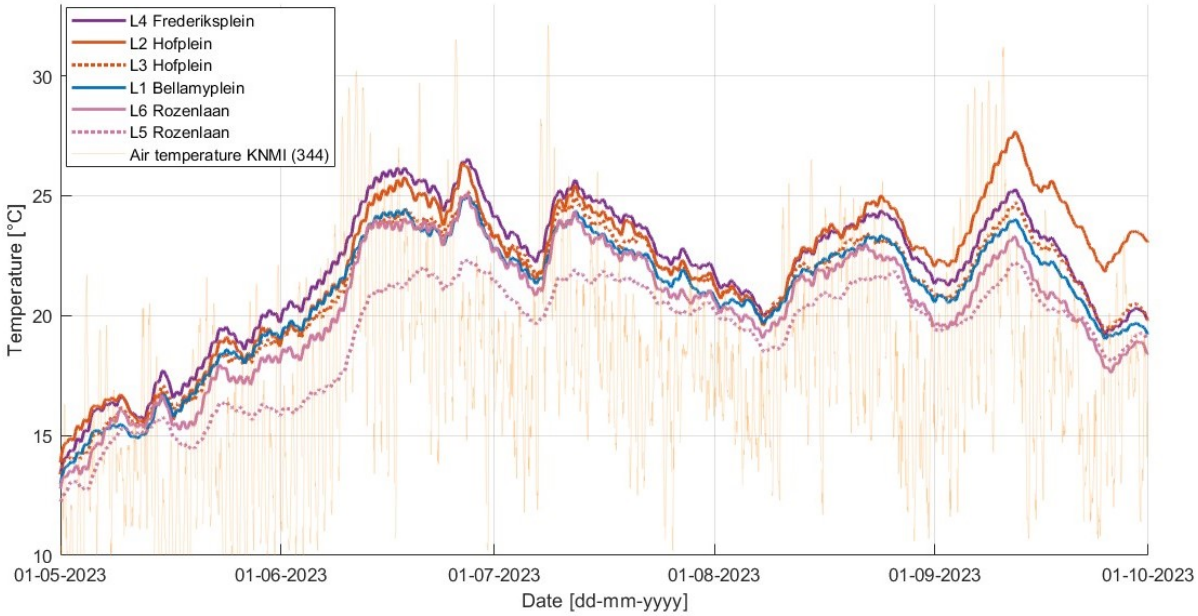

Figure 4.3.: The measured mean soil temperature at 0.8 m depth for locations in Rotterdam.

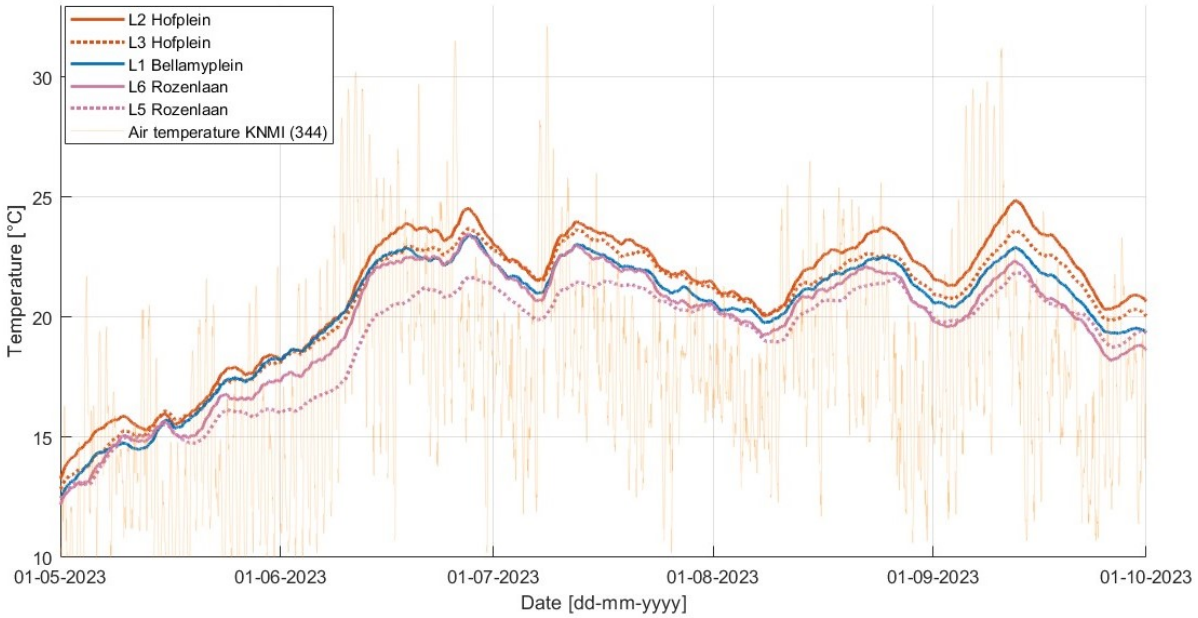

Figure 4.4.: The measured mean soil temperature at 1 m depth for locations in Rotterdam.

The figures show a similar progression of soil temperature at all locations, at either 0.8 or 1 m depth. The weather conditions are one thing that all locations have in common, so the similar progression (and thus times that maxima occur) can be attributed to the weather conditions. The different magnitude of soil temperature at each location (at the same depth) can be attributed to more local circumstances, e.g. presence of shade. The difference in soil temperature (at a particular depth) between locations is not constant. In general, the differences in magnitude of the soil temperature between the locations is larger when considering 0.8 m depth. At 1 m depth, the soil temperature measurements at the locations converge more. So, e.g., at 0.8 m depth, locations L2 and L5 differ more in soil temperature than they differ at 1 m depth at the same time. This indicates that the deeper the pipes are located, the less sensitive they are to local circumstances, also to ones related to level of urbanization, e.g. anthropogenic heat sources.

The influence of level of urbanization was analysed by comparing the soil temperature at 1 m depth in TGV to the temperature at locations in Rotterdam. Figure 4.5 shows the soil temperatures, all measured below concrete tiles. As shown in Figure D.16, the weather conditions in TGV and Rotterdam are similar. Therefore, this is most probably not a cause of the different observed soil temperatures. This graph shows that the soil temperature at 1 m depth in TGV, which is not an urban area, is higher (location B) than locations in Rotterdam or as high as (location A) location L2 Hofplein, which is located in the city centre of Rotterdam. This indicates the influence of local aspects (e.g. type of top layer), independent of how urbanized an area is.

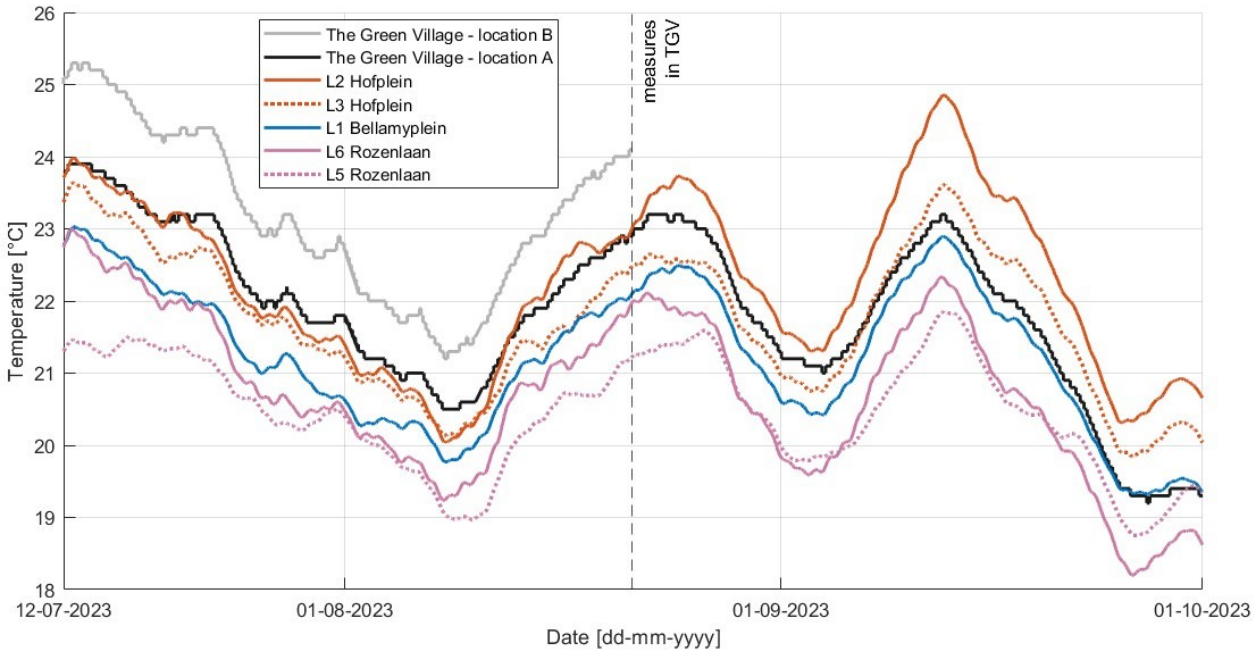

Figure 4.5.: The measured soil temperature at 1 m depth for locations in Rotterdam and in TGV. Measurements at location B in TGV are only provided for the period before measures were applied.

4.1.3. Depth

Rotterdam: 0.8 vs 1 m

The maximum and average temperatures of the measurements presented in Figure 4.3 and 4.4 are provided in Table 4.1. At 1 m depth, the soil temperature is lower than at the more shallow depth of 0.8 m. The measured soil temperature at the five locations does not reach the 25 °C

in the analysed time frame at 1 m depth. At 0.8 m depth, the 25 °C is exceeded several times and sometimes for several days. This is mostly the case for location L2 and L4 (Figure 4.3). The average soil temperature at 0.8 m depth was 0.1 - 1.0 °C higher (on average 0.6 °C for the five locations) than the mean soil temperature at 1 m depth, as can be derived from Table 4.1.

Table 4.1.: Mean and maximum measured soil temperature [°C] at 0.8 and 1 m depth at locations in Rotterdam, for the period May 1 to October 1 2023.

Depth	Soil temperature	L1 Bellamyplein	L2 Hofplein	L3 Hofplein	L4 Frederiksplein	L5 Rozenlaan	L6 Rozenlaan
0.8 m	**Mean [°C]**	20.9	22.0	21.1	21.9	19.2	20.3
	Maximum [°C]	25.0	27.7	25.2	26.5	22.3	25.1
1 m	**Mean [°C]**	20.2	21.0	20.5	-	19.1	19.7
	Maximum [°C]	23.4	24.9	23.7	-	21.9	23.5

Figure 4.3 and 4.4 show that the gradient is steeper for 0.8 m depth: the temperature difference between a trough and peak is bigger. So, there is more daily fluctuation at 0.8 m depth, resulting in an erratic course of the soil temperature. Overall, the general course of increase and decrease of the soil temperature is similar at both depths at a certain location. Figure F.5 in Appendix F displays the soil temperature at both depths for one location, location L2. The peaks and troughs occur at similar times, although a bit earlier for 0.8 m depth compared to 1 m depth. For example, the peak of the soil temperature at L2 occurs on September 12 06:00 (till 07:00) for 0.8 m depth, and at September 12 12:00 (till 17:00) for 1 m depth, so a few hours later. This delay at 1 m depth indicates that the soil temperature is more sensitive to short time changes of weather conditions at 0.8 m depth than at 1 m depth.

The figures (4.3 and 4.4) also show that the maximum soil temperatures at both depths occur in periods of elevated air temperatures. As the rate of heating at 0.8 m depth is larger, leading to a more substantial heating, the difference in soil temperature between the depths increases during warm periods. Since the progression is similar for all locations at both depths, this accounts for all locations. The increased differences of the maximum measured (during warm periods) soil temperatures between the depths prove this, as can be derived from Table 4.1. The maximum soil temperature at 0.8 m depth can be 0.4 - 2.8 °C higher (on average 1.6 °C for the five locations) than the maximum at 1 m depth. This is a larger difference than the average difference in soil temperature between the two depths (0.1 - 1.0 °C, on average 0.6 °C). The maximum difference between the two depths occurs at location L2, on September 11 2023, where the soil temperature at 0.8 m depth is 2.9 °C higher than at 1 m depth (Figure F.5).

TGV: 0.7 vs 1 m

Figure F.4 in Appendix F shows the soil temperature at 0.7 and 1 m depth below concrete tiles in TGV, including the days that measures were applied at location B. Considering the period before any measures were applied, the figure shows that 25 °C is sometimes exceeded at both locations A and B. Especially at location B and/or at 0.7 m depth, the soil temperature can reach high temperatures. The figure also shows that the soil temperature at location B experiences more daily fluctuation at 0.7 m depth than location A, meaning a larger difference between the minimum and maximum daily soil temperature. The temperature at location B is consistently higher than at location A when considering the time before measures were applied. At 0.7 m depth, this difference can increase to almost 4 °C. At 1 m depth, the soil temperature at location B is generally 1 - 1.5 °C higher.

Table 4.2 shows the mean soil temperatures at location A and B, for the period before any measures were applied. Both mean and maximum soil temperature are lower at 1 m compared to at 0.7 m. The difference between the mean soil temperature at 0.7 m and 1 m depth is 1.1 °C for

location A, and 1.9 °C for location B. The maximum difference between the two depths occurs on August 17 2023 for location B, when the soil temperature at 0.7 m depth is 4.3 °C higher than at 1 m depth. At location A, the maximum difference between the depths also occurs on August 17, and the difference is 1.8 °C.

Table 4.2.: Mean and maximum measured soil temperature [°C] below concrete tiles in TGV, for the period before any measures were applied, so July 12 to August 21 2023.

Depth	Soil temperature	Location A	Location B
0.7 m	**Mean [°C]**	23.3	25.1
	Maximum [°C]	26.7	30.7
1 m	**Mean [°C]**	22.2	23.2
	Maximum [°C]	23.9	25.3

4.1.4. Vegetation

The results for the measured soil temperature at 1 m depth below 'Vegetation in sandy soil', 'Vegetation in 40 cm roof substrate', and 'Concrete tiles' in TGV is presented in Figure 4.6. The graph provides when measures were applied, which influences the soil temperature below 'Concrete tiles - location B'. Table 4.3 presents the maximum and average soil temperature at 1 m depth below each ground coverage type. The mean and maximum values were calculated for periods when no measures were yet applied to the concrete tiles. So, for location B, the period August 1 to August 21 was considered.

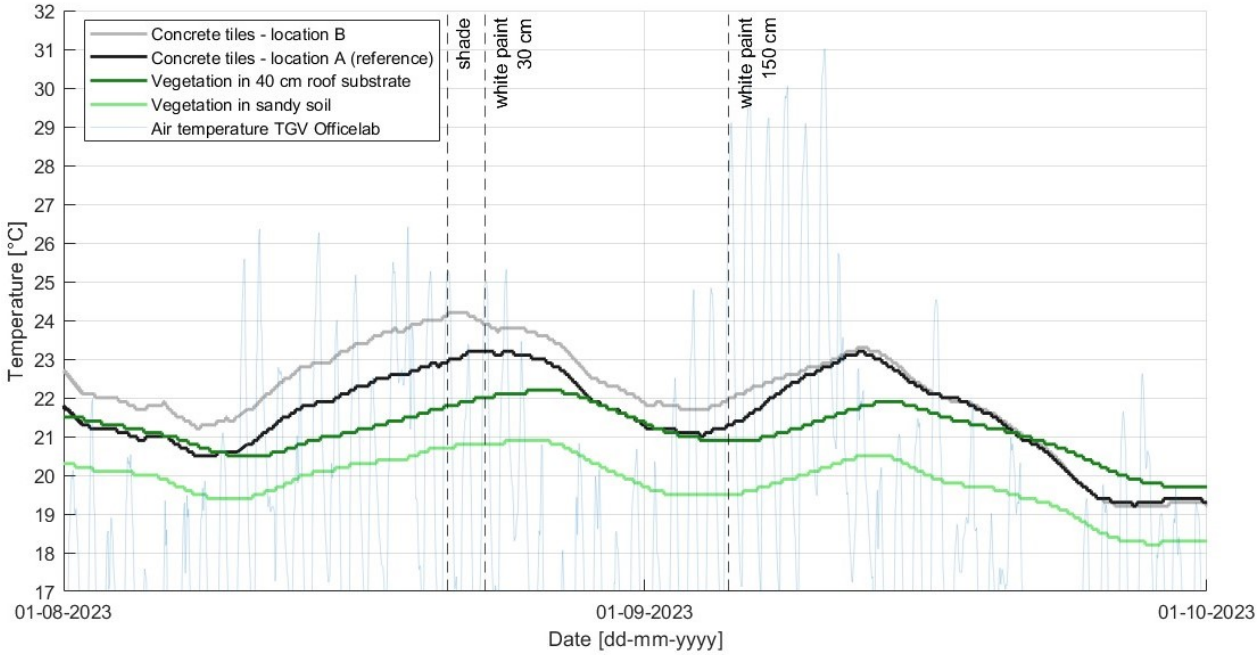

Figure 4.6.: The measured soil temperature at 1 m depth below vegetation in sandy soil, vegetation in 40 cm roof substrate, and concrete tiles in TGV.

For this period of two months, the soil temperature below the ground coverage type 'Vegetation in sandy soil' consistently remains the lowest. Even with air temperatures around 30 °C, the soil temperature at 1 m depth remains around 20 °C. The soil temperature at 1 m depth below 'Concrete tiles' is the highest. Only after the tiles have been painted white, the soil below the concrete tiles was able to reach temperatures lower than ´Vegetation in 40 cm roof substrate´,

but never lower than 'Vegetation in sandy soil'. As can be derived from Table 4.3, the difference between the mean soil temperature below 'Concrete tiles' and 'Vegetation in sandy soil' is 1.8 - 2.5 °C at 1 m depth (when considering the same periods). The difference in mean soil temperature below 'Vegetation in 40 cm roof substrate' and 'Concrete tiles' is smaller: 0.4 - 1.4 °C at 1 m depth. When considering the period August 1 to October 1, the mean soil temperature at 1 m depth below ´Vegetation in sandy soil´ is 1.4 °C lower than below ´Vegetation in 40 cm roof substrate´. This might suggest that the type of substrate matters for the working principle of vegetation.

Table 4.3.: Mean and maximum soil temperature [°C] at 1 m depth below different types of ground coverage. For concrete tiles - location B, the period before measures were applied is considered so August 1 to August 21 2023. No measures were applied at location A, so the full period (August 1 to October 1 2023) is analysed for this location.

Soil temperature at 1 m depth	**Period**	**Vegetation in 40 cm roof substrate**	**Vegetation in sandy soil**	**Concrete tiles - location A (reference)**	***Concrete tiles - location B***
Mean [°C]	01-08-2023 - 01-10-2021	21.2	19.8	21.6	-
	01-08-2023 - 21-08-2023	*21.1*	*20.0*	-	*22.5*
Maximum [°C]	01-08-2023 - 01-10-2023	22.2	20.9	23.2	-
	01-08-2023 - 21-08-2023	*21.8*	*20.7*	-	*24.2*

The provided air temperature of TGV in the graph shows that periods with elevated air temperatures coincide with high measured soil temperatures. The more pronounced gradient between a trough and peak indicate that the soil beneath concrete tiles experiences the most rapid rate of heating and the most substantial heating, in comparison to the soil beneath vegetation. The soil below concrete tiles responds fast to changing weather conditions: when air temperatures increase, the soil below concrete tiles is the first to heat. This results in an even larger difference in soil temperature compared to below vegetation during warm periods. Similarly, the cooling of the soil (as a result of a decline in air temperature) adheres to a consistent order, so the soil beneath concrete tiles initiates the cooling phase. Figure 4.7 shows more clearly the delay of heating and cooling of the soil below a certain ground coverage type, which is a zoomed-in section of Figure 4.6. This figure also shows that the difference in soil temperature between the ground coverage types increases during times of elevated air temperatures. For location A, the temperature below concrete tiles was on average 1.8 °C higher at 1 m depth compared to the temperature below vegetation in sandy soil, in the two analysed months (Table 4.3: 21.6-19.8=1.8 °C). This difference increases during a warm period, up to 2.7 °C on September 12 2023 (Location A, Figure 4.7).

Table 4.4 presents the duration of heating for each ground coverage type. During this warm period, the concrete tiles at location B were already painted white, covering a width of 30 cm. On September 5, this coating was expanded to a width of 150 cm. This white paint affects the temperature below the concrete tiles at location B. Therefore, only location A is used to represent the soil temperature below 'Concrete tiles' for the comparative analysis, and therefore only location A is included in the table. The short time of the peak of soil temperature below concrete tiles shows the rapid response to weather conditions.

Table 4.4.: Heating of the soil [°C]at 1 m depth below three different ground coverages for the period August 30 to September 17 2023, as presented in Figure 4.7.

Ground coverage type	**From [°C]**	**To [°C]**	**Heating [°C]**	**Duration heating**	**Duration peak**	**Notes**
Concrete tiles (location A)	21.0	23.2	2.2	8.2 days	8.5 hours	Heats and cools first
Vegetation in sandy soil	19.5	20.5	1.0	6 days	2 days	Heats second First to reach maximum
Vegetation in 40 cm roof substrate	20.9	21.9	1.0	6.2 days	1.6 days	Heats up last, 3 days after concrete tiles

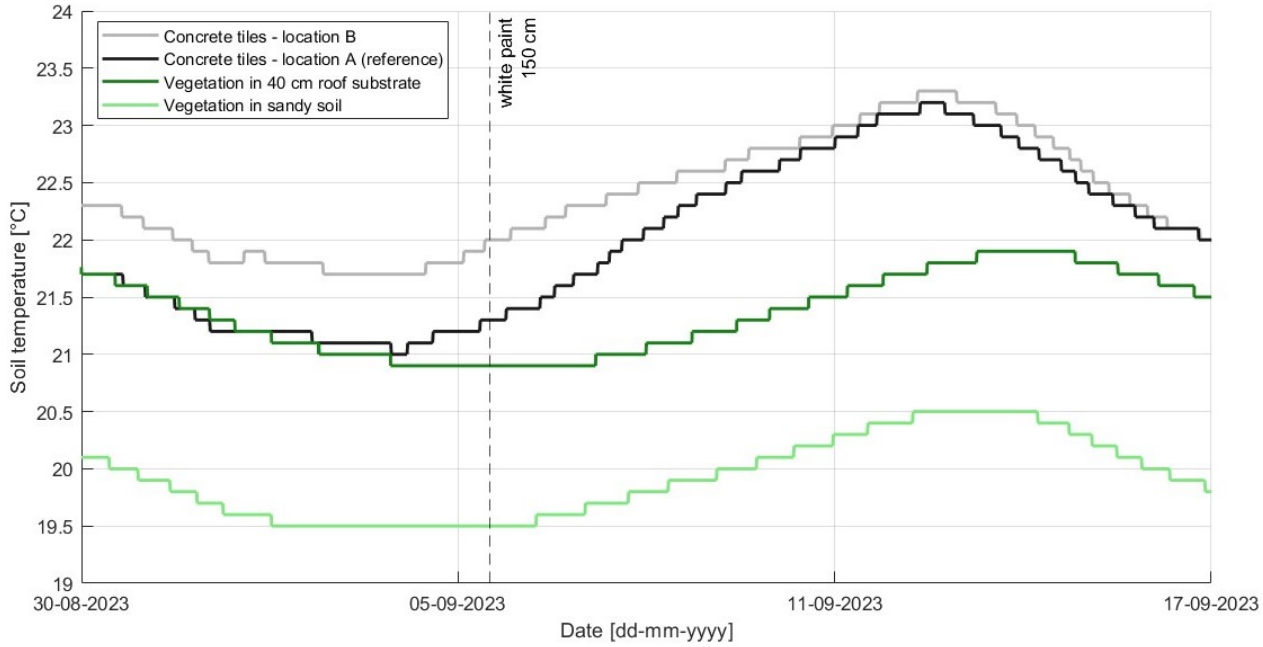

Figure 4.7.: The measured soil temperature at 1 m depth below vegetation in sandy soil, vegetation in 40 cm roof substrate, and concrete tiles in TGV for the period August 30 to September 17 2023. White paint was already present on location B, and was widened to 150 cm on September 5 2023.

Bare substrate and Growth vegetation

As reference for the working principle of vegetation, bare substrate was also analysed. The outcome is provided in Appendix F, Figure F.2. This figure shows that, when there is no vegetation yet, the soil temperature of sandy soil is initially higher compared to the soil with 40 cm roof substrate at the upper level. The soil temperature of bare sandy soil is maximally 0.5 °C higher. Figure F.3 in the same appendix shows the further progression of the soil temperature for (vegetation in) sandy soil and 40 cm roof substrate. The vegetation in sandy soil grew faster than the vegetation in 40 cm roof substrate. Around mid June, the vegetation in the sandy soil was grown, whereas the vegetation in roof substrate only consisted of some sprouts. While the vegetation in sandy soil grew, the temperature of sandy soil reduced, to temperatures below what is measured in soil with 40 cm roof substrate. This clearly shows that the cooling of the soil is a result of vegetation.

4.1.5. Shade

Permanent shade

The soil temperature at 0.8 and 1 m depth for the two locations in Rotterdam (Hofplein Figure 3.8: L3 in the shade, L2 not in the shade) is presented in Figure 4.8. Figure 4.9 zooms in on a warm period. Figure 4.8 shows that the soil temperature at location L2 is generally higher compared to the temperature at location L3. The progression (time of peaks and drops) of the soil temperature at both locations is similar, although the location in the shade (L3) shows less daily fluctuation. The occurrences of peaks and troughs are around similar times, where generally the peak of location L3 in the shade occurs 1 or 2 hours earlier than at location L2.

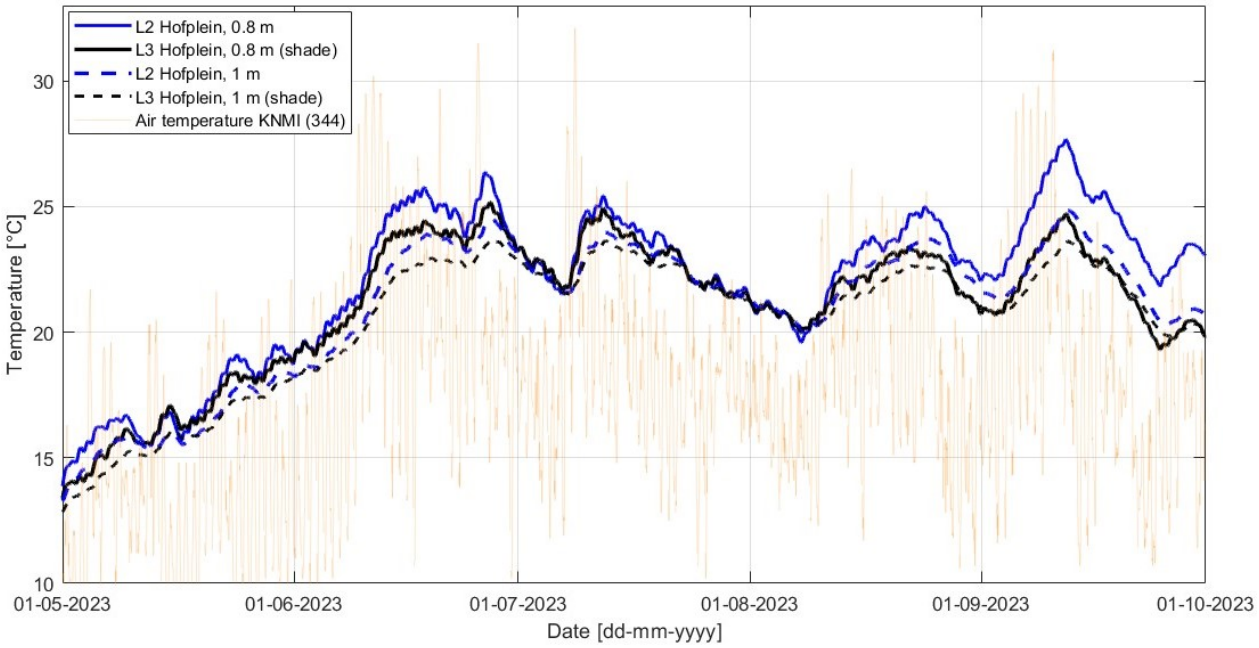

Figure 4.8.: The measured mean soil temperature at 0.8 and 1 m depth at Hofplein in Rotterdam. Location L3 is stationed in the shade.

Table 4.5 provides a summary of the average soil temperature at both locations, both for the whole analysed period (Figure 4.8) and for the warm period (Figure 4.9). For the whole period, the maximum values are also provided. At 0.8 m depth the effect of shade is larger: the temperature in the shade is on average 0.9 °C lower. At 1 m depth, the temperature is on average 0.5 °C lower. This shows that the difference between the two locations, and thus the effect of shade, decreases as the depth increases. The values in the table also confirm what can be observed visually in Figure 4.8: it seems that the difference in soil temperature between the locations is smaller for periods with lower air temperature (this accounts for both depths). For example, the soil temperatures at both locations approach each other at both depths at the end of July, which is a period with lower air temperatures. The mean values in the table indeed show that during warm periods, the temperature difference between shade and no shade is larger compared to the difference averaged over the entire five months. When only such warm period is analysed, the temperature in the shade is on average 2.1 °C lower at 0.8 m depth and on average 0.8 °C lower at 1 m depth. The biggest difference (see Figure 4.9) for 0.8 m depth appears on September 12, 05:00, where the soil temperature at location L2 is 3 °C higher than at location L3. On the same day, but at 12:00, the maximum difference appears at 1 m depth. This difference is 1.3 °C.

Table 4.5.: Mean soil temperature [°C] at two locations in Rotterdam, for the whole period of the analysis and of a warm period. For the whole period, the maximum values are also provided. Location L3 is stationed in the shade.

Period	**Depth**	**L2**	**L3 (shade)**	**Difference L2 (no shade) - L3 (shade)**
01-05-2023 - 01-10-2023	0.8 m	Mean: 22.0 Max: 27.7	Mean: 21.1 Max: 25.2	Mean: 0.9 Max: 2.5
	1.0 m	Mean: 21.0 Max: 24.9	Mean: 20.5 Max: 23.7	Mean: 0.5 Max: 1.2
30-08-2023 - 17-09-2023	0.8 m	Mean: 24.6	Mean: 22.5	Mean: 2.1
	1.0 m	Mean: 22.9	Mean: 22.1	Mean: 0.8

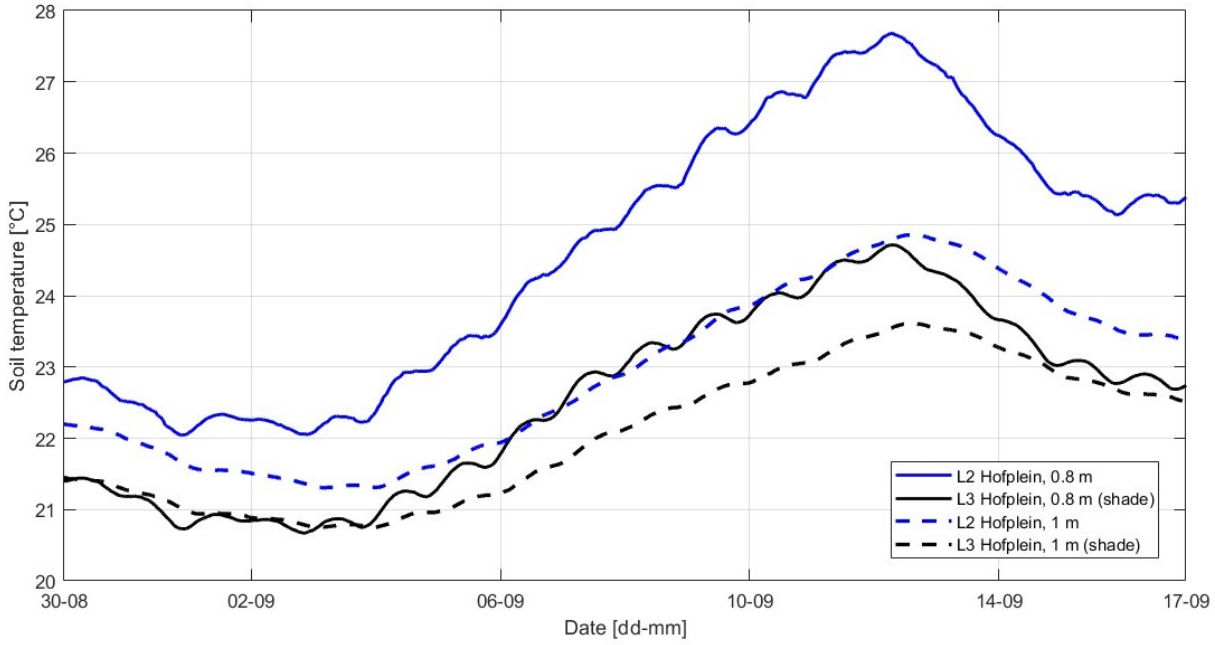

Figure 4.9.: The measured mean soil temperature at 0.8 and 1 m depth at Hofplein in Rotterdam, for August 30 to September 17 2023. Location L3 is stationed in the shade.

Temporary shade

Figure 4.10 shows the soil temperature at 0.7 and 1 m depth, where shade was created with a partytent from August 21 11:00 to August 23 10:00, on location B.

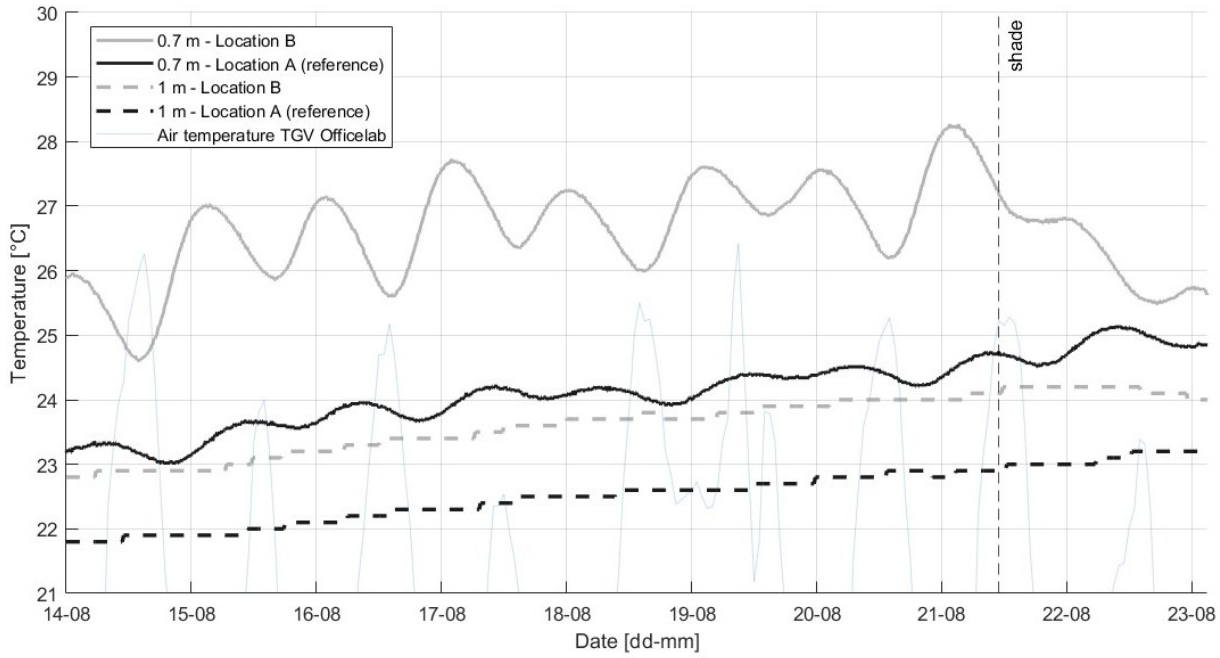

Figure 4.10.: The measured soil temperature at 0.7 and 1 m depth below concrete tiles in TGV. Temporary shade is created on top op the sensor at location B.

Whereas the influence on 1 m depth is small (0.1 °C), the influence on 0.7 m depth is noteworthy. The creation of shade results in a rather stable soil temperature at this depth during the day, with almost no temperature rise (solely 0.1 °C) in the night. This differs from days where no shade was created, where the temperature in the night could increase with 2 °C. So, the daily fluctuation reduces due to the shade. Table 4.6 shows the mean and maximum temperatures at location B specifically for the same period of measurements as presented in Figure 4.10, to quantify the absolute and relative decrease in soil temperature that this location experienced. The figure and table show that the night before shade was created, the soil temperature at 0.7 m depth in the night was maximally 28.3 °C. After one day of creation of shade the temperature was maximally 26.8 °C in the night. After a second day of creation of shade, the soil temperature during the night was maximally 25.8 °C. So, the soil temperature in the night (this is the maximum soil temperature) decreases 1 - 1.5 °C at 0.7 m depth at the location where shade is created. Relatively, this is a decrease of 5.0 % after the first day creation of shade and 3.7 % after the second day, which might indicate that shade initially has more effect. Although the soil temperature reduces, it still exceeds the 25 °C threshold. Still, the figure and table shows that after 2 days (so temporary) creation of shade, the soil temperature at location B decreased at both depths. The air temperature also reduced these days, but as the soil temperature at location A still increased at both depths, the creation of shade can be considered as a cause for the decreasing temperature.

Table 4.6.: Mean soil temperature [°C] at location B before (14-08-2023 - 21-08-2023) and after (21-08-2023 - 23-08-2023) temporarily shade was created on the concrete tiles, including the average air temperature [°C] and solar radiation [W/m^2].

Period		Air temperature [°C]	Solar radiation [W/m^2]	Soil temperature 0.7 m depth [°C]	Soil temperature 1 m depth [°C]
Before	**Mean**	20.3	195.8	26.7	23.5
	Max	26.4	814.8	28.3	24.1
After	**Mean**	19.5	170.4	26.2	24.16
	Max	25.3	771.0	1st night 26.8, 2nd night 25.8	24.20

Because location A and B cannot be compared one-to-one, as they showed different soil temperatures at same depths from the beginning, the temperature reduction can be estimated by using location A as reference and considering the soil temperature difference between location A and B. The soil temperature at location B was first approximately 3 °C higher at 0.7 m depth (see Figure 4.10) than at location A. After creation of shade for two days, the difference reduced to approximately 1 °C. This means that the total effect of temporary shade on concrete tiles was around 2 °C (B relative to A: +3, then +1)

4.1.6. White paint

As discussed in Section 4.1.3, the soil temperature at location B was higher at both 0.7 and 1 m depth compared to location A, before any measures were applied at location B. The maximum temperature exceeded 25 °C at both depths at location B, abundantly at 0.7 m depth. Figure 4.11 shows the soil temperatures for the period when the concrete tiles at location B were painted white. After the tiles were painted white, the soil temperature at location B decreased to values lower to experienced before, even though air temperatures reached higher levels than before the tiles were painted white. Also, the daily fluctuation at 0.7 m depth reduces as a result of this measure: the difference between day and night soil temperature decreases.

Just as for the effect of temporary shade, the temperature reduction can be estimated by using location A as reference and considering the soil temperature difference between location A and B. As can be observed visually in Figure 4.10, the difference in soil temperature between locations A and B reduces after applying 30 cm white paint on the concrete tiles at location B. The temperature at location B regularly reduces to values lower than at location A. Around two days after widening to 150 cm, the soil temperature at location B remains below the soil temperature at location A.

The soil temperature at location B keeps decreasing, enlarging the difference with location A. In values: location B was first approximately 3 °C higher at 0.7 m depth than at location A. After applying white paint 30 cm, the soil temperatures diverged to similar temperatures at location A (i.e. 0 °C difference). Then, after widening the white paint to 150 cm, location B reduced to approximately 1 °C lower than at location A. This means that the total effect of white paint on the concrete tiles, in cooling of the soil, was around 4 °C (B relative to A: +3, then +0, then -1).

With regard to the soil temperature at 1 m depth, the difference between location A and B also decreases compared to the period before measures were applied, especially after the white paint was widened to 150 cm. After around nine days that the white paint was widened to 150 cm, the soil temperature at location B reduces to similar soil temperatures as at location A for this depth. The temperature reduction can again be estimated by using location A as reference and considering the soil temperature difference between location A and B. This shows that the effect of white paint can be estimated to be 1 °C.

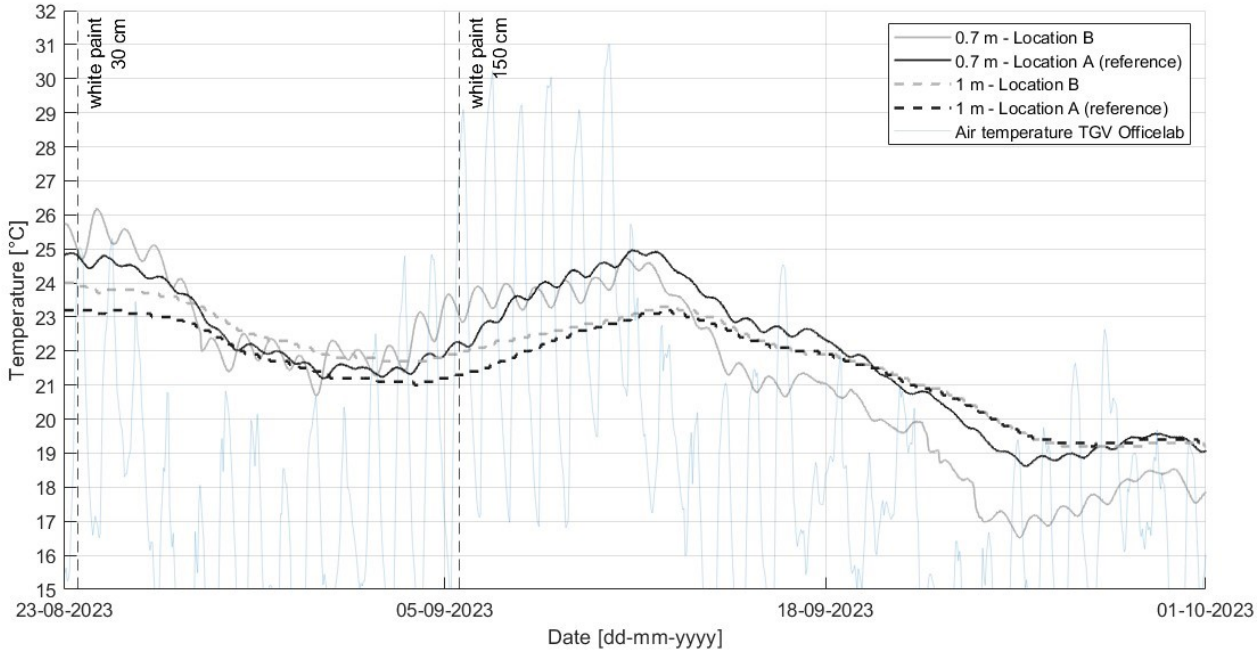

Figure 4.11.: The measured soil temperature at 0.7 and 1 m depth below concrete tiles in TGV. White paint 30 cm was applied on August 23 11:00, and white paint 150 cm on September 5 12:00. Location A is used as reference: no measures are applied on top of this sensor.

Table 4.7 presents the mean and maximum soil temperature for location B specifically, separating the periods before and after the tiles at this location have been painted white. The average air temperature and solar radiation for these periods are also provided. The table shows that there is a reduction in maximum and mean soil temperature at both analysed depths after the white paint was applied. The mean soil temperature has reduced with 3.8 °C at 0.7 m depth, and with 1.5 °C at 1 m depth. Relatively, this is a decrease of 15.1 % at 0.7 m depth and 6.5 % at 1 m depth.

Table 4.7.: Mean soil temperature [°C] at location B before (12-07-2023 - 21-08-2023) and after (23-08-2023 - 01-10-2023) the concrete tiles were painted white, including the average air temperature [°C] and solar radiation [W/m^2].

Period		Air temperature [°C]	Solar radiation [W/m^2]	Soil temperature 0.7 m depth [°C]	Soil temperature 1 m depth [°C]
Before	**Mean**	18.5	183.0	25.1	23.2
	Max	26.4	910.7	30.7	25.3
After	**Mean**	18.3	102.9	21.3	21.7
	Max	31.0	678.0	26.2	23.9

The table also shows a decrease in mean air temperature (of 0.2 °C) and solar radiation (of 80.1 W/m^2) for the period after the tiles have been painted white. This can also cause the lower soil temperatures at both depths. Therefore, a scatterplot was made to more clearly show which soil temperatures were measured before and after the tiles were painted white, for the same air temperature or amount of solar radiation. The period before any measures were applied is July 12 - August 21 2023 11:00, and the period after the concrete tiles at location B were painted white is August 23 11:00 - October 1 2023. Because white paint affects 0.7 m most, the scatterplots were made for this depth only. The scatterplots are presented in Figure 4.12. The scatterplots show that when considering the same air temperature or solar radiation, the soil temperature at 0.7 m depth has clearly reduced after the tiles have been painted white. Especially Figure 4.12a clearly shows the effectiveness of white paint: also for higher air temperatures around 30 °C, the soil temperature at 0.7 m depth remains below 25 °C. The measurements of 'After painted white' still show some soil temperatures above 25 °C (maximally 26.2 °C), but this originates from the first days after the white paint was applied on the tiles. After these first days, the temperature remained below 25 °C, just as on 1 m depth. The last time the temperature exceeded the 25 °C threshold was on August 26 2023, 04:00.

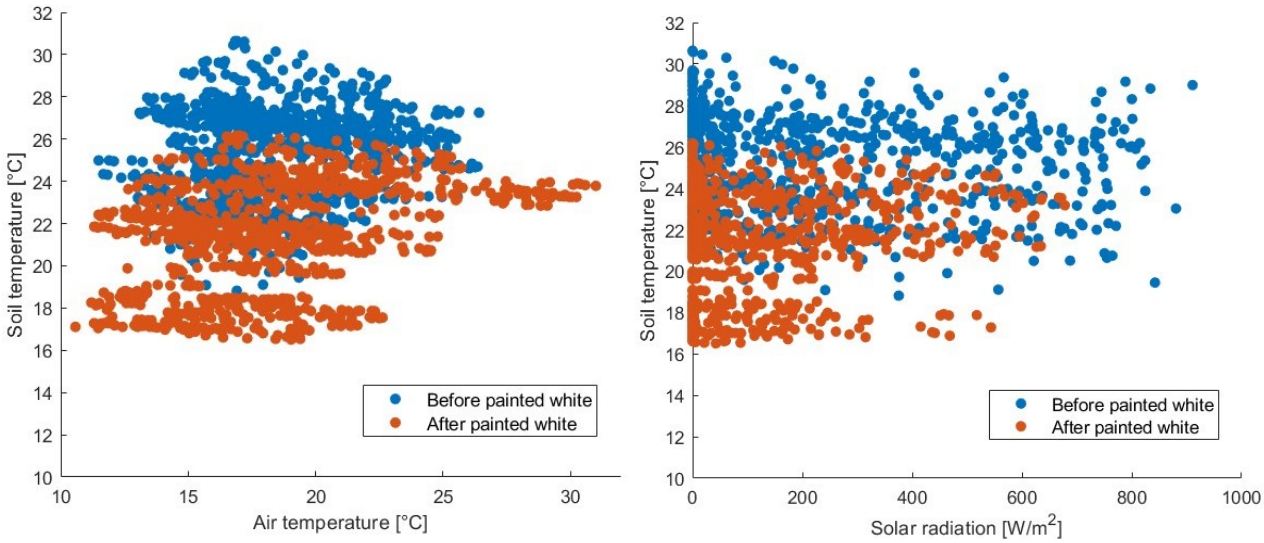

(a) Soil temperature at 0.7 m depth below concrete tiles versus air temperature, in TGV

(b) Soil temperature at 0.7 m depth below concrete tiles versus solar radiation, in TGV.

Figure 4.12.: Scatterplots of soil temperature at 0.7 m depth versus air temperature and solar radiation, before measures were applied and after tiles were painted white.

4.2. Simulations versus measurements

4.2.1. Prediction effect Level of urbanization (three urban types)

The measurements and simulations for Rotterdam, so with the meteorological data of KNMI as input, are provided in Figure 4.13 for 0.8 m depth and in Figure 4.14 for 1 m depth. Figure 4.15 (location A) and 4.16 (location B) show the measured and modelled soil temperature at 0.7 and 1 m depth below concrete tiles in TGV, so with weather data of the Officelab as input.

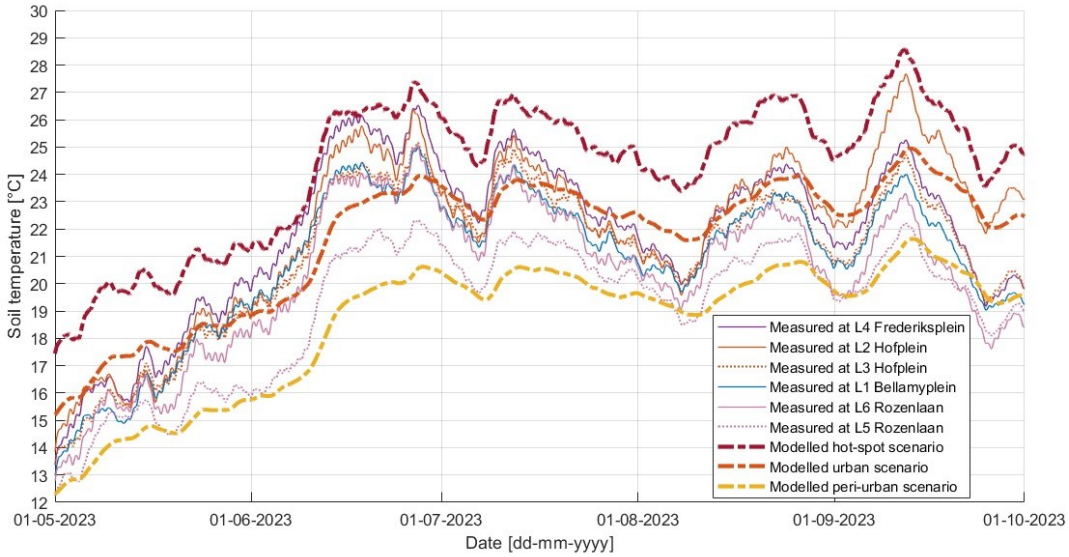

Figure 4.13.: The measured and modelled soil temperature at 0.8 m depth in Rotterdam. The modelled situation is provided both for the urban and hot-spot scenario.

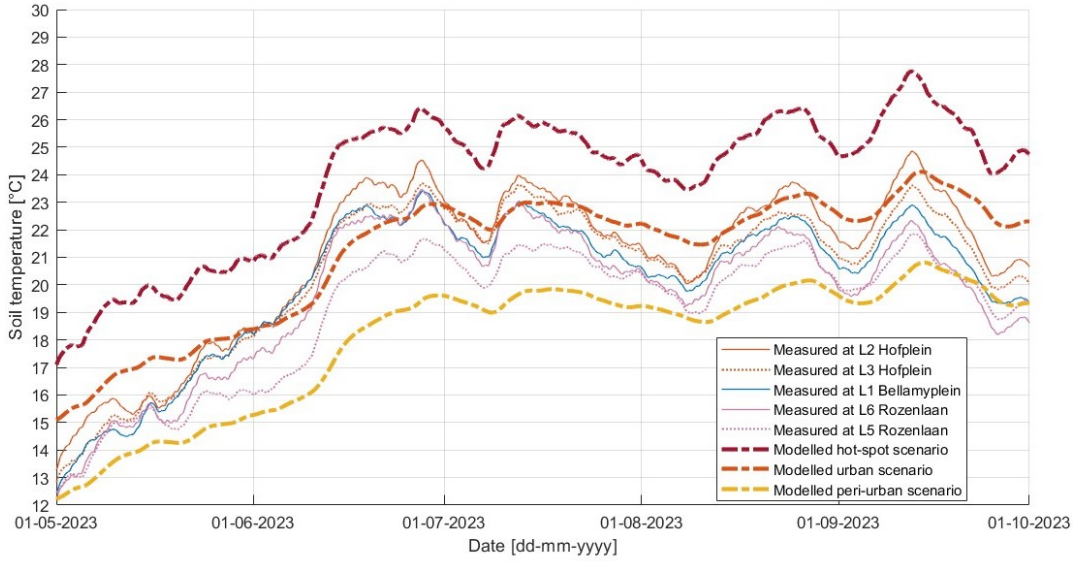

Figure 4.14.: The measured and modelled soil temperature at 1 m depth in Rotterdam. The modelled situation is provided both for the urban and hot-spot scenario.

Some general observations can be made about the three urban types based on these figures of Rotterdam and TGV. In general, the soil temperature model simulates the progression of the soil temperature well. The increase and decrease of the soil temperature occur at similar periods, although at a different rates. For example, the magnitude of the decrease in the simulations is smaller compared to what is measured, resulting in higher temperature values at the troughs of the graph. Still, this course provides proper projections by the simulation about when minimum (troughs) and maximum (peaks) soil temperatures occur in reality. The proper estimation of the progression in time also becomes clear when analyzing the soil temperature at location A (Figure 4.15). The measured soil temperature at 0.7 m depth lowers to values below the temperature at 1 m depth approaching October. The model accurately simulates this. It also predicts well that the temperature at 0.7 depth reaches above 1 m depth again before the end of the analysed period.

The daily fluctuation which is experienced at the more shallow depths of 0.8 and 0.7 m in reality is not properly simulated. Of the three urban types, the hot-spot scenario simulates the daily fluctuation most accurately. The progression of the hot-spot scenario also aligns most with location B in TGV, where the temperature at 0.7 m depth occasionally drops below the temperature at 1 m depth. The hot-spot scenario simulates this at the right times, whereas the urban and peri-urban scenario do not (Figure 4.16).

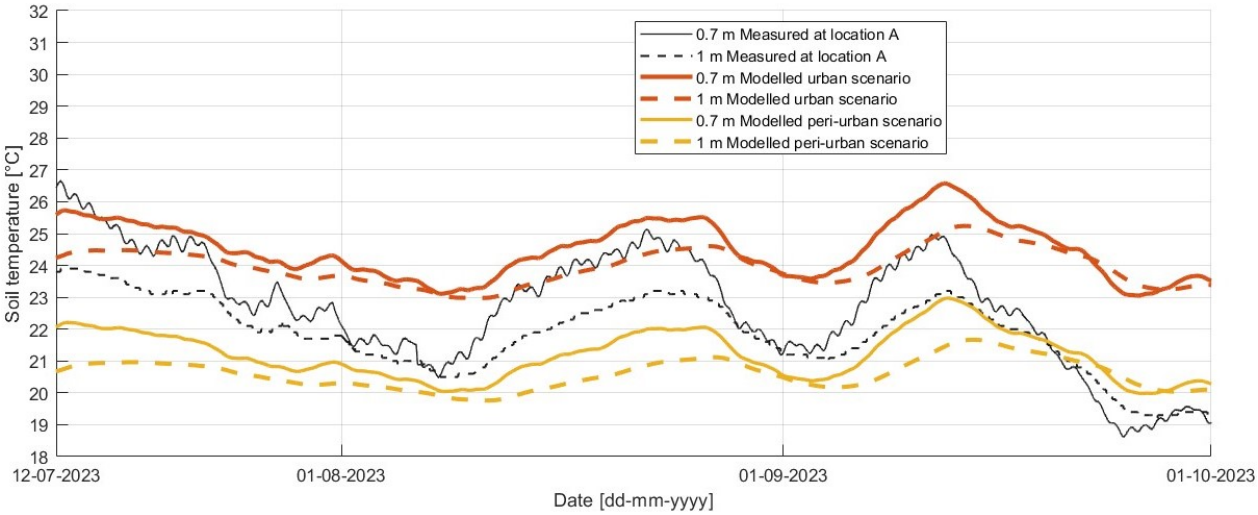

Figure 4.15.: The measured and modelled soil temperature at 0.7 and 1 m depth in TGV, at location A (reference). The modelled situation is provided for the peri-urban and urban scenario.

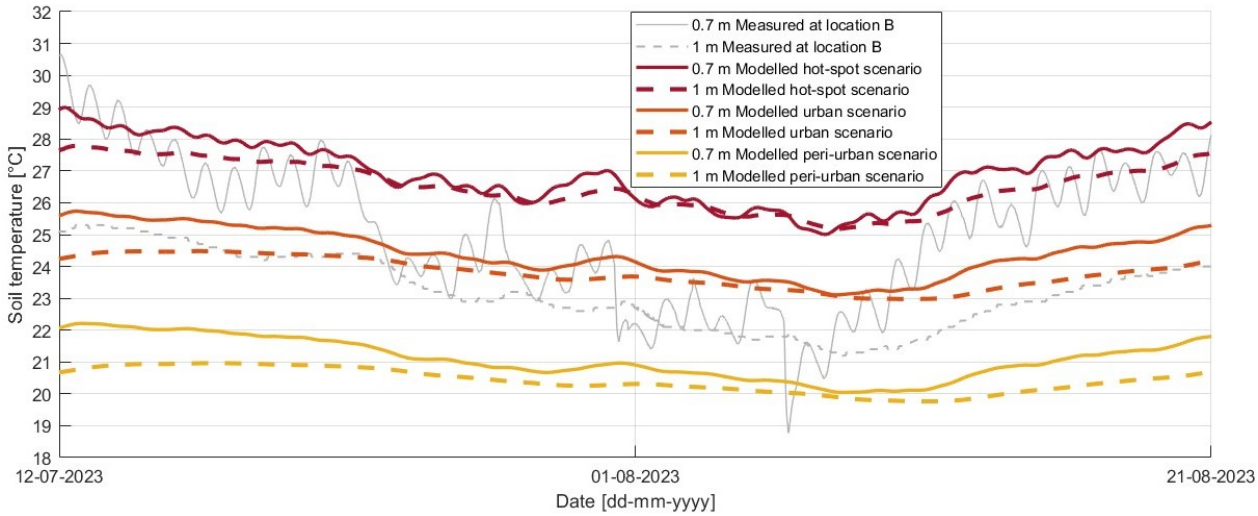

Figure 4.16.: The measured and modelled soil temperature at 0.7 and 1 m depth in TGV, at location B. The modelled situation is provided for the peri-urban and urban scenario.

With regard to the magnitude, it seems that the hot-spot scenario can be suitable as upper limit (during critical days with elevated air temperatures) for the more shallow depths of 0.7 and 0.8 m. This scenario can still slightly overestimates the peaks, but at location B in TGV the measurements can sometimes also be even higher than simulated with the hot-spot scenario. For 1 m depth, the urban scenario provides a better fit. The measurements in Rotterdam clearly show that the urban scenario falls within the spectrum encompassed by locations exhibiting both the highest and lowest measured soil temperatures. For both the measurements in Rotterdam and in TGV accounts that the soil temperature at 1 m depth can also lean towards the peri-urban scenario.

Still, this peri-urban scenario generally underestimated the temperatures at all locations and at both depths. Only in times of lower air temperatures, so from mid September to October, and in May at 0.8 m depth, the peri-urban scenario approaches the measurements.

4.2.2. Prediction effect Depth

Rotterdam: 0.8 vs 1 m

Table 4.8 shows the difference between the mean soil temperatures at the depths 0.8 and 1 m, determined based on measurements and simulations with the three urban types. The table shows that the simulations predict that 0.4 - 0.5 °C cooling of the soil can be gained by locating pipes at 1 m depth instead of 0.8 m, whereas in reality the gain ranges from 0.1 to 1.0 °C. The average of the five locations is 0.8 °C reduction of the mean soil temperature at 1 m compared to 0.8 m depth, so more than expected with modelling for all three urban types. In reality, the maximum difference occurs at location L2 on September 11 2023, and is 2.9 °C (Section 4.1.3). Figure F.6 in Appendix F provides the simulations for the three urban types for 0.8 and 1 m depth. This shows that the simulation rightly predicts more difference in soil temperature between 0.8 and 1 m depth in times of elevated air temperatures. The maximum difference that can occur between 0.8 and 1 m depth is expected to be 1.5 °C in the analysed period, based on simulating the hot-spot scenario. So, this is around two times less than the maximum difference that occurs in reality.

Table 4.8.: Mean measured and simulated soil temperature [°C] at 0.8 and 1 m depth, for the period 01-05-2023 - 01-10-2023.

	L1 measured	L2 measured	L3 measured	L4 measured	L5 measured	L6 measured	Peri-urban simulated	Urban simulated	Hot-spot simulated
0.8 m depth	20.9	22.0	21.1	21.9	19.2	20.3	18.6	21.7	24.3
1 m depth	20.2	21.0	20.5	-	19.1	19.7	18.1	21.2	23.9
Difference 0.8 m - 1 m depth	0.7	1.0	0.6	-	0.1	0.6	0.5	0.5	0.4

TGV: 0.7 vs 1 m

Table 4.9 shows the difference in mean soil temperature between 0.7 and 1 m depth, both for the measurements and for simulations. This table provides the means of the measurements and simulations presented in Figure 4.15 (location A) and 4.16 (location B). So, for location B, the period before any measures were applied is considered (July 12 to August 21), and all three urban types were simulated. The table shows that the simulation predicts a smaller temperature reduction which can be gained by locating at 1 m depth instead of at 0.7 m depth, than is measured. This accounts for location B peculiarly: the difference in mean soil temperature between the two depths (0.7 - 1 m depth) is 1.9 °C based on the measurements, and 0.4 - 0.7 °C based on the simulations with the three urban types. So, the model predicts that the reduction in mean soil temperature is less than half of what is measured at location B in case the pipes are located at a depth of 1 m compared to 0.7 m. Of the three urban types, the hot-spot scenario underpredicts the reduction in mean soil temperature due to increasing the depth most.

With regard to the maximum difference, the simulation also predicts less than what is measured in reality. This can also be observed visually in Figure 4.15 (location A) and 4.16 (location B): the difference between the depths fluctuates more in reality and reaches larger differences than simulated. For location A, the simulation (both peri-urban and urban) predicts a maximum difference between the two depths on September 12 2023, where the temperature at 0.7 m depth is expected to be 1.5 °C higher than at 1 m depth. In reality, the measurements show a maximum difference of 2 °C between the two depths at location A, occurring one day earlier. At location

B, the measured maximum difference between 0.7 and 1 m depth was 5.6 °C just after the installation of the sensors (July 12 2023), and later (the second highest difference) was 4.3 °C (on August 17 2023). The three urban scenarios predict a maximum difference between the depths of 0.9/1.3/1.4 °C (depending on the urban type). So, the reduction in soil temperature by increasing the depth is underestimated by the model for both location A and B in TGV.

Table 4.9.: Mean soil temperature [°C] measured in TGV below concrete tiles, and simulated mean soil temperature for the same periods.

Depth	Period	Location A - reference measured	Location B measured	Peri-urban simulated	Urban simulated	Hot-spot simulated
0.7 m	**12-07-2023 - 01-10-2023**	22.7		21.2	24.5	
	12-07-2023 - 21-08-2023		25.1	21.1	24.4	26.9
1 m	**12-07-2023 - 01-10-2023**	21.9		20.6	24.0	
	12-07-2023 - 21-08-2023		23.2	20.4	23.8	26.5
Difference 0.7 m - 1 m	**12-07-2023 - 01-10-2023**	0.8		0.6	0.5	
	12-07-2023 - 21-08-2023		1.9	0.7	0.6	0.4

4.2.3. Prediction effect Vegetation

Figure 4.17 shows the measured and modelled soil temperature at 1 m depth below vegetation and concrete tiles as ground coverage. Only location A is presented to represent concrete tiles, as there were no measures applied at this location.

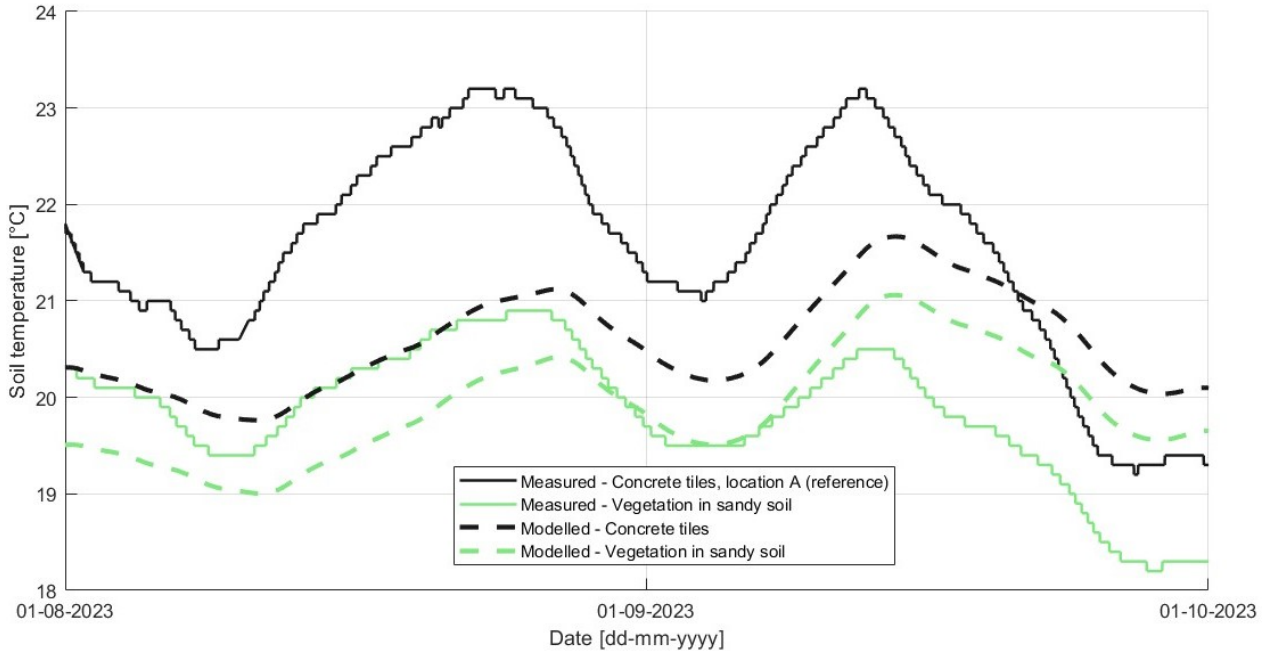

Figure 4.17.: The measured and modelled soil temperature at 1 m depth in TGV. The modelled situation is provided both for the peri-urban scenario, with grass=0 & a_{SS}=0.14 or grass=1 & a_{SS}=0.19. The measurements of vegetation in sandy soil are derived from the registered measurements by logger z6-20597.

The figure shows a similar progression for the measurements and the outcome of the model, with peaks and troughs at same times. However, the rate of increase and decrease is faster for the measurements compared to the rate predicted by the simulation. With regard to the difference in temperature between the two ground coverage types, the figure shows that for both the measurements and simulation, the difference is rather constant. However, the magnitude of the difference between concrete tiles and vegetation as ground coverage is in reality larger than predicted with modelling.

Table 4.10 provides an overview of mean soil temperature at 1 m depth below concrete tiles and vegetation as ground coverage, and the difference in means between these two types of top layer. This is provided for both the measured and simulated soil temperature. The measured mean soil temperature below vegetation is 1.8 °C lower compared to below concrete tiles, while the model predicts a difference of 0.7 °C in the mean soil temperature between the two types of top layers. This predicted difference is approximately 2.5 times less than what is measured. With regard to the maximum difference between concrete tiles and vegetation as ground coverage, the simulation also underpredicts the difference. For instance, on September 12 2023, the measured soil temperature at 1 m depth below concrete tiles was 2.7 °C higher than below vegetation. The model predicts a difference of only 0.6 °C on this day. Thus, in reality, more than 4.5 times as much difference occurred. The maximum difference between the two ground coverage types which is predicted by the model for this analysed period is 0.8 °C. This is still around 3.5 times less than the measured maximum difference. So, the temperature reduction which could be gained by changing the ground coverage type from concrete tiles to vegetation is larger in reality than what the soil temperature model predicts.

Table 4.10.: Measured and simulated mean soil temperature [°C] at 1 m depth. Below concrete tiles and vegetation as ground coverage, for the period 01-08-2023 - 01-10-2023. For the simulation, the peri-urban scenario was used.

Ground coverage type	**Vegetation in sandy soil measured**	**Concrete tiles - location A measured**	***Difference***	**Grass simulated**	**Concrete tiles simulated**	***Difference***
Mean [°C]	19.8	21.6	*1.8*	19.9	20.6	*0.7*

4.2.4. Prediction effect Shade

Figure 4.18 shows the measured and expected (simulated) soil temperature at 0.8 m depth for a location in the shade and not in the shade. Figure F.7 in Appendix F shows the same, but for 1 m depth. The figures for both 0.8 and 1 m depth show that the simulation especially wrongly predicts a rather constant difference in soil temperature between a location with or without presence of shade. This does not align with the fluctuating difference of the measurements. At 0.8 m depth, the difference expected by the simulation is around 1 °C for the entire analysed period. The maximum difference which can occur between shade and no shade in the analysed period is 1.3 °C according to the simulation at 0.8 m depth, and maximally 1.2 °C at 1 m depth. In reality, the difference in soil temperature between shade and no shade fluctuates at both 0.8 m and 1 m depth. Shade can cause a difference up to 3 °C at 0.8 m depth in times of elevated air temperatures. Also at times, the presence of shade results in no difference in the measured soil temperature compared to a location without shade. The simulated difference can also sometimes be in the same range (1 °C) as occurs in reality, but because the simulated difference remains rather constant while the measurements fluctuate, the simulation more often over- or underpredicts the effect of shade.

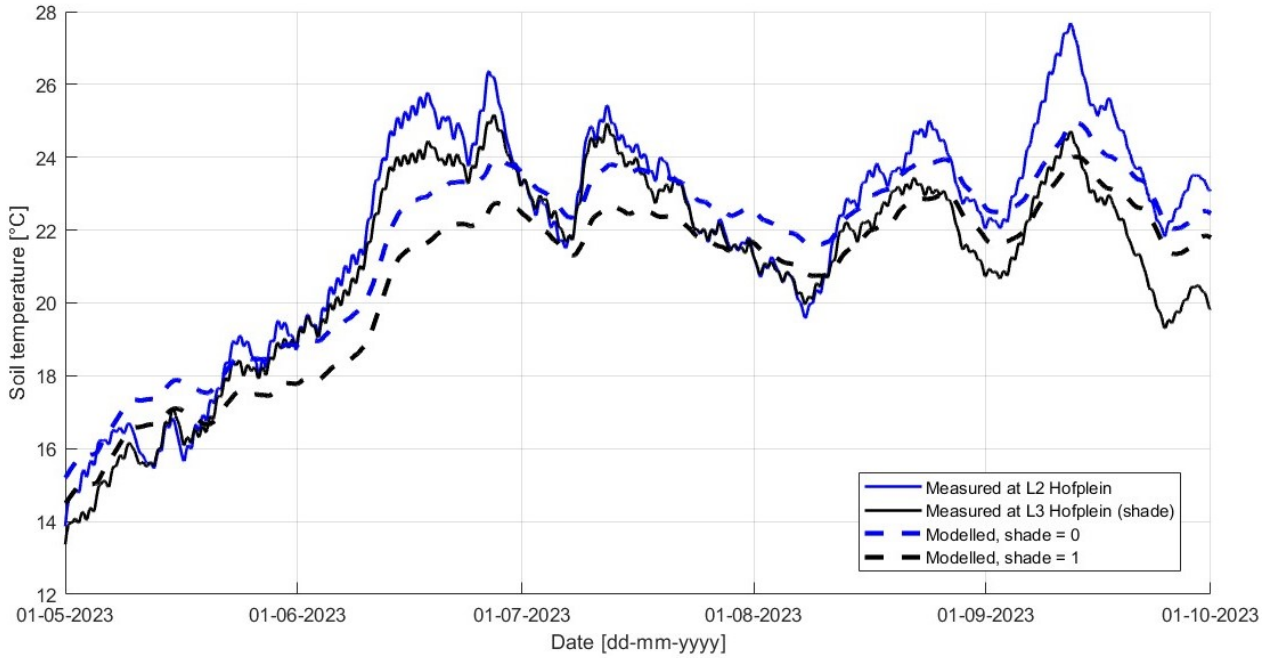

Figure 4.18.: The measured and modelled soil temperature at 0.8 m depth at Hofplein in Rotterdam. The modelled situation is provided both for the urban scenario, with shade=0 or shade=1.

Table 4.11 displays the mean soil temperatures at depths of 0.8 and 1 m for locations with and without shade, for both measured and simulated soil temperature. Additionally, the table shows the difference in mean soil temperature between locations with and without shade. As the measured soil temperature of locations in the shade sometimes equals the measurements of locations without shade, this results in a smaller difference in means between shade and no shade. Consequently, the differences in mean soil temperature between locations with and without shade for measurements and simulations provide limited information. However, the table does reveal that the model incorrectly assumes the same average effect of shade at both 0.8 and 1 m depth, whereas in reality, the effect of shade decreases with depth.

Table 4.11.: Measured and simulated mean soil temperature [°C] for the effect of shade, for the period 01-05-2023 - 01-10-2023. For the simulation, the urban scenario was used.

Depth	L2 measured	L3 (shade) measured	*Difference*	no shade simulated	shade simulated	*Difference*
0.8 m	22.0	21.1	*0.9*	21.7	20.7	*1.0*
1 m	21.0	20.5	*0.5*	21.2	20.2	*1.0*

4.2.5. Prediction effect White paint

The measurements and simulation of the soil temperature at 0.7 m depth, as a result of applying white paint on concrete tiles on August 23 2023, are provided in Figure 4.19. The full period from the day of installation of the sensors to October 1 2023 is provided in Figure F.8 in Appendix F. On September 21 2023, the graph which simulated the white painted tiles (transition to another albedo) joins the simulation of a constant albedo of 0.85. This is almost a month later than the day that the albedo changed from 0.14 to 0.85. So, the simulation expects a transition period of nearly a month. A similar statement cannot be made for the reality, as there were no measurements performed below permanent white painted tiles.

With regard to the magnitude of the effect, the simulation predicts the soil temperature at 0.7 m depth to reduce in this period with approximately 1 °C (i.e. the difference between albedo of 0.14 and 0.85). In reality, the total effect of white paint on concrete tiles, in cooling of the soil, was estimated to be 4 °C (Section 4.1.6). This shows that the actual cooling effect of white paint, so increasing the albedo, is more than can be expected by simulating the situation.

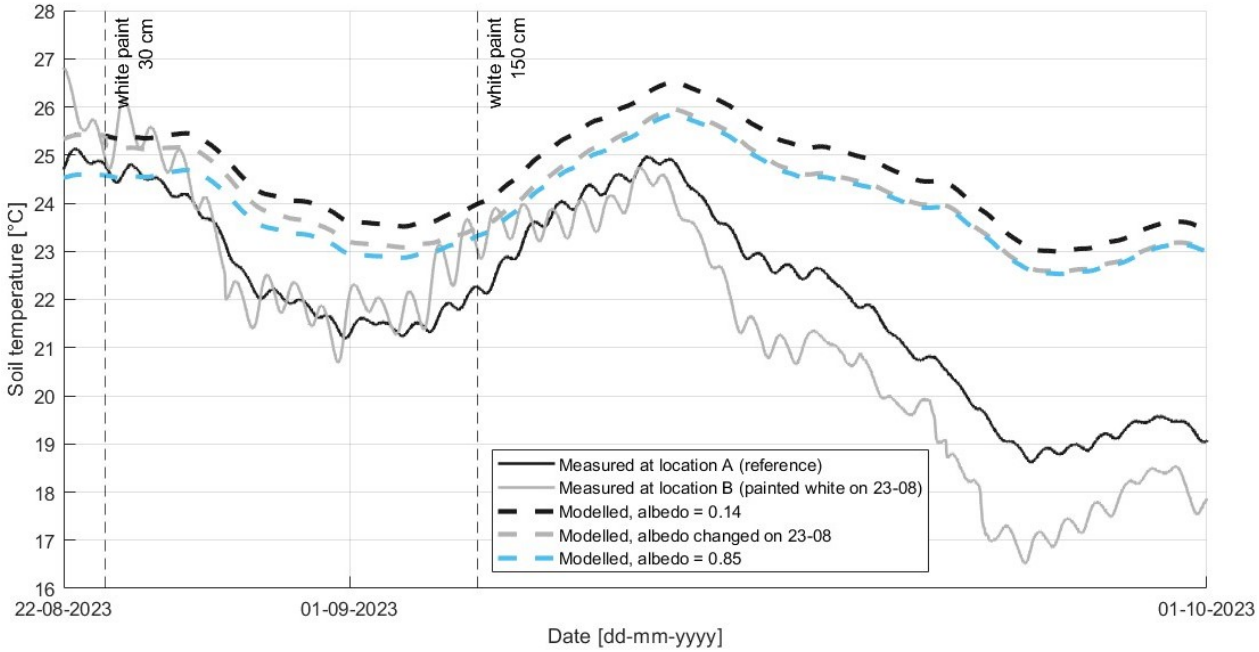

Figure 4.19.: The measured and modelled soil temperature at 0.7 m depth in TGV, where location B has been painted white. The modelled situation is provided for the urban scenario, with a_{SS}=0.14, a_{SS}=0.85, and for a change from 0.14 to 0.85 on August 23.

4.3. Summary of effect of measures

Table 4.12 summarizes the quantified effect on the soil temperature of the analysed measures. It presents the differences between the mean observed temperatures and between the maximum observed values for particular periods, as a result of the measure. This is relative to the soil temperature below a regular concrete tile, so the difference can be seen as gain in soil temperature reduction as a result of e.g. vegetation as top layer instead of concrete tiles. The difference between the maximum values is not the same as the maximum difference. The maximum differences can be larger on specific days, when one is at its maximum, and the other is not. Therefore, the table also provides the maximum observed difference (observed on a specific day). The maximum difference that can occur according to the model is also provided in the table (in italics).

Soil temperature / Measure	Period analysis (2023)	Depth	
		0.7 / 0.8 m	**1 m**
Concrete tiles – vegetation in sandy soil	Aug 1 – Oct 1 (A) Aug 1 – Aug 21 (B)		Difference in mean value: 1.8 (A) – 2.5 °C (B), avg A&B = 2.2 °C Difference in max value: 2.3 (A) – 3.5 °C (B), avg A&B = 2.9 °C Max difference on specific day: 2.7 °C on Sept 12 (A) & 3.4 °C on Aug 22 (B) *Model: max difference 0.8 °C*
Concrete tiles – vegetation in 40 cm roof substrate	Aug 1 – Oct 1 (A) Aug 1 – Aug 21 (B)		Difference in mean value: 0.4 (A) – 1.4 °C (B), avg A&B = 0.9 °C Difference in max value: 1.0 (A) – 2.4 °C (B), avg A&B = 1.7 °C Max difference on specific day: 1.4 °C on Sept 12 (A) & 2.4 °C on Aug 22 (B)
Concrete tiles no shade – permanent shade	May 1 – Oct 1 Aug 30 – Sept 17	Difference in mean value: 0.9 °C Difference in max value: 2.5 °C Max difference on specific day: 3 °C on Sept 12 *Model: max difference 1.3 °C*	Difference in mean value: 0.5 °C Difference in max value: 1.2 °C Max difference on specific day: 1.3 °C on Sept 12 *Model: max difference 1.2 °C*
Concrete tiles – temporary shade	Aug 14 – Aug 21 vs Aug 21 – Aug 23	At location B specifically: - Decrease in mean value: 0.5 °C - Decrease in max value: 1.5 °C Relative to A, total estimated effect: 2 °C	±0 °C
Concrete tiles – white paint	July 12 – Aug 21 Vs Aug 21 – Oct 1	At location B specifically: - Decrease in mean value: 3.8 °C - Decrease in max value: 4.5 °C Relative to A, total estimated effect: 4 °C *Model, total effect: 1 °C*	At location B specifically: - Decrease in mean value: 1.5 °C - Decrease in max value: 1.4 °C Relative to A, total estimated effect: 1 °C
Concrete tiles Depth 0.8 m – 1 m	May 1 – Oct 1	Difference in mean value: 0.1 (L5) – 1.0 °C (L2), avg L1,L2,L3,L5,L6 = 0.6 °C Difference in max value: 0.4 (L5) – 2.8 °C (L2), avg L1,L2,L3,L5,L6 = 1.6 °C Max difference on specific day: 2.9 °C at L2 on Sept 11 *Model max difference: 1.5 °C*	
Concrete tiles Depth 0.7 m – 1 m	July 12 – Aug 21	Difference in mean value: 1.1 (A) – 1.9 °C (B), avg A&B = 1.5 °C Difference in max value: 2.8 (A) – 5.4 °C (B), avg A&B = 4.1 °C Max difference on specific day: 4.3 °C at B on Aug 17 *Model max difference: 1.4 °C*	

Table 4.12.: Summary of the effect of measures. The colors indicate the analysed depth, with light yellow representing a depth of 0.7 m, and darker yellow representing a depth of 0.8 m. The table also provides the maximum effect predicted by the model.

5. Discussion and Recommendations

5.1. Discussion of measurements and Recommendations implementation measures

5.1.1. Ground coverage type: horizontal/vertical

As stated in Section 2.10, it remains unclear how far from the DWDS vegetation can have an influence. Although this was not the main focus of this thesis, the horizontal temperature profiles of the HeatSquare can offer first insights into the extent to which certain ground coverages influence soil temperature horizontally. The results showed that the effect of a ground coverage type mainly affects the soil temperature in vertical (in-depth) direction. However, the manual installation of the DTS cable did not result in a completely straight cable. This might have led to inexact determinations of the LAF at transitions to a different ground coverage type, affecting the interpretation of the horizontal temperature profiles.

The results confirm that the (type of) top layer affects the soil temperature. The observed soil temperatures below certain types of top layer align with the theory about functioning of modifications as described in Section 2.10.3, which are relying on the heat transfer as described in Appendices A and B. The soil temperature below dark pavement heats the most as expected, because of the low albedo. The soil temperature below vegetation is the lowest, as expected because of evapotranspiration and a higher albedo of green compared to other colors like black (Table 3.2). Other more remarkable magnitudes are the temperature below one of the plots of 'Vegetation in sandy soil' (the fourth one) and below 'Pavement, light' (the first one), in Figure 4.1 and 4.2. One would expect a cooling effect below 'Vegetation in sandy soil' because of the evapotranspiration of vegetation. However, the measurements below that top layer show rather high values. The reason for this might be that this plot of land is excavated regularly, because of maintenance to the innovation which is installed here. As visible in Figure 3.11, this repeatedly resulted in bare substrate at this location, thereby lowering the albedo and evapotranspiration. Either this or the presence of the innovation 'Urban Rainshell' in itself could be the reason for the higher soil temperature here. As rainwater is collected and treated within the system, it may undergo processes that generate heat. This heat can then transfer to the surrounding soil, causing an increase in soil temperature. The reason for the larger temperature drop below one plot 'Pavement, light', compared to the other plot with the same top layer type, can be contributed to the presence of picnic tables and also often a partytent at that location. The shade created by these objects is probably the reason for the drop in soil temperature, in line with the working principle of shade as described in Section 2.10.3.

Nevertheless, it is important to highlight that this measurement set-up does not result in identical soil temperatures each time below the same ground coverage type, as this was not the only variable parameter. So, the soil temperature was also influenced by other local conditions. Also, the length of a plot, and therefore of the cable below a certain ground coverage type, differs each time. When the plot is shorter, this gets more affected by the surrounding ground coverage types. This is also visual in the graphs: not all plots seem wide enough to reach the maximum or minimum soil temperature. The type of top layer on the surrounding plots also differ per plot, meaning that the boundary conditions are not equal, and this also affects the soil temperature. Additional factors influencing the measurements include calibration, which affects accuracy, and the possibility of issues with proper soil contact along the cable. In such instances, the measurements may not accurately reflect the actual soil temperature.

Still, the results show that the top layer significantly influences the soil temperature. Therefore, changing the top layer type or applying modifications the top layer can reduce the soil temperature, where the modifications can be based on the working principles as described in Section 2.10.3. So, installing the mains below darkly colored pavement should be avoided. Instead, a top layer with a high albedo, vegetation, or shade should be used. The top layer type can be changed on the already existing DWDS, by replacing the concrete tiles. Another possibility is applying modifications to the existing top layer. Also, the top layer can be installed simultaneously with the installation of new pipes. As the influence of the top layer mainly works in vertical direction, the top layer is recommended to be changed, installed, or modified directly on top op the distribution main.

5.1.2. Level of urbanization

The comparison between measurements within Rotterdam shows that locations within an urban area experience different soil temperatures, depending on local circumstances. Comparing these measurements to the measurements in TGV, show a contradiction with the expected SSUHI effect. As described in Section 2.3, the SSUHI expects the soil temperature in urban areas to be higher than in its surroundings, but the measurements in TGV (i.e. 'surroundings') show similar or even higher soil temperatures as/than in Rotterdam (i.e. 'urban'). This already indicates that simulating soil temperatures based on three types related to level of urbanization might not be desirable. Rather, the focus should be on other local influences such as the type the top layer. Section 5.2.1 elaborates on what this implies for the soil temperature model. The differences in soil temperature between locations is larger at more shallow depths. So, deeper pipes are less sensitive to local circumstances. This also means that possible (local) measures are less effective for pipes which are already located deeper. This aligns with what is described in Section 2.7.2: a deeper level means that the amplitude of diurnal variability is dampened in the soil. Larger depths typically correspond to a greater damping depth, which means that deeper layers are less influenced by external conditions.

5.1.3. Depth

The six measurement locations in Rotterdam show that the threshold of 25 °C was never exceeded at 1 m depth. The maximum soil temperature at this depth is 24.9 °C, measured at location L2. However, it must be kept in mind that location L4 Frederiksplein (with a broken sensor at 1 m depth) could have resulted in temperatures higher than 25 °C at this depth, because this location also shows the highest temperatures at 0.8 m depth, in Figure 4.3. Still, the mean and maximum measured soil temperatures at 0.8 and 1 m depth show that the soil temperature is lower at a deeper level. The results also show that the soil temperature is more sensitive to short time changes of weather conditions at 0.8 m depth than at 1 m depth, with peaks occurring earlier at 0.8 m depth. This aligns with what is described in Section 2.7.2: a deeper level means less dependency of short time weather changes, because the amplitude of diurnal variability is dampened in the soil, and a delay of peak values occurs. The results of measurements in TGV show the same: the mean and maximum soil temperature decrease at a deeper level, aligning with Figure 2.3 in Chapter 2.

Therefore, locating the mains at a deeper level in the sub-surface means that the pipes are surrounded by lower soil temperatures. During times with elevated air temperatures, the difference between locating at a shallower or deeper depth is even larger, making a deeper location even more beneficial. The measurements in TGV compared to Rotterdam indicate that the difference between 0.7 and 1 m is larger compared to between 0.8 and 1 m. Although this is based on

different analysed periods, this aligns with the fact that soil temperature decreases as depth increases. So, more temperature reduction can be gained when replacing pipes from 0.7 to 1 m depth, instead of relocating from 0.8 to 1 m depth. However, this does not matter much, as relocating existing pipelines to a greater depth is not necessarily recommended anyway, because this requires excavation of the soil and it disturbs the present infrastructure in the ground. In Rotterdam specifically, 1 of 18 digging movements results in damage to a pipeline (as described in Section 2.7.2). So, increasing the depth of all vulnerable pipelines will turn out to be expensive because of the need for excavation and the incidental damage to present infrastructure in the subsurface. Therefore, relocating the pipes to a deeper level can be done for short lengths, but it is primarily recommended when installing new pipes. The recommended depth of at least 1 m can be incorporated in the NEN7171, such that this minimal depth is secured for new construction in public areas.

5.1.4. Vegetation

The results show that the soil below vegetation in sandy soil is cooler than when the vegetation grows in roof substrate (even though sandy soil is initially warmer when considering bare soil without vegetation). This could mean that the type of substrate matters for the cooling effect of vegetation. However, another contributing factor to the difference is the type of vegetation. The species and their height differ in the substrates, as presented in Figure 3.3. Section 2.10.3 already addressed that height of vegetation matters for the soil temperature: for taller vegetation (50-90 cm), diurnal ground surface temperature and ground heat flux variations are smaller. This indicates that the air temperature fluctuations are more effectively dampened by thicker canopy, resulting in higher soil temperatures in the night, and lower temperatures during daytime. Although this diurnal fluctuation is not visible at 1 m depth, the height might contribute to the consistently lower soil temperatures at a deeper level. The creation of shade by higher plants also contributes to lower soil temperatures. Besides, their deeper roots which allow for more water uptake from a deeper soil level for evapotranspiration, also cools the soil. Therefore, proper statements about the type of substrate in which vegetation is most effective cannot be made based on these results.

Still, independent of the soil in which vegetation grows in, the results clearly indicate that vegetation cools the soil, as was expected based on the theory presented in Section 2.10.3. Thus, compared to concrete tiles, the soil temperature below vegetation is lower. So, reduction in soil temperature could be gained by replacing the existing concrete tiles above the DWDS with vegetation. During critical days (with elevated air temperatures), the difference in soil temperature between concrete tiles and vegetation is even larger, increasing the gain. The advantage of replacing concrete tiles with vegetation is that it does not require relocation of the pipes. However, given that all distribution mains in Rotterdam are currently at the vulnerable depth of 0.7 m, all below grey concrete tiles, this measure might still require lots of construction work, and possibly not all sidewalks at vulnerable locations can become vegetated due to practical considerations. Either way, it is also possible to install vegetation at the same time as installing new pipes. For installation of new pipes, the predetermined road layout, which localizes the drinking water pipes below the sidewalk, can be reconsidered. Meaning, the manual 'Handboek Beheer Ondergrond' (Manual Subsoil Management) could include a recommendation advising for installing distribution mains next to the sidewalk if vegetation is already present there. Besides the fact that vegetation cools the soil, it also has positive side effects for the area in which it is implemented. The livability of a city can be increased with more green spaces, because it positively affects air pollution and noise. And besides the fact that vegetation lowers temperatures in the soil, it also reduces the air temperature. Therefore, the UHI effect gets reduced, resulting in less heat stress and more human comfort.

5.1.5. Shade

Permanent shade

The results show that shade cools the soil, which could be expected based on the functioning of shade described in Section 2.10.3. The effect of shade, in cooling the soil at both depths, increases in times of elevated air temperatures. The cloud cover and solar radiation progression have also been analysed to provide a similar statement, but the relation between these aspects and increased difference in soil temperature between the two locations was less clear. Either way, this means that the effectiveness in reducing the soil temperature which could be gained by (re)locating pipes in the shade is even larger during critical warm periods. Relocating existing mains into the shade is not necessarily recommended, for the same reasons to avoid relocating existing pipes to a greater depth: to avoid excavation, disturbance to the existing underground infrastructure, and damage. Rather, the premise should be that new pipes are installed in permanent shade. Especially at a more shallow depth, shade is effective in cooling the soil. So, possibly, an even higher temperature reduction can be expected at 0.7 m depth caused by shade, than is now observed at 0.8 m depth. Therefore, especially when new pipes would still be installed at 0.7 m depth in the future, it is highly recommended to ensure that these pipes are at least installed in the shade. Creating permanent shade is something what needs to be considered in urban planning, as the shade creation depends on the lay-out and heights of buildings, and of the time of the year (position of the sun). These are factors which cannot be changed manually or short-term, so these aspects must be considered beforehand. Shade maps (like Figure 3.8) can help to show where shade occurs during different times in the year. This can show on which side of the road the distribution mains need to be installed to realise permanent presence of shade. This recommendation can be incorporated in the 'Handboek Beheer Ondergrond' (Manual Subsoil Management) of the municipality of Rotterdam. After this effort, the advantage of using permanent shade as measure is that is does not require frequent manual labor or other adjustments after installation of the mains.

Temporary shade

Temporarily creating shade cools the soil at 0.7 m depth, but to what extent cannot be conclusively determined. This is because the air temperature also decreased, and one-to-one comparison to reference location A was not performed because location A consistently had lower soil temperatures, also before any modifications were performed to location B. Proper statements about whether the measure could (eventually) be effective in lowering the soil temperature below 25 °C can also not be made, because shade was created for only two days. Besides the questionable effectiveness, the measure is accompanied by limitations. Using a partytent to create temporary shade demands regular displacement of the tent, such that the shade remains at the right place. This requires manual labor and it is not really efficient if everywhere in an urban area partytents need to be displaced. Taking these limitations into account, besides the fact that the reduction in soil temperature is not much, especially not at 1 m depth, this measure is not necessarily recommended. This does not detract from the possibility that temporary shade may have less limitations and is more effective when using other ways to create shade. There are also other objects which create temporary shade but do not require regular displacement. At the beginning of the summer or when a warm period is expected, for instance, modular urban trees can be deployed, or sidewalks can be covered by canopies.

Both results of the effect of shade, either permanent or temporary, show that shade has less effect on a deeper level. This aligns with the discussion in Section 5.1.2 stating that (local) measures are less effective for pipes which are already located deeper. Both results also show that shade causes

less daily fluctuation. This might be caused by the decreased incoming shortwave and outgoing longwave radiation due to shade, as discussed in Section 2.10.3.

5.1.6. White paint

The observed effect of white paint on concrete tiles also aligns with the discussion in Section 5.1.2 stating that (local) measures are less effective for pipes located at greater depths. The larger relative decrease in soil temperature at 0.7 m depth at location B specifically indicates that white paint is more effective in cooling the soil at this shallower depth compared to 1 m depth. While the results regarding the effect of shade had already confirmed this, the difference in effect of white paint between both depths may be even more pronounced, as this has potentially even led to lower soil temperatures at 0.7 m compared to 1 m depth (as shown in Figure 4.11). This trend was observed at location B starting from September 13, whereas normally one would expect higher soil temperatures at shallower depths. One possible contributing factor could be lower air temperatures during this period. However, at other locations which experience this same decrease in air temperature this does not cause a similar effect. This is illustrated in Figure F.5 for location L2 in Rotterdam, where the soil temperature at 1 m depth remains below that at 0.8 m depth even as air temperatures decrease approaching October. Therefore, the reduction in soil temperature at 0.7 m depth to values lower than at 1 m depth at location B suggests that the cooling effect of white paint is much more pronounced at the shallower depth of 0.7 m. Although a similar trend is observed at location A (almost a week later), it is worth noting that the temperature at 0.7 m at location A also rises above that at 1 m depth again before the end of the analysed period. Figure 4.6 also provides an insight into the effect of white paint at 1 m depth compared to vegetation as ground coverage at this depth. This figure shows that 'Concrete tiles - location B', so the white tiles, reduced to soil temperatures below 'Vegetation in 40 cm roof substrate', but 'Vegetation in sandy soil' remained approximately 1 °C cooler. So, white paint on concrete tiles might be most valuable for distribution mains at 0.7 m depth.

The soil temperature at 0.7 m depth has consistently remained below 25 °C just a few days after the tiles have been painted white, even with high air temperatures around 30 °C. So, the white coating is effective in reducing the soil temperature at this depth. However, this measure also has some downsides. White paint on concrete tiles goes against the standardized ground coverage types as stated in the manual 'Handboek Rotterdamse stijl'. The white surface disrupts the existing aesthetics of the urban area and could potentially be visually discomforting for individuals. Besides, when paint is used to whiten the tiles, this might cause a slippery road, especially when it rains and the coating gets wet or when it freezes. However, this risk can be reduced by adding anti-slip agents to the paint, or by manufacturing and using concrete tiles which are white colored instead of grey. Moreover, the maintenance of the white coating necessitates manual labor as regular cleaning is required to preserve its high albedo. When the high albedo is not maintained, the effectiveness of the measure reduces. Although some limitations can be conquered, implementing this measure will necessitate several adjustments to current practices, particularly the need for revision of the 'Handboek Rotterdamse Stijl'. Hence, while this measure may not be the primary option due to its limitations and need for revisions, it can prove useful in times of necessity. Given that all pipes in the city are currently at the vulnerable depth of 0.7 m, solutions that are effective at this depth and do not necessitate relocating all pipes or extensive construction work can be highly beneficial during times of need. Since this measure can be applied to the existing top layer, it can be easily applied without requiring much manual labor, making it feasible for short-term execution.

5.1.7. Summary Recommendations implementation measures

Among all analysed measures, changing concrete tiles to vegetation results in the most significant reduction in soil temperature based on the measurements (as presented in Table 4.12). This aligns with the study of Blokker and Pieterse-Quirijns (2012), which showed that changing the top layer to vegetation assures the most cooling of the soil temperature at 1 m depth, as discussed in Section 2.10.3. Given that green spaces in urban areas increase the livability of a city, this measure is preferred. Applying white paint to existing concrete tiles can be implemented promptly during urgent situations. This approach is particularly advantageous considering that all distribution mains are currently situated at a shallow depth of 0.7 m, making them susceptible to high soil temperatures. Figure 5.1 provides an impression of how this would appear. For new pipes, locating at at least 1 m depth and in the shade is highly recommended.

For all discussed measures, an integral approach is required before implementation. The situation affects the municipality and the drinking water companies, because they share a joint responsible. Drinking water companies are responsible for the quality, whereas the measures (determination of the depth and the location of the green areas) do not fall under their influence, so cooperation between both is crucial. Workshops with these parties, including research institutes like KWR and other relevant stakeholders, are recommended. In this way, by collaboration and exchanging knowledge, negative consequences as a result of high drinking water temperature can be prevented.

Figure 5.1.: An impression of white tiles on the existing concrete tiles on the sidewalk.

5.2. Discussion of simulations versus measurements and Recommendations improvement and use of soil temperature model

5.2.1. Progression simulation based on three urban types

The simulations compared to the measurements (Section 4.2.1: Prediction Level of urbanization (three urban types)) show that even for the locations in TGV, which could be expected to be a peri-urban location based on the definition, the peri-urban scenario underestimates the soil temperature. The urban or even the hot-spot scenario predicts the soil temperatures in TGV better. Only at the end of the analysed time frame, approaching October, the soil temperature at location A lowers to temperatures below the peri-urban type. However, this is probably not related to the fact that TGV is less urbanized. It could be caused by the widened white paint on the concrete

tiles at location B, which could possibly also influence the soil temperature at location A, as a top layer also influences the soil temperature in other directions than solely vertically. Remarkably, the model even simulates well that the soil temperature at 0.7 m depth in TGV location A reduces to values lower than at 1 m depth, when approaching October, and before the end of the analysed period is increases again above 1 m depth. This shows that the progression is well simulated, so the soil temperature model is considered to be suitable for predicting in which period (many) peaks in soil temperatures will occur. To function as prediction, this does require right climate predictions, to use as input. This prediction could help in planning of when measures should be applied, such that preparations for the implementation of the (temporary) measures can be executed in time.

Apart from the precise representation of the progression, the model could be improved to enable better estimations of the magnitude, and thus the effect of measures. Currently, the outcome of the simulation is mainly based on a differentiation in three urban types, regarding whether a location is situated in an urban area or in its surroundings (expressed via the input of the three urban types). Comparing measurements to the simulation of the three urban types shows that the daily fluctuation is best predicted by the hot-spot scenario. When considering the difference in input between the three urban types, the higher thermal conductivity could be the reason for this, because this soil thermal property facilitates faster heat transfer through the materials, resulting in quicker response to changes in weather conditions. Therefore, it is recommended to use a soil thermal conductivity of at least 2.6 W/m/K in all simulations with the soil temperature model, to properly reproduce the daily fluctuation. The results of the comparative analysis between measured and predicted (simulated) effects of depth, vegetation, and shade also allow for recommendations regarding other aspects that should carry more weight in the simulation.

5.2.2. Prediction Effect of measures

Prediction effect Depth

Which urban type simulates the magnitude of the soil temperature best, depends on the depth. For a more shallow depth (0.7 and 0.8 m), the hot-spot scenario can function as a upper limit or 'worst-case' scenario. At 1 m depth, the urban scenario estimates the soil temperature best. The fact that which urban type suits best is related to which depth one considers, already indicates that the differences in soil temperature between depths is underestimated by the model when considering one urban type. The simulations of soil temperatures at two depths confirm this. For a bigger difference between the depths, so 0.7 m versus 1 m depth, the model especially underpredicts the difference in soil temperature between the two depths. For a slighter difference, so 0.8 m versus 1 m depth, the model still underestimates, although less than for 0.7 m versus 1 m. Overall, the model underestimates the effectiveness in cooling of the soil of (re)locating pipes to a deeper level.

This suggests that it might be appropriate to differentiate input parameters based on depth. As discussed in Section 5.1.2, shallower depths are more sensitive to local circumstances. To reflect this in the simulation, the model could be set such that it uses different parameters up to a depth of 0.8 m. Local circumstances include heat sources. So, the input for anthropogenic heat (QF) could be set higher for the first 0.8 m, and the empirical coefficient a3 (which is used in the calculation of heat storage) could be a larger negative value. From 0.8 m depth onwards, heat sources influence the soil temperature less, so these values can be set lower (QF) or less negative (a3). In this way, the difference in soil temperatures between two depths increases, which is more realistic.

Prediction effect Top layer

Section 4.2.3 (Prediction Concrete tiles vs Vegetation) showed that the difference between vegetation and concrete tiles is expected to be less (by the model) than what was observed in reality at location A. The difference would be even larger if location B was chosen to represent concrete tiles instead of location A, because the soil temperature at this location is higher than at location A (Figure F.4). Also, the difference between the two top layer types is possibly even larger at 0.7 m depth, but no measurements were performed at this depth below vegetation. Still, the comparative analysis by using 1 m depth at location A already indicates that the model underpredicts the cooling effect of vegetation. Given the significant influence of the top layer on soil temperature, the soil temperature model should incorporate more differentiation related to the type of top layer. This means that infiltration, which is currently neglected in the model, should be included. As described in Appendix A, the decision to neglect infiltration in the current model is based on the assumption that urban drainage systems instantly remove excess water, preventing prolonged surface retention that could facilitate significant infiltration. Additionally, the presumed compaction of urban soil reduces its permeability, further restricting infiltration potential. In semi-paved areas, although drainage systems may still rapidly collect excess water, semi-paved surfaces could permit some infiltration depending on factors like surface porosity and compaction. Similarly, vegetated areas typically encourage greater infiltration compared to paved surfaces due to the presence of vegetation and organic matter, which can enhance soil porosity and permeability. Therefore, to give more weight to the type of top layer, infiltration should be considered. Infiltration affects the amount of water availability in the soil, subsequently impacting evapotranspiration and, consequently, the cooling effect. Currenlty, the available water at the surface is calculated for each time step (t), based on the storage level of the previous time step (Ci(t-1)) and the precipitation of the current time step (P(t)), see Equation B.29 in Appendix B. This equation could be changed to:

$$\begin{aligned}
&\text{If } E_p(t) < C_i(t-1) + P(t) - R_{\text{inf}}(t): \quad E_a(t) = E_p(t) \quad \text{and} \quad C_i(t) = C_i(t-1) + P(t) - E_p(t) - R_{\text{inf}}(t) \\
&\text{If } E_p(t) > C_i(t-1) + P(t) - R_{\text{inf}}(t): \quad E_a(t) = C_i(t-1) + P(t) - R_{\text{inf}}(t) \quad \text{and} \quad C_i(t) = 0
\end{aligned} \tag{5.1}$$

Also, hard-coded parameters related to ground coverage type could be made variable, or fragmented into more alternatives. This would allow for the representation of a wider range of top layer types. This accounts for the empirical coefficients a1, a2, and a3, which determine the calculated heat storage and thus the heating. The coefficient a3 currently depends on the urban type in the simulation, whereas it should depend on the ground coverage type (Table A.1 in Appendix A). The values a1 and a2 only distinguish between pavement or grass, but they could also be differentiated to represent more types of top layer. The same applies to the maximum storage capacity, Si, which currently only distinguishes between pavement and grass. Si eventually influences LvE, and therefore the cooling effect.

Prediction effect Shade

The fact that the model wrongly assumes a rather constant different in soil temperature between a location in the shade and not in the shade is most likely because the model overlooks the influence of cloud cover. Cloud cover uniformly creates shade across all locations, resulting in no differentiation between locations with or without shade. Currently, when shade is set to 0 (no shade), the model does not take into account that this has no impact when there is cloud cover everywhere, which blocks the solar radiation anyway. The measurements show that in reality, this cloud cover results in similar soil temperatures at both a location in the shade and not in

the shade. It is recommended to include the cloud cover, which is originally also present in the meteorological data of the KNMI, in the simulation. In the current soil temperature model, the cloud cover is stored, but nothing happens with it afterwards. This cloud cover must also set the boundary conditions and can then be used as conditional statement in Equation B.2 in Appendix B. The presence of shade or no shade should only be considered when there is no cloud cover everywhere. When there is cloud cover everywhere, shade falls on every location, so this situation is comparable to the situation of shade=1. The cloud cover is provided in eights in the weather data of the KNMI, where 9 means that the sky is invisible. So, a possible statement could be:

If cloudcover ≤ 8, then:

$$R_{global} = R_{solar} * (1 - shade) \tag{5.2}$$

If cloudcover > 8, then:

$$R_{global} = 0 \tag{5.3}$$

When considering all measures, the model predicts the effect of permanent shade to be the largest. The maximum difference that can occur at 1 m depth between a location in the shade and a location not in the shade is predicted to be 1.2 °C. This does not align with the measurements, which show that the maximum difference which can occur at 1 m depth is between vegetation and concrete tiles as ground coverage (see Table 4.12: 2.7 °C). The simulation of shade also indicates that the model does not predict much difference in effect of measures between two depths. Whereas in reality, the effect of measures reduces with depth.

5.2.3. Use of soil temperature model

Comparing the measurements to the simulations has indicated in which way the model can be improved. After changing aspects in the model based on these preliminary recommendations, the measurement data can be used to calibrate the model again, to more accurately decide on the set parameters (e.g. QF, a3). The improved model can be validated with measurements. New simulations with the improved soil temperature model can be made with the climate scenarios of KNMI as meteorological data input. This can provide better predictions of the magnitude of the problem in the future, such that responsible parties can participate properly and in time. Currently, most awareness is given to locations which can be assigned to be hot-spots. As the hot-spot scenario was found to generally overestimate the observed soil temperatures, the new simulations might result in a smaller number of expected exceedances in the future (compared to the numbers presented in Table 2.1). However, the same hazardous components, most importantly the hazardous concrete tiles as type of top layer and shallow depth, possibly apply at more locations (independent of how urbanized an area is), compared to the specific properties which would lead to assigning a location to be a hot-spot. This probably results in a bigger number of locations which can be classified as vulnerable locations for high soil temperatures and thus high drinking water temperatures. This increases the need for effective measures, in which the soil temperature model can also help. With more focus on the influence of the depth and top layer, it is possible to make better predictions of the temperature reduction which can be gained by particular measures, also of ones not considered in this thesis research. The more accurate predicted effectiveness of a measure helps in better decision-making about implementation of particular measures. The model can also help to predict how much time it takes to reach full effectiveness of a measure. For example, the simulation of white paint on tiles indicated a transition period of nearly a month to reach full effectiveness. Such prediction could help in deciding when to start implementing the measure, such that it functions as intended in time.

5.3. Limitations

In delineating the scope of this research, it is necessary to acknowledge certain limitations to the methodology that impact the generalizability of the findings. Remarks related to the interpretation of the results and strengths and limitations about possible measures were already addressed in the prior sections.

Related to the methodology, most measurement depths were prescribed before the research topic was determined. This led to installation of the DTS cable at 10/30 cm and 60 cm depth, and in Rotterdam the sensors were installed at 0.8 m depth. These depths differ from the depth of the distribution mains in Rotterdam specifically (0.7 m). Therefore, it was not possible to quantify the soil temperature at this relevant depth of the distribution mains in each analysis. However, expect for the DTS, most measurement locations did include the depth of 1 m, which is the general depth in the Netherlands and therefore relevant for analysis. Still, even when the depth is relevant to analyse, it must be kept in mind that the actual depth where measurements were collected might not be exactly similar to the depth mentioned in the analyses. This is because of the manual installation of the DTS cable and sensors, which is not as precise as desired. This means that the depth of the cable is not exactly 60 cm (at all locations) and the exact depths of the point temperature sensors might also differ from the desired 0.7 m or 1 m. So, it is possible that deviations from the intended depths could introduce bias into the measurements.

Also, when interpreting the results, it is important to note that the impact of soil moisture has not been explicitly examined, despite its significant role in determining soil thermal properties (Table 2.9.2). An increase in the moisture content of a sandy soil reduces the thermal diffusivity of the soil, resulting in slower heating. In the simulation, soil moisture was considered through input parameters for thermal properties. A fixed moisture level between 50% to 100% was assumed, as outlined in Section 2.9.2. Soil moisture was not factored into the comparison of soil temperatures between measurement locations, as the moisture content was not measured at most locations. Nevertheless, it is crucial to consider that variations in moisture content contribute to differences in soil temperature between two locations as it determines the thermal diffusivity. This remark is related to the generalizability of the findings. For instance, when comparing the soil temperature between a location with and without shade, disparities which are now attributed to shade in this thesis research might also be caused by differing moisture levels. However, given similar weather conditions between the locations which are compared, and typically a constant water table level in the summer (as described in Section 2.9.2), it is likely that soil moisture levels remained relatively consistent across locations, and therefore the conclusions about the effect of measures remain valid. Only for comparing vegetation in sandy soil with vegetation in roof substrate, the soil type obviously differs, of which roof substrate retains a lot of moisture (as described in Section 3.2.1). The sensor at 1 m depth indeed showed a higher moisture content in the plot with roof substrate. Still, the vegetation in sandy soil experienced lower soil temperatures, so it appears that water availability was not a limiting factor.

Apart from the moisture content, also other aspects vary locally, possibly causing heating or cooling of the soil. The differences in measured soil temperatures at location A and B below concrete tiles on the Hydrogen Square highlight the dependence on local circumstances. Location A and B are near each other, below the same ground coverage type, prone to the same weather conditions, but still location A exhibits consistently lower soil temperatures at both depths and less daily fluctuation at 0.7 m depth. This might be caused by the difference in soil moisture, which was explicitly addressed for location A and B in Section 3.2.2. Other causes for differences can be an imprecise installation, leading to a disparity in depth compared to the depth at another location, shade of the electricity boxes, the nearer presence of vegetation at location A, or a combination of factors. Either way, the disparities between location A and B underscore the highly localized variability of soil temperatures. This local variation is related to the interpretation of the results. As

even locations near each other can experience significant differences, the results of the measurements provide an insight, but do not necessarily apply in general. All measurement locations are prone to different local circumstances, complicating a one-to-one comparison between locations. For example, for the difference between vegetation and concrete tiles, the cooling effect of vegetation which is determined based on the measurements might also be partly dedicated to other local circumstances. For the analysis of permanent shade accounts the same: location L2 and L3 are both stationed at Hofplein, but presence of shade or no shade are not the only differences which may cause other soil temperatures. The soil type of both locations was assumed similar based on the one drilling profile representing L2 and L3 (Figure D.15), but in reality this soil type can vary locally as soils are heterogeneous. This would affect the heat transfer in the soil and can therefore also contribute to the difference in soil temperature between the two locations. The presence of anthropogenic heat sources also influences soil temperature. As mentioned in Section 2.7.2, the district heating system is situated below the road, so not below the sidewalk like the DWDS. However, since the sensors at the measurement locations in Rotterdam were installed for different purposes, they may be positioned closer to the district heat system than the distribution mains would.
In the simulation, this local variability can be excluded: in the simulation one can differ only one aspect, e.g. presence of shade by setting the input shade=1, while all other factors (parameters) remain the same. This must be kept in mind when interpreting the comparisons between the measured and modelled effect. Additionally with regard to the comparison between measurements and the simulation, the number of measurement locations was limited. For instance, none of the six locations in Rotterdam measured values as estimated with the hot-spot scenario, but this does not mean that there are no locations which experience these high temperatures, as the measurement locations were not risk-driven determined.

Lastly, there are limitations related to factors which cannot be influenced. Most importantly, the weather conditions. More warm days would have provided a larger data set with more useful data, as warm days raise vulnerability to high soil temperatures. It is relevant to analyse which soil temperatures occur during these instances and whether measures are (still) effective. However, a heat wave can be simulated, but not 'engineered'. Nevertheless, there were enough warm days during the analysis to allow for the formulation of recommendations. As weather is hard to predict, this also complicated the time planning. The modifications to the concrete tiles on the Hydrogen Square could have possibly be distributed more equally, such that creating temporary shade would have been possible for more days. However, choices had to be made and priorities were given to the white paint, after just 2 days of creation of shade. Still, this enabled to make statements about temporary creation of shade, which was complemented with the measurements of locations in Rotterdam to make statements about shade.

6. Conclusions and Future research suggestions

6.1. Conclusions

The research for this thesis has provided results to answer the following research question: *How do ground coverage types or modifications to ground coverage quantitatively influence soil temperature at the depth of distribution mains?*

This can be answered via three sub-questions:

1. What is the quantified soil temperature at 0.7 and 1 m depth, measured beneath various types of (modified) ground coverage?

The quantified (measured) effect of the analysed measures on soil temperature was summarized in Table 4.12. Overall, the measured effect of the measures align with the theory described in Section 2.10.3. The paved areas with a low albedo cause higher soil temperatures, whereas vegetation, a higher albedo, or shade result in lower soil temperatures. The soil temperature at a more shallow depth is more affected by local measures applied to the top layer. So, measures are less effective for pipes which are already located at a greater depth. However, also less temperature reduction is needed at a greater depth, as the soil temperatures are already lower there.

2. How do the measurements compare to the outcome of the soil temperature model, and how can the model be improved and used?

This question was answered by a comparative analysis between measurements and simulations of the general progression of soil temperature in time and the effect of measures. The progression is highly accurately simulated, so the simulated time of peaks align with when the peaks are measured. Therefore, the soil temperature model can be used in planning of when measures need to be prepared and implemented. However, the measurements demonstrated that the model underpredicts the effect of all considered measures. The maximum difference according to the model is also provided in Table 4.12. This shows that this is less for all measures compared to the maximum difference that can occur in reality. To enable better prediction of the effect of measures, the simulated magnitude can be improved by carrying more weight to other aspects, instead of primarily relying on categorizing locations into three urban types based on their level of urbanization, which currently determines the input of the model. Given that the measurements in Rotterdam and TGV show a contradiction with the expected SSUHI effect, and that the top layer has much influence on the soil temperature, this aims to put more weight to aspects related to the top layer, by differentiating parameters related to the top layer more and improving the effect of shade by including a conditional statement in the model. Related to the depth, a higher thermal conductivity and a differentiation in input parameters per depth might be suitable. The soil temperature model which includes these changes, should be calibrated again with the measurement data. The improved model can be validated with measurements and used for more accurate simulations. This can help to more accurately research the scope of the problem (i.e. expected number of exceedances in the future), to anticipate properly. Moreover, it can more accurately predict the effectiveness of all possible measures. This can contribute to more informed decision-making about implementation of particular measures.

3. Is modifying the ground coverage a feasible mitigation measure to prevent the temperature of drinking water from exceeding 25 °C?

The results of the measurements clearly confirm the influence of the (type of) top layer on the soil temperature at both considered depths. So, modifying the top layer can reduce the soil

temperature, and therefore potentially avoid exceedances of the 25 °C threshold in drinking water. Table 4.12 shows that changing concrete tiles to vegetation has the most gain in soil temperature reduction based on the measurements. Given that green spaces in urban areas also increase the livability of a city, this measure is preferred. The measure of applying white paint on existing concrete tiles can be implemented during times of urgency, particularly for distribution mains at 0.7 m depth.

The maximum differences (Table 4.12) are observed on days with elevated air temperatures. This also applies to different types of top layers: the discrepancies between various top layers increase during warm periods. This is favorable, as these are the days when cooling is most necessary, given that soils are most vulnerable to high soil and consequently drinking water temperatures during these periods. Via the top layer, measures do not disrupt the existing network in the sub-surface, which is valuable as pipelines are engineered with a lifespan of at least 50 years. By maintaining the network as it is, (costly) excavation, inconvenience for residents, and damage to the current underground infrastructure can be avoided. So, because it is effective, also during critical days, and because modifications to the top layer do not require relocation of pipes, modifying the top layer is considered a feasible measure to cool the soil. Changing, installing, or modifying the top layer should be done directly on top of the distribution main, as the horizontal temperature profiles showed that the top layer mainly influences the soil temperature in vertical (in-depth) direction. For new pipes, it is highly recommended to locate them at a depth of at least 1 m and in the shade.

In general, an integral approach is recommended to determine which measures must be implemented. This includes collaboration of the municipality and the drinking water companies, as well as research institutes. By cooperating, the most suitable and effective measures can be implemented, to secure provision of drinking water with high quality.

6.2. Suggestions for future research

There are much possibilities for future research regarding this topic. The ones which are most related to the research for this thesis, which could possibly function as a follow-up study, are addressed here. First of all, as the results also showed that the effect of a measure decreases with depth, it is possible that a single measure does not avoid heating of the soil sufficiently. So, especially if a distribution main is already situated at a depth of 1 m and still experiences significant heating, a single measure may prove insufficient to cool the soil. In such cases, a combination of measures may be necessary. Therefore, future research to the effect of combinations of measures is recommended, based on both measurements and modelling, as this thesis research already showed that they can differ significantly. Measurements of the effect of measures are recommended at 0.7 and 1 m depth, over a longer period of time, such that more weather conditions can be analysed (e.g. a heat wave). This enables to indicate whether the analysed measures have the potential to completely avoid exceedances of the 25 °C threshold, for a large variety in weather conditions.

To gain more knowledge about the effect of white paint, it would be interesting to research the effect on the soil temperature for different widths of white paint. When a smaller width is found to have a similar effectiveness, this reduces the influence on the existing aesthetic of the urban area and reduces the limitations associated with the white paint. Given that the top layer also affects the soil temperature in other directions than solely vertical, is recommended to set a reference location far from the tiles on which white paint is applied, such that the reference soil temperature is certainly not affected. It is also recommended to ensure that the soil temperature at both locations are similar prior to modifications to one of the two locations. This enables a proper insight into the absolute effect of the measure on the temperature, without bias.

Besides, it is recommended to study the effect of pavement watering, which is a way to slow

down the process of heating, in case the humidity is low. Therefore, this is a possible temporary measure, just as temporarily creating shade. It is also relevant to propose other temporary measures, as they can be useful for areas which do not experience heating often, so it might be undesirable or not cost-effective to implement a permanent solution. These temporary measures can be applied when soil temperature extremes are expected, based on the prediction of the soil temperature model.

To provide more insight into the effect of particular types of top layer, it is recommended to analyse the progression in time. Also, it is recommended to make equally sized plots with a certain ground coverage type, such that they are all equally influenced by their surroundings. The length of the plot must be long, such that there is no interfering of surrounding plots and their temperatures (influenced by their own top layer type). Then, eventually a rather steady temperature can be reached in the middle of the plot. Ideally, all plots exhibit the same boundary conditions, and other external conditions. It is also interesting to gain more insight in how much a top layer affects the surrounding soil temperature in lateral direction. To research this, the DTS technique is recommended due to its high spatial resolution, but the locations of the transition to another ground coverage type need to be determined more precisely than for this thesis research. This can be achieved by putting an ice pack on the DTS cable, resulting in a temperature drop, indicating the relevant LAF.

To properly interpret the risk of high soil temperatures, it would be valuable to gain more insight in the relation between soil temperature and drinking water temperature, as this eventually affects the drinking water quality. The water temperature model in the software application EPANET-MSX can be used. This water temperature model allows calculating the temperature at each location in the distribution network, assuming a constant soil temperature over 24 hours. The outcome of the predictions with the improved soil temperature model at the depth of a distribution main can be used as assumption of that constant soil temperature. Another possibility to relate the soil temperature to the drinking water temperature, is the use of DTS in the DWDS itself, which is already the aim of Evides to utilize in the near future, although for the purpose to detect leakages. Additionally, the soil temperature measurements can be extended with measurements at the drinking water taps which are connected to the analysed distribution mains. Both can show the temperatures which actually occur in the distribution mains and/or at the tap. This relation to the drinking water temperature, especially in case of risk-driven monitoring, can provide more insight into vulnerable areas. Similarities between these locations can help identifying the hazards, such that it is known where the risky areas are (to be expected), and measures can be implemented at the right locations.

While climate change in itself causes the problem of rising drinking water temperatures, climate change also causes transitions. One of these transitions is the energy transition. This will result in more (or larger) heat sources (district heating system, higher capacity electricity cables) in the sub-surface. It is important to research to what extent these heat sources influence the surrounding soil temperature. If the soil temperature increase due to the heat sources outweigh the temperature reduction caused by measures, more research is necessary to facilitate the formulation of recommendations regarding the minimum required distance between these heat sources and the DWDS. Another transition involves the adaptation of more water-saving innovations. It is interesting to analyse the effect of a decrease in drinking water demand, because this increases the residence times. Possibly, this can result in less effect of the proposed measures.

The additional knowledge acquired through these proposed research initiatives can contribute to emphasizing the urgency of the issue. Simultaneously, it can provide a more precise understanding of the effects of implementing (new) measures to reduce the temperature of drinking water, building on this thesis research.

List of references

C. Agudelo-Vera. Aanpak om de hotspots in het leidingnet terug te dringen. *KWR BTO 2018.024*, 2018.

C. Agudelo-Vera and M. Blokker. Climate change impact on the drinking water distribution network temperature. 2014.

C. Agudelo-Vera and M. Blokker. Finding (subsurface) anthropogenic heat sources that influence temperature in the drinking water distribution system. pages 1–9, 2016.

C. Agudelo-Vera and M. Blokker. Sub-surface urban heat island (ssuhi) - sources and effects on drinking water. pages 1–18, April 2017.

C. Agudelo-Vera, M. Blokker, P. van der Wielen, and B. Raterman. Drinking water temperature in future urban areas. *KWR BTO 2015.012*, pages 1–81, February 2015.

C. Agudelo-Vera, M. Blokker, de Kater H, and R. Lafort. Identifying (subsurface) anthropogenic heat sources that influence temperature in the drinking water distribution system. *Drinking Water Engineering and Science*, 10:83–91, 2017. doi: https://doi.org/10.5194/dwes-10-83-2017.

C. Agudelo-Vera, M. Blokker, and C. Quintiliani. Maatregelen tegen ongewenste opwarming van het drinkwater in het leidingnet. *KWR BTO 2020.015*, 2020.

V.F. Bense, T. Read, and A. Verhoef. Using distributed temperature sensing to monitor field scale dynamics of ground surface temperature and related substrate heat flux. *Agricultural and Forest Meteorology*, 220:207–215, 2016. ISSN 0168-1923. doi: https://doi.org/10.1016/j.agrformet.2016.01.138. URL `https://www.sciencedirect.com/science/article/pii/S0168192316301496`.

J. Bessembinder, R. Bintanja, R. van Dorland, C. Homan, B. Overbeek, F. Selten, and P. Siegmund. Knmi'23 - klimaatscenario's voor nederland. pages 1–64, 2023.

M. Blokker and I. Pieterse-Quirijns. Model voor de berekening van de watertemperatuur in het leidingnet. *H2O*, 23:46–49, 2010.

M. Blokker and I. Pieterse-Quirijns. Scenariostudies voor beperken invloed klimaatveranderingen op temperatuur en kwaliteit drinkwater in het net. *KWR BTO 2012.017*, 2012.

M. Blokker and I. Pieterse-Quirijns. Modeling temperature in the drinking water distribution system. *American Water Works Association*, pages 19–28, 2013. doi: http://dx.doi.org/10.5942/jawwa.2013.105.0011.

M. Blokker, P. Horst, A. Moerman, S. Mol, and R. Wennekes. Haalbaarheid van maatregelen tegen ongewenste opwarming van drinkwater in het leidingnet. *KWR 2014.057*, 2014.

M. Blokker, A. Moerman, and C. Agudelo-Vera. Drinkwatertemperatuur, bedreigingen en kansen. *TVVL Magazine*, 2017.

Centraal Bureau voor de Statistiek. Inwoners per gemeente, 2023. URL `https://www.cbs.nl/nl-nl/visualisaties/dashboard-bevolking/regionaal/inwoners`. (accessed: 07.09.2023).

S. Chapman, J. Watson, A. Salazar, M. Thatcher, and C. McAlpine. The impact of urbanization and climate change on urban temperatures: a systematic review. *Landscape Ecol*, 32:1921–1935, 2017. doi: DOI10.1007/s10980-017-0561-4.

B. des Tombe, B. Schilperoort, and M. Bakker. Estimation of temperature and associated uncertainty from fiber-optic raman-spectrum distributed temperature sensing. *Sensors*, 20(8), 2020. ISSN 1424-8220. doi: 10.3390/s20082235. URL https://www.mdpi.com/1424-8220/20/8/2235.

Gemeente Rotterdam. Standaard wegindelingen k & l, 2009. URL https://archief12.archiefweb.eu/archives/archiefweb/20221125210917/http://www.rotterdam.nl/apps/rotterdam.nl/wonen-leven/leidingenbureau/Bijlage-I-Standaard-wegindelingen-KL.pdf. (accessed: 01.06.2023).

Gemeente Rotterdam. Rotterdamse stijl - handboek openbare ruimte - toolkit. 2020.

Gemeente Rotterdam. Handboek beheer ondergrond rotterdam 2022. pages 1–93, 2022.

Gemeente Rotterdam. Boorprofielen dossiernummers 2013-0020, mvf21109, mvf16231, 2015-0132, and ib-2019-0188. 2023.

P. Gentine, D. Entekhabi, and B. Heusinkveld. Systematic errors in ground heat flux estimation and their correction. *Water Resources Research*, 48:9541–, September 2012. doi: 10.1029/2010WR010203.

C. Grimmond and T. Oke. An evapotranspiration-interception model for urban areas. *Water Resources Research*, pages 1739–1755, July 1991. doi: 10.1029/91WR00557.

Inspectie Leefomgeving en Transport. Drinkwaterkwaliteit 2021. pages 1–42, November 2022.

A. Klein Tank, J. Beersma, J. Bessembinder, B. van den Hurk, and G. Lenderink. Knmi '14 climate scenarios for the netherlands. pages 1–34, 2015.

L. Klok, S. Zwart, H. Verhagen, and E. Mauri. The surface heat island of rotterdam and its relationship with urban surface characteristics. *Resources, Conservation and Recycling*, 64:23–29, 2012.

KNMI. Klimaatviewer, 2023a. URL https://www.knmi.nl/klimaat-viewer. (accessed: 12.09.2023).

KNMI. Uurwaarnemingen weerstations, 2023b. URL https://www.daggegevens.knmi.nl/klimatologie/uurgegevens. (accessed: 06.09.2023).

H. Lee, K. Calvin, D. Dasgupta, G. Krinner, A. Mukherji, P. Thorne, ..., and Z. Zommers. Synthesis report of the ipcc sixth assessment report (ar6): Longer report. *Intergovernmental Panel on Climate Change, Climate Change 2023*, pages 1–85, 2022.

Y. Mao. Changing patterns of thermal behaviour of concrete pavements in diurnal periods. pages 1–15, September 2022.

M. Meerkerk and R. Beuken. Richtlijn drinkwaterleidingen buiten gebouwen: ontwerp, aanleg en beheer (gebaseerd op nen-en 805:2000). PCD 3:2020, October 2020.

G. Mihalakakou. On estimating soil surface temperature profiles. *Energy and Buildings*, 34:251–259, March 2002. doi: 10.1016/S0378-7788(01)00089-5.

NEN. Normcommissie - ordening van ondergrondse netwerken, 2023. URL https://www.nen.nl/normcommissie-ordening-van-ondergrondse-netwerken. (accessed: 02.08.2023).

P. Oguntunde, A. Ajayi, and N. van de Giesen. Tillage and surface moisture effects on bare-soil albedo of a tropical loamy sand. *Soil & Tillage Research - SOIL TILL RES*, 85:107–114, January 2006. doi: 10.1016/j.still.2004.12.009.

T. Oke. The distinction between canopy and boundary-layer urban heat islands. *Atmosphere*, 14 (4):268–277, 1976. doi: 10.1080/00046973.1976.9648422.

T. R. Oke. The energetic basis of the urban heat island. *Quarterly Journal of the Royal Meteorological Society*, 108(455):1–24, 1982. doi: https://doi.org/10.1002/qj.49710845502.

Overheid Lokale wet- en regelgeving. Handboek kabels en leidingen 2018, n.d. URL `https://lokaleregelgeving.overheid.nl/CVDR625666#d3305593e37`. (accessed: 01.06.2023).

Overheid Wettenbank. Drinkwaterregeling, 2023. URL `https://wetten.overheid.nl/BWBR0030152/2022-12-21#Bijlage3`. (accessed: 07.04.2023).

J. Selker, L. Thevenaz, H. Huwald, A. Mallet, W. Luxemburg, N. van de Giesen, M. Stejskal, J. Zeman, M. Westhoff, and M. Parlange. Distributed fiber-optic temperature sensing for hydrologic systems. *Water Resources Research*, 42:1–8, 2006. doi: doi:10.1029/2006WR005326.

E. Stache, B. Schilperoort, M. Ottelé, and H. Jonkers. Comparative analysis in thermal behaviour of common urban building materials and vegetation and consequences for urban heat island effect. *Building and Environment*, 213:108489, 2022. ISSN 0360-1323. doi: https://doi.org/10.1016/j.buildenv.2021.108489.

I.D. Stewart and T. Oke. Local climate zones for urban temperature studies. *Bulletin of the American Meteorological Society*, 93:1879–1900, December 2012. doi: 10.1175/BAMS-D-11-00019.1.

The World Bank. Urban population (% of total population) - netherlands, 2022. URL `https://data.worldbank.org/indicator/SP.URB.TOTL.IN.ZS?end=2022&locations=NL&start=1960&view=chart`. (accessed: 21.02.2024).

J. Uber and J. Boxall. Multi-species network water quality modeling: Current examples, future potential, and research needs. *Proceedings of the Tenth International Conference on Computing and Control for the Water Industry*, 2010.

United Nations. 64/292. the human right to water and sanitation, 2010. URL `https://documents.un.org/doc/undoc/gen/n09/479/35/pdf/n0947935.pdf?token=bwNZb967AahbpOwPU6&fe=true`.

D. Van der Kooij, B. Wullings, and P. van der Wielen. Invloed van temperatuurstijging op nagroei van micro-organismen in het leidingnet. 2009.

M. Van der Molen, I. Pieterse-Quirijns, A. Donocik, and E. Smulders. Eigenschappen bodem en oppervlak beïnvloeden temperatuurstijging rond drinkwaterleidingen. *H2O*, 7:33–35, 2009.

P. Van der Wielen. Invloed van temperatuur op groei van opportunistische ziekteverwekkers in drinkwater. *KWR BTO 2020.036*, pages 1–39, July 2020.

J. Van Vossen, S. Stofberg, and C. Agudelo-Vera. Effectiviteit maatregelen tegen opwarming drinkwater in leidingen. *KWR BTO 2019.080*, pages 1–70, November 2019.

J. Versteegh and H. Dik. De kwaliteit van het drinkwater in nederland, in 2006. pages 1–48, 2007.

World Health Organization. Guidelines for drinking-water quality. pages 1–583, 2022.

A. The functioning of the soil temperature model

General operation and energy balances

The soil temperature model was developed by KWR and Dutch water companies and it runs on MATLAB®. It is defined in MATLAB® as USVAT: Urban Soil Vegetation Atmosphere Temperature Model. The soil temperature model includes different influences on the soil temperature, including the meteorological conditions, the environment (rural versus urban), soil type, land cover, and level of urbanization. Van der Molen et al. (2009) first developed a micrometeorology model, which was slightly adapted and used by Blokker and Pieterse-Quirijns (2013). This model of Blokker and Pieterse-Quirijns (2013) enabled prediction of the soil temperature at various depths. It considered weather and environmental conditions, but it solely simulated soil without vegetation, therefore it neglected evapotranspiration. Moreover, anthropogenic heat emissions and the heat storage capacities of the buildings were not taken into account in the model. However, this model forms the base for the simulation of the soil temperature in later studies. Agudelo-Vera et al. (2015) extended the existing soil temperature model by including the three lacking aspects: the urban evapotranspiration, anthropogenic heat emissions, and the heat storage capacities of the buildings. To include these processes, literature values reported by Stewart and Oke (2012) were used.

The soil temperature model considers four layers:

- the atmosphere (atm)
- the Roughness Layer (RL)
- the Soil Surface (SS)
- the soil

Figure A.1 provides a visualisation of the model, containing the four layers. The Roughness Layer represents the layer between the atmosphere. For built-up areas, the height of the Roughness Layer depends on the spatial distribution and heights of buildings. The Soil Surface represents the layer where air properties can be changed by, for example, vegetation or buildings (Blokker and Pieterse-Quirijns, 2013).

The model calculates the heat transfer between the atmosphere and through the soil. Two energy balances are used to describe this heat transfer: the energy balance in the Roughness Layer and in the Soil Surface. The energy balances describe how the net radiation received at the land surface, Rnet, is distributed between evapotranspiration (latent heat flux, LvE), sensible heat flux (H), and substrate heat flux (Gsub) (i.e. soil heat flux). Between the atmosphere and the Roughness Layer and between the Roughness Layer and the Soil Surface energy is transferred by convection. The energy between the Soil Surface and the soil and further through the soil is transferred by conduction.

Heat transfer in Roughness Layer

The heat transfer in the Roughness Layer is driven by two sensible heat fluxes (H): between the Roughness Layer and the atmosphere (RL $\rightarrow$ atm), and between the Soil Surface and the Roughness Layer (SS $\rightarrow$ RL). The total heat transfer between the Soil Surface and the atmosphere is described by equation A.1, which is similar as in the original soil temperature model of 2013.

$$\rho \cdot C_p \cdot h_{RL} \cdot \frac{dT_{RL}}{dt} = H_{SS \rightarrow RL} - H_{RL \rightarrow atm} = \rho \cdot C_p \cdot \frac{T_{SS} - T_{RL}}{R_g} + \rho \cdot C_p \cdot u_* \cdot T_* \tag{A.1}$$

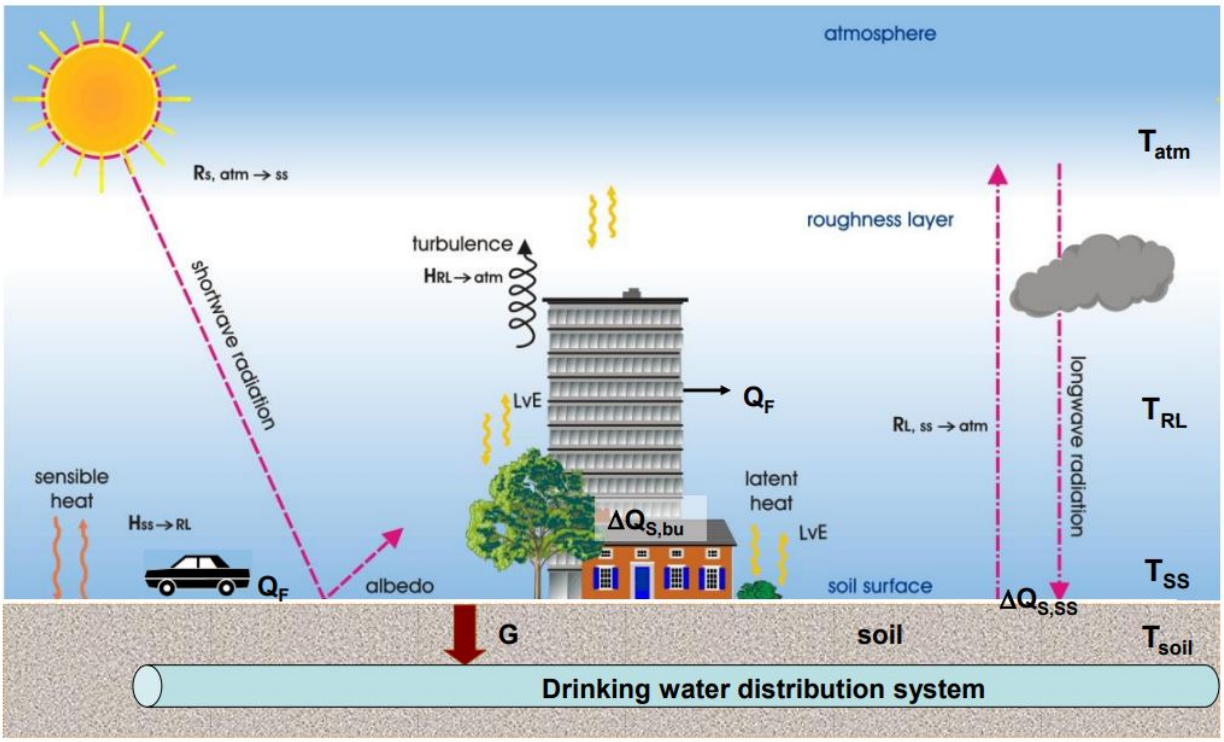

Figure A.1.: Schematic heat transfer in a urban setting (Agudelo-Vera et al., 2015).

When equation A.1 is rewritten, the temperature in the Roughness Layer (T_{RL}) can be solved numerically via equation A.2. This results in equation B.30 in Appendix B.

$$h_{RL} \cdot \frac{dT_{RL}}{dt} = \frac{T_{SS} - T_{RL}}{R_g} + C_D \cdot u \cdot (T_{atm} - T_{RL}) \cdot f_h \tag{A.2}$$

Heat transfer at Soil Surface

The heat transfer at the Soil Surface in an urban area of the original version of 2013 was complemented with anthropogenic heat (QF) emissions and heat storage (dQs) in the extended version of 2015. The heat transfer is driven by the parameters in the right-hand side of equation A.3.

$$\rho_{\text{soil}} \cdot C_{p,\text{soil}} \cdot \frac{dT_{\text{soil}}}{dt} = \frac{d}{dz_{\text{soil}}} \left(R_{\text{net}} + Q_F - H_{\text{SS}\rightarrow\text{RL}} - dQ_S - LvE\right) \Big|_{z=0} + \frac{d}{dz_{\text{soil}}} G \tag{A.3}$$

Explanations about the parameters in this equation are provided in Appendix B, of which Rnet, the net radiation, is also visualised with the pink arrows in Figure A.1. This net radiation is the sum of incoming shortwave and incoming and outgoing longwave radiation. The sun emits shortwave radiation towards the surface. The net shortwave radiation which is absorbed by the land surface depends on the albedo. The albedo is defined as the ratio of reflected to incoming radiation at a surface, over all the wavelengths of solar irradiation. The albedo of a surface determines how much radiation is reflected. When the surface is light (e.g. white), the albedo is higher, so more radiation is reflected. On the other hand, dark materials have a low albedo (Stache et al., 2022). Besides dark materials, urban areas ('rough areas') are also known to have a smaller albedo. This is due to multiple reflections between vertical and horizontal facets. These facets determine the canyon aspect ratio, which is the ratio of the canyon height to canyon width, so the height of the surrounding buildings along the street divided by the width of the street. Urban albedo declines with increased canyon aspect ratio (Agudelo-Vera et al., 2015). However, the model does not include this effect of canyon in the model.

The amount of longwave radiation reaching the Soil Surface depends on the cloud cover and atmospheric composition (greenhouse gasses). When looking from the perspective of the Soil Surface, it is both an incoming flux and an outgoing flux. The incoming flux depends on the emissivity of the surface and the atmospheric temperature. The outgoing longwave radiation depends on the surface temperature of the ground.

In summary, Rnet is the incoming shortwave radiation of the sun, which is adjusted by the albedo, plus the longwave radiation from the atmosphere to the soil surface minus the longwave radiation from the soil surface to the atmosphere.

Urban evapotranspiration

The level of urban development, expressed via the land cover in specific, determines the urban evapotranspiration, which is a combination of both transpiration and evaporation. It is the transformation from water to water vapor into the atmosphere. When this process occurs at the water/surface-air or soil-air interface, it is called evaporation. It is called transpiration when the process of vaporization of water happens at the surface of plants. For simplification, both processes of transpiration and evaporation are combined into evapotranspiration, which is used in this thesis as well, representing the total flux of water vapor into the atmosphere. The phase change of liquid water to water vapor (as long as there is sufficient water available) requires energy, where latent heat is produced (Stache et al., 2022). This leaves less energy available for the soil, so this process has a cooling effect on the soil.

In the soil temperature model, the potential evapotranspiration (ET_{pot}) is assumed as reference evapotranspiration, which can be calculated with the adapted Penman-Monteith method for urban areas (Grimmond and Oke, 1991). This method is more elaborated in Appendix B.

Evapotranspiration requires water, depending on factors such as infiltration. Infiltration (I) refers to the process of water passing through the ground surface into the pores of the soil, and entering the groundwater system. In the soil temperature model, infiltration is neglected for the calculation of evapotranspiration. This is based on the assumption that in urban areas the drainage system will collect the excess water instantly, and also and due to increasing compaction of the urban soil which is less permeable.

Heat storage

The heat storage flux (dQs) defines the net absorption and release of energy by sensible heat changes of all surfaces and objects. In an urban system, this storage heat flux is considerably larger than in rural areas. This is attributed to the greater effective mass contributing to the diurnal thermal storage, stemming from the increased roughness of the city and the larger heat transfer surface area resulting from the geometry of buildings. So in urban areas, more of the soil (in depth) contributes to the diurnal energy balance (Agudelo-Vera et al., 2015). The size of the storage heat flux depends on the surface material. The ground coverage type determines the empirical coefficients a1, a2, and a3, which are used to calculate the heat storage. Literature values of these empirical coefficients for different surface covers are presented in Table A.1. This table shows a big range for the coefficients. The coefficients which are eventually used in the model are presented in Appendix C, as a result of calibration for Rotterdam in the summer. In the simulation, the values a1 and a2 depend on the ground coverage type (grass or pavement), and the coefficient a3 depends on the urban type. These urban types and their related parameters are presented in Section 2.9.3. The equation for the heat storage is presented in Appendix B, equation B.24.

Table A.1.: Literature values of the coefficients to determine heat storage (Agudelo-Vera et al., 2015).

Surface cover	a1	a2 [h]	- a3 [W/m^2]
Grass	0.32	0.54	27.4
Rooftop	0.17-0.82	0.10-0.57	17.0-55.7
Concrete	0.81-0.85	0.32-0.48	28.5-79.9
Asphalt	0.36-0.82	0.23-0.68	19.3-150.0

Anthropogenic heat emissions

Anthropogenic heat (QF) is heat that is related to human activities, including waste heat from heating and cooling of buildings, transportation, manufacturing, lighting, and metabolism of humans and animals. By conduction, convection, and radiation, these sources heat the atmosphere. The contribution of QF to the urban energy balance is largely a function of latitude and season of the year (Agudelo-Vera et al., 2017). There are several methods for determining anthropogenic heat. A study by TNO has found an average anthropogenic heat for Rotterdam during the summer of 53.9 W/m^2. The contributions of considered sources are visible in Table A.2.

Table A.2.: Reported average anthropogenic heat for Rotterdam during the summer, assessed by TNO (Agudelo-Vera et al., 2015).

Source	[W/m^2]
Large sources	48
S&ME's	0.3
Traffic	3.2
Body	0.2
Cooking	0.5
Electrical appliances	0.5
Lighting	0.4
Air conditioning	0.8
Total	**53.9**

Another way to determine the anthropogenic heat is by considering the Local Climate Zone (LCZ). A set of zones were developed by Stewart and Oke (2012), to standardize description of surface structure and cover because cities present a separate micro-climate that can modify precipitation and wind patterns. The typology of urban zones ease the determination of parameters for the model, in this case of anthropogenic heat. For Rotterdam, LCZ=2-3, so between compact midrise (2) and compact low-rise (3). This means QF can be assumed to be smaller than 75 W/m^2 (Agudelo-Vera et al., 2015). However, it must be noted that this applies to the average of the entire city. When one would consider a smaller scale, in different areas of the city, a different LCZ could be assigned to each specific area, leading to different parameters.

The LCZ also determines the Sky View Factor (SVF) which is defined as the fraction of the visible sky from the total possible sky hemisphere at a certain location. SVF is not considered, although this is a determining factor for the local climate since it affects wind directions and reflection of radiation, which influences soil temperature. At micro scale it is therefore important to consider the SVF in the energy balance. At larger scales, at neighbourhood or city level, SVF might be considered to be less relevant, because of the variation of geometry of buildings (Agudelo-Vera et al., 2015).

Although anthropogenic heat shows annual and diurnal patterns, the heat is added as a constant value in the model due to a lack of detailed information. As shown in this section, the value for anthropogenic heat depends on the method of defining it. The values which are eventually used in the model are a result of calibration and depend on the urban type (peri-urban/ urban/ hot-spot). The values are presented in Section 2.9.3.

Advection

Some assumptions of the model were already mentioned: infiltration is neglected, and the Sky View Factor (SVF) and the effect of canyon on the albedo are not taken into account. The model also neglects advection. The process of advection results from spatial differences of surface characteristics, for example in surface temperature or roughness. It is a process on long time and spatial scales, and it is atmospherically driven. The setting of the city, such as whether it is located along the coast or in a valley, influences the extent and direction of these interactions on a larger scale than the city itself. Meanwhile, within the city, the uneven distribution of urban surfaces, whether at the property or neighborhood level, impacts the horizontal exchange of energy and the mixing. Agudelo-Vera et al. (2015) explain that the horizontal advection is negligible in urban energy balance calculations, supported by small values measured in a city next to the sea with a sea breeze. Since the surface temperature is mostly determined by local processes, the larger scale process of advection, which mainly influences the atmosphere, is considered to be irrelevant for the surface temperature and therefore the model does not take advection into account.

B. Equations of the soil temperature model in MATLAB®

The soil temperature model includes the surface types ground (pavement) or green (grass). The fraction of surface types in the modelled area depends on whether the parameter 'grass' is set 0 or 1. When grass=0, the area is 100 % pavement. When grass=1, the area is assumed to be 100 % grass. These surface types determine the maximum storage capacity (Si). The maximum storage capacity is set at 0.48 for ground (pavement), and 1.0 for green (grass).

The anthropogenic heat (QF) is taken into account in the model as a constant value, based on literature values as addressed in Section A and Table A.2. Each urban type (peri-urban/ urban/ hot-spot) has its own value for anthropogenic heat as a result of the calibration, which are presented in Section 2.9.3. The anthropogenic heat is an input value and it is not transformed in the code. It is solely used in the formulas for evaporation and the change of soil temperature. Both of these formulas are presented later in this section.

The model takes a time step of 60 seconds (dt). Then, the model considers the soil layers. It is modelled as a grid of depths from -5.5 to 0 meter with spacing of 0.05 meter.

The first equation in the model calculates the drag coefficient. The drag coefficient refers to the change of temperature and velocity of air resulting from existing trees and buildings. It can later be used to calculate the friction velocity and friction temperature. It is a constant value which can be calculated with the equation:

$$C_D = \frac{\kappa^2}{(\ln(z/zo))^2} \tag{B.1}$$

The boundary conditions are set by the meteorological data. The boundary conditions include the date, solar radiation [W/m^2], wind direction [degrees], average wind speed [m/s], temperature (from weather data file (e.g. KNMI) + 273.15, so in [K]), and precipitation [mm]. The precipitation is later transformed to [mm/min] (Rain_time) instead of [mm/h]. These boundary conditions are interpolated to get boundary conditions for each time step. The RL temperature is set equal to the atmosphere temperature.

To calculate the incoming longwave radiation, the emissivity has to be known. To calculate e_{eff}, the model uses a beta distribution with shape paremeters of alpha=14.8616 and beta=1.6411, by using the function 'e_eff_from_betarnd.mat'. The condition is that $e > 0.7$, so the coding ensures that all elements in e_{eff} are equal or above 0.7. This is because the emissivity varies between 0.7 for clear skies and 1 for overcast skies (Blokker and Pieterse-Quirijns, 2013).

Then, the rest of the code calculates the latent heat for vaporization (LvE) per surface type (i), the water storage in each surface type (Ci), the latent heat for vaporization for the total area (LvET), the net radiation (Rnet), the potential evapotranspiration (Ep), and the actual evapotranspiration (Ea). All these parameters are pre-allocated at 0.

To calculate the storage in the surface, there are several variables of interest. These are empirical values, dependent on the surface type. The values for a_1 and a_2 are provided in Appendix C, and a_3 is input of the model, depending on the urban type of which the values are presented in Section 2.9.3. These values differ from the literature values presented in Figure A.1, but are the result of the calibration.

In case of shade [0/0.5/1], the solar radiation is adjusted, because not everything is direct shortwave radiation when there is presence of shade. The (interpolated) solar radiation of the meteorological data file is then multiplied by (1-shade).

$$R_{global} = R_{solar} * (1 - shade) \tag{B.2}$$

This adjusted radiation (=R_{global}, so including consideration of shade), is used to calculate the shortwave radiation. The shortwave radiation, from atmosphere to the soil, is affected by the angle at which it hits the surface of the earth. Since the Netherlands is a flat country, the incoming short-wave radiation is equal to the solar radiation which is measured by the weather station (and adjusted by shade). The albedo of the surface determines how much of this R_{global} is reflected as shortwave radiation. So, Rs is given by:

$$R_{shortwave} = R_{global} * (1 - a_{SS}) \tag{B.3}$$

The longwave radiation can be calculated by using the already calculated e_{eff}:

$$R_{longwave} = e_{eff} * \sigma * T_{atm}^4 \tag{B.4}$$

In this equation, T_{atm} is the interpolated boundary condition, taken from the meteorological data file.

The emitted longwave components from the soil to the atmosphere depend on the surface temperature of the soil (T_{SS}) and is given by:

$$R_{longwave} = \sigma * T_{SS}^4 \tag{B.5}$$

Then, the model parameterizes the surface layer. First, Richardson's bulk number (R_{ib}) is calculated. This is a dimensionless number, which determines whether convection is free or forced (Blokker and Pieterse-Quirijns, 2013).

$$R_{ib} = \frac{g \cdot z}{0.5 \cdot (T_{\text{atm}} + T_{\text{RL}})} \cdot \frac{T_{\text{atm}} - T_{\text{RL}}}{u^2} \tag{B.6}$$

Richardson's bulk number indicates the stability of the atmosphere and the surface layer. The stability of the atmosphere depends on the temperature gradient: if $T_{RL} >= T_{atm}$, then $R_{ib} < 0$. This means that the atmosphere is considered unstable. If $T_{RL} < T_{atm}$: $R_{ib} > 0$ and the atmosphere is considered stable. The calculation of f_m and f_h depend on this stability, as can be seen in equations B.7 and B.8.

$$\text{if } T_{RL} \geq T_{\text{atm}}: \quad \begin{aligned} f_m &= 1 - \frac{10 \cdot \text{Ri}_b}{1 + 75 \cdot C_D \cdot \sqrt{\frac{z}{z_o}} \cdot \sqrt{|\text{Ri}_b|}} \\ f_h &= 1 - \frac{15 \cdot \text{Ri}_b}{1 + 75 \cdot C_D \cdot \sqrt{\frac{z}{z_o}} \cdot \sqrt{|\text{Ri}_b|}} \end{aligned} \tag{B.7}$$

$$\text{else}: \quad \begin{aligned} f_m &= \frac{1}{1 + \frac{10 \cdot \text{Ri}_b}{\sqrt{1+5 \cdot \text{Ri}_b}}} \\ f_h &= \frac{1}{1 + 15 \cdot \text{Ri}_b \cdot \sqrt{1 + 5 \cdot \text{Ri}_b}} \end{aligned} \tag{B.8}$$

Then, f_m is used to calculate the friction velocity of wind, and f_h is used to calculate the friction temperature. These friction parameters are corrected values of the temperature and the wind velocity, because vegetation like trees and buildings change these two parameters as they are experienced at the SS. They are defined as:

$$u_* = u \cdot \sqrt{C_D \cdot f_m} \tag{B.9}$$

$$T_* = C_D \cdot \frac{u}{u_*} \cdot (T_{atm} - T_{RL}) \cdot f_h \tag{B.10}$$

The model then calculates heat, moisture, and carbon fluxes in the surface layer. The sensible heat flux between the Roughness Layer and the atmosphere is given by:

$$H_{RL \to atm} = -1 * \rho * C_p * u_* * T_* \tag{B.11}$$

The heat flux between the Soil Surface and the Roughness Layer is given by:

$$H_{soil \to RL} = \frac{\rho \cdot Cp \cdot (T_{soil}(\text{end}) - T_{RL})}{Rg} \tag{B.12}$$

The flux resistance R_g [s/m] is associated with the transfer of heat and moisture from the SS to the RL.

Then, the temperature gradient in the soil is calculated with the diff function in MATLAB® and this gradient is used to add the ground heat flux (G) to the receiving layer, with:

$$G = \lambda_{soil} \cdot -1 \cdot \text{temperature gradient soil} \tag{B.13}$$

The last value of the ground heat flux is initialized to zero, after which the ground heat flux is updated to the rest of the layers.

Then, the model calculates evapotranspiration and heat storage. To enable this calculation, the psychometric constant (γ) is calculated first. The psychometric constant is the rate of change of saturation vapor pressure with temperature.

$$\gamma = \frac{C_p \cdot (po/100)}{0.622 \cdot L_v} \tag{B.14}$$

Now, resistances are calculated. The aerodynamic resistance (ra) is a measure of the resistance to water vapor transfer caused by the movement of air over a surface. The boundary layer resistance (rb) is the resistance between the surface and the atmosphere. The equations for ra and rb are given by:

$$\text{ra} = \frac{1}{0.007 + 0.0056 \cdot u} \tag{B.15}$$

$$\text{rb} = 1.1 \cdot u_*^{-1} + 5.6 \cdot u_*^{1/3} \tag{B.16}$$

To relate ra and rb, K is calculated.

$$K = \frac{(rs/ra)/(ra - rb)}{rs + rb \cdot (s/\gamma + 1)} \tag{B.17}$$

The net allwave radiation at the surface is the shortwave radiation received by surface plus the longwave emitted by the atmosphere minus the longwave radiation emitted by surface and absorbed by atmosphere. Given in an equation, this is:

$$R_{\text{net}} = R_{shortwave,atm \rightarrow soil} + R_{longwave,in} - R_{longwave,soil \rightarrow atm} \tag{B.18}$$

The slope of the saturation vapour pressure curve (s) can be calculated according to equation B.19 and is valid for values of air temperature up to 313 K (40 °C). This s is eventually used to calculate the evaporation.

$$s = \frac{L_v \cdot M_w \cdot 0.6108 \cdot \exp\left(\frac{17.27 \cdot (T_{\text{atm}} - 273.15)}{T_{\text{atm}} - 35.8}\right) \cdot 10}{1000 \cdot R \cdot T_{\text{atm}}^2} \tag{B.19}$$

The vapour pressure of the air (e_a) can be assumed equal to the saturation vapour pressure (e_s).

$$e_a = e_s = 1000 \cdot 0.6108 \cdot \exp\left(\frac{17.27 \cdot (T_{\text{atm}} - 273.15)}{T_{\text{atm}} - 35.8}\right) \tag{B.20}$$

This e_a (equal to e_s) can be used to calculate the vapour pressure deficit of air. This is the difference between the saturation vapor pressure and the actual vapor pressure of the air.

$$V = \frac{(610.7 \cdot 10^{7.5 \cdot (T_{\text{atm}} - 273.15)/(T_{\text{atm}} - 35.8)}) - e_a}{100} \tag{B.21}$$

Stomatal conductance (rs) values are a measure of the ability of the leaf surface to transfer water vapor to the surrounding air. It is the inverse to the surface conductance (gs), meaning:

$$r_s^{-1} = g_s = G_1 \cdot \sum_{i=1}^{n} (f_i \cdot g_{i,\max} \cdot \frac{LAI}{LAI_{\max}}) \tag{B.22}$$

For the whole area, fi=1, so this gives:

$$rs = \frac{1}{G1 \cdot 1 \cdot g_{i,\max} \cdot \frac{\text{LAI}}{\text{LAI}_{\max}}} \tag{B.23}$$

Then, the heat storage per surface type is considered. The heat storage per surface type is:

$$\Delta Qs = a1 \cdot Rnet + a2 \cdot \frac{dRnet}{dt} + a3 \tag{B.24}$$

For the whole area:

$$dQ_s = \sum \left(\left([a_1\ a_2\ a_3] \cdot \begin{bmatrix} R_{\text{net}}(t) \\ \frac{R_{\text{net}}(t) - R_{\text{net}}(t-1)}{dt} \\ 1 \end{bmatrix} \right) \cdot \text{Area} \right) \tag{B.25}$$

Then, the available water in the surfaces (Ci) is calculated by adding the already present water (of the previous time step) and the precipitation (of the current time step). This Ci is updated later.

For each surface, The W is calculated.
If the available water Ci is larger or equal to the maximum storage capacity (Si): W=1.
Else, so if Ci $<$ Si, W can be calculated by:

$$W = \frac{K-1}{K-\frac{Si}{Ci}} \tag{B.26}$$

The W then determines the new rss which replaces rs in LvE.

$$\text{rss} = \left(\frac{W}{rb \cdot \left(\frac{s}{\gamma}+1\right)} + \frac{1-W}{rs+rb \cdot \left(\frac{s}{\gamma}+1\right)} \right)^{-1} - rb \cdot \left(\frac{s}{\gamma}+1\right) \tag{B.27}$$

With the calculated dQs and rss, the latent heat flux due to evaporation from each surface can be calculated with Penman-Montheith. This reference evaporation for each surface is calculated with:

$$\text{L}_\text{v}\text{E} = \frac{s \cdot (R_\text{net} + QF - \Delta Qs) + \text{Cp} \cdot \rho \cdot \frac{V}{ra}}{s + \gamma \cdot (1 + \frac{rss}{ra})} \tag{B.28}$$

This LvE is assumed as potential evapotranspiration. For each surface, the potential evapotranspiration in mm (Ep) is determined by multiplying LvE [W/m^2] with the time step dt and by dividing it by Lv, which is the latent heat of vaporization (=2.45$e10^6$ J/kg).

The actual evapotranspiration (Ea) depends on the available water content Ci and precipitation P. Available water at the surface is calculated for each time step (t), based on the storage level of the previous time step (Ci(t-1)) and the precipitation of the current time step (P(t)). Ea (in [mm]) takes the minimum value of either the potential evapotranspiration or the available water content for a surface. This Ea updates for each surface the potential evapotranspiration LvE (=Ea*Lv/dt) and available water content Ci (Ci=Ci-Ea) for each time step. The updated LvE is used to calculate the actual evapotranspiration for the whole area, by multiplying this LvE with the area. This gives the actual evapotranspiration for the whole area: LvET. Summarizing, the relation between Ci, P, Ea, and Ep is:

$$\begin{aligned} &\text{If } E_p(t) < C_i(t-1) + P(t): \quad E_a(t) = E_p(t) \quad \text{and} \quad C_i(t) = C_i(t-1) + P(t) - E_p(t) \\ &\text{If } E_p(t) > C_i(t-1) + P(t): \quad E_a(t) = C_i(t-1) + P(t) \quad \text{and} \quad C_i(t) = 0 \end{aligned} \tag{B.29}$$

As mentioned in Section 2.9, the infiltration is neglected.

Based on the energy balance provided in Appendix A, equation A.1, the change of temperature in the Roughness Layer can be calculated:

$$\Delta T_{RL} = \frac{dt}{h_{RL} \cdot \rho \cdot Cp} \cdot (H_{soil \to RL} - H_{RL \to atm}) \tag{B.30}$$

This ΔT_{RL} updates the temperature of the Roughness Layer.

Based on the energy balance provided in equation A.3, the change of temperature of the soil can be calculated. This is under the assumption that the thermal conductivity of the soil is independent of z. The actual evapotranspiration is used in the calculation. Furthermore, equation B.13 is used to calculated G, equation B.18 for R_{net}, and B.12 for $H_{soil \to RL}$.

$$\Delta T_\text{soil} = \frac{dt}{dz_\text{soil} \cdot \rho_\text{soil} \cdot Cp_\text{soil}} \cdot (G + \text{Isfc} \cdot (-H_{\text{soil} \to \text{RL}} + R_\text{net} - \text{LvET} + QF - dQs)) \tag{B.31}$$

In this equation, Isfc is an array containing zeros, where the last value is set to 1. This is to ensure that only the top soil layer has an interaction with the Roughness Layer and atmosphere, and that for the deeper layers only the heat transfer through the soil is calculated. This ΔT_{soil} updates the temperature of the soil layer. The temperature of the soil layer is transferred back to Celsius in the end of the code.

To calculate the soil temperature, the soil temperature model first runs with inclusion of only the first year of meteorological data. This run is performed to set the initial temperature profile of the soil which serves as staring point for the full simulation. For the first run, the initial temperature of the soil layers is set to 4 °C. For the final simulation, which uses the full meteorological dataset, the output of the run with only the first year of weather data (stored as 'initialisation') is used as the input T_soil.

Some of the input depends on the urban type which is considered, as presented in Section 2.9.3. Two parameters differ for each: G1 and z. These values can be found in Appendix C. The other input parameters (scenario_name, a_soil, grass, and shade) depend on the measurement location.

C. Parameters of the soil temperature model

a_1 = empirical value to estimate heat storage [-] = 0.8 for ground (pavement), 1 for green (grass)
a_2 = empirical value to estimate heat storage [s] = 30 for ground (pavement), 30 for green (grass)
a_3 = empirical value to estimate heat storage, depending on urban type [W/m^2]
α_i = albedo of surface type i [-]
α_{veg} = albedo of vegetation [-]
C_D = drag coefficient in relations for friction velocity and friction temperature [-]
C_i = interception state of the canopy of the ith surface [mm]
C_p = heat capacity of air [J/kg/K] = 1004.67 J/kg/K
$C_{p,soil}$ = heat capacity of soil [J/kg/K]
e_a = vapour pressure of air [Pa]
e_s = saturation vapour pressure [Pa]
E_{act} = Actual Evapotranspiration [mm]
E_{pot} = Potential Evapotranspiration [mm]
f_h = factor, that incorporates the surface roughness and atmospheric stability [-]
f_i = fraction cover [-]
f_m = stability factor [-]
G = heat flux into the ground [W/m^2]
G1 = parameter related to the maximum surface conductance [mm/s] = 11.54 mm/s for urban and hot-spot or 14.97 for peri-urban
g = gravitational constant [m/s^2] = 9.81 m/s^2
$g_{i,max}$ = maximum conductance values for the surface type i [m/s] = 0.005 m/s
g_s = surface conductance [m/s]
H = sensible heat flux [W/m^2]
h_{RL} = height of the air column representing roughness layer [m] = 10 m
k = overall heat transfer coefficient [$W/m^2/K$]
K = relates r_a and r_s [-]
LAI = Leaf Area Index [-] = 1.0
LAI,max = maximal Leaf Area Index [-] = 1.1
L_v = latent heat of vaporization [J/kg] = $2.45e10^6$
LvE = latent heat due to evaporation [W/m^2]
M_w = molecular weight of water [g/mol] = 18 g/mol
m = number of layer in ground [-]
P = precipitation [mm]
p = pressure [hPa]
po = standard air pressure [Pa] = $101.3e10^3$ Pa
ΔQ_s = heat storage [W/m^2]
QF = anthropogenic heat [W/m^2]
R = molar gas constant [8.314 J/mol/K]
r_a = aerodynamic resistance [s/m]
r_b = mean boundary layer resistance [s/m]
r_s = surface resistance [s/m]
r_{ss} = redefined surface resistance [s/m]
R_g = flux resistance, associated with heat transfer from SS to RL [s/m] = 30 s/m
R_{global} = global radiation [$J/m^2/s$]
$R_{l,in}$ = incoming long wave radiation [$J/m^2/s$]
$R_{l,SS\rightarrow atm}$ = outgoing long wave radiation [$J/m^2/s$]
R_{net} = net radiation [W/m^2]
$R_{s,atm\rightarrow SS}$ = incoming shortwave radiation [$J/m^2/s$]

Ri_b = Richardson's bulk number [-]
s = slope of saturation vapour [hPa/K]
S_i = maximum storage capacity of the surface i [mm]
T_{atm} = atmospheric temperature [K]
T_{RL} = temperature in the roughness layer [K]
T_{soil} = temperature of soil [K]
T_{SS} = temperature of soil surface [K]
T_* = friction temperature [K]
t = time [s]
u = wind velocity [m/s]
u_* = friction velocity of wind [m/s]
V = vapour pressure deficit of the air [hPa]
W = function of the amount of water on the canopy of the individual sufaces (C_i) relative to the canopy surface water storage capacity (S_i) [-]
z = height at which the wind speed is determined [m] = 10 m
z_0 = roughness length [m] = 1 m
z_{soil} = depth in the ground [m]
α = constant in beta probability density function for ϵ_eff
β = constant in beta probability density function for ϵ_eff
ϵ_{eff} = effective or apparent emissivity [-]
γ = psychrometric constant [hPa/K]
κ = von Karman's constant [-] = 0.4
λ_{soil} = thermal conductivity of soil [W/m/K]
ρ = density of air [kg/m^3] = 1.18 kg/m^3
ρ_{soil} = density of soil [kg/m^3]
σ = Stefan-Boltzmann constant [$W/m^2/K^4$] = 5.67e10^{-}8 $W/m^2/K^4$

Original equations in MATLAB®code:

$$K = \frac{\left(\frac{rs}{ra}\right)}{\left(\frac{ra}{rb}\right)} \Bigg/ \left(rs + rb \cdot \frac{s}{\gamma + 1}\right) \tag{C.1}$$

Has been changed to: K=((rs/ra)/(ra-rb))/(rs+rb*(s/gamma+1)) (equation B.17).

And:

$$\mathrm{L_vE} = \frac{s \cdot (R_{\mathrm{net}} + QF - \Delta Qs) + \mathrm{Cp} \cdot \rho \cdot \frac{V}{ra}}{s + \frac{\gamma}{1 + \frac{\mathrm{rss}}{ra}}} \tag{C.2}$$

Has been changed to: LvE=(s*(Rnet+QF-dQs)+Cp*rho*V/ra)/(s+gamma*(1+rss/ra)) (equation B.28).

D. Measurement locations

D.1. The Green Village (TGV)

Figure D.1.: Map of The Green Village.

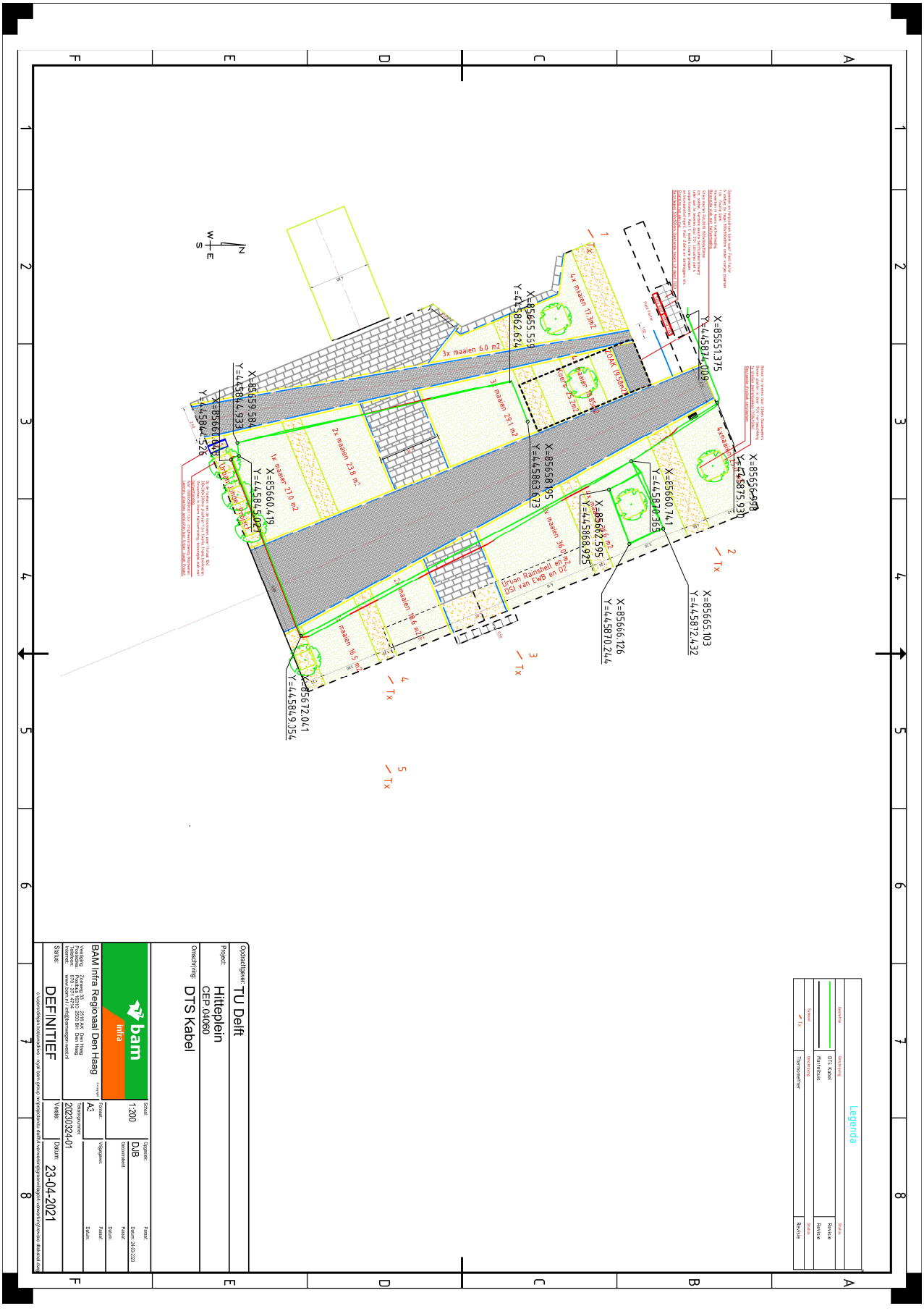

Figure D.2.: Map of the HeatSquare in The Green Village, including the path of the DTS cable.

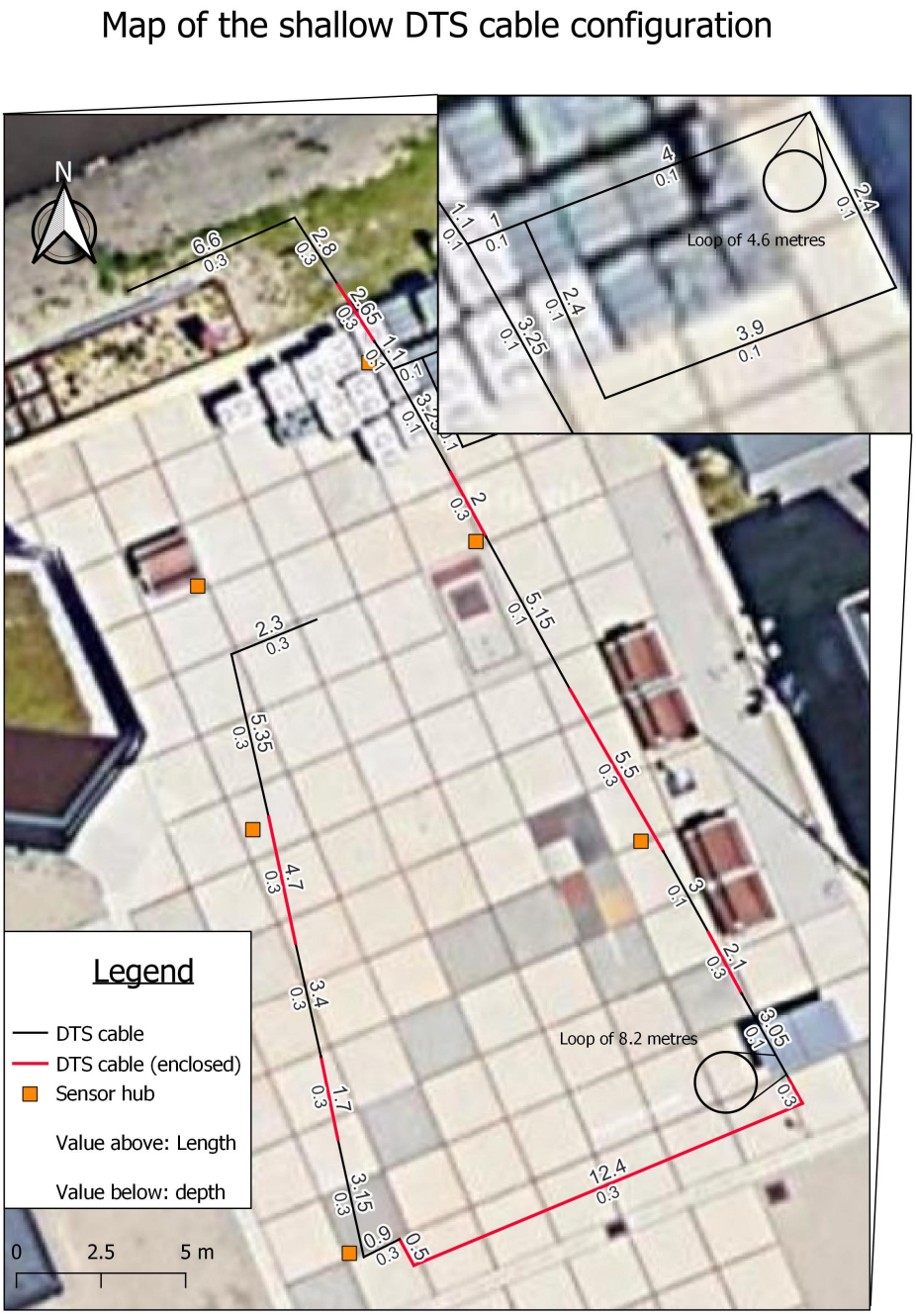

Figure D.3.: The shallow cable configuration on the HeatSquare.

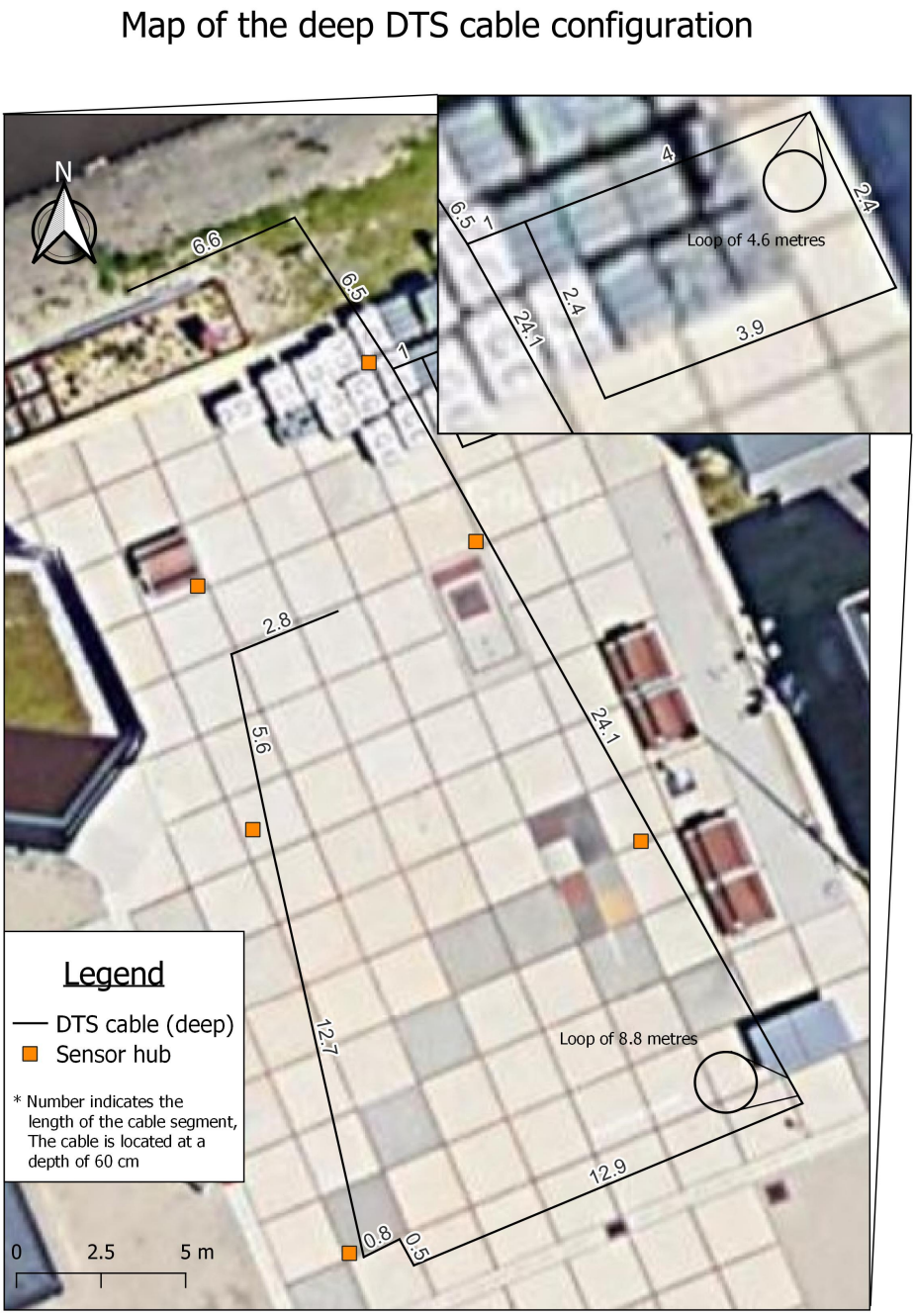

Figure D.4.: The deep cable configuration on the HeatSquare.

D.2. Rotterdam

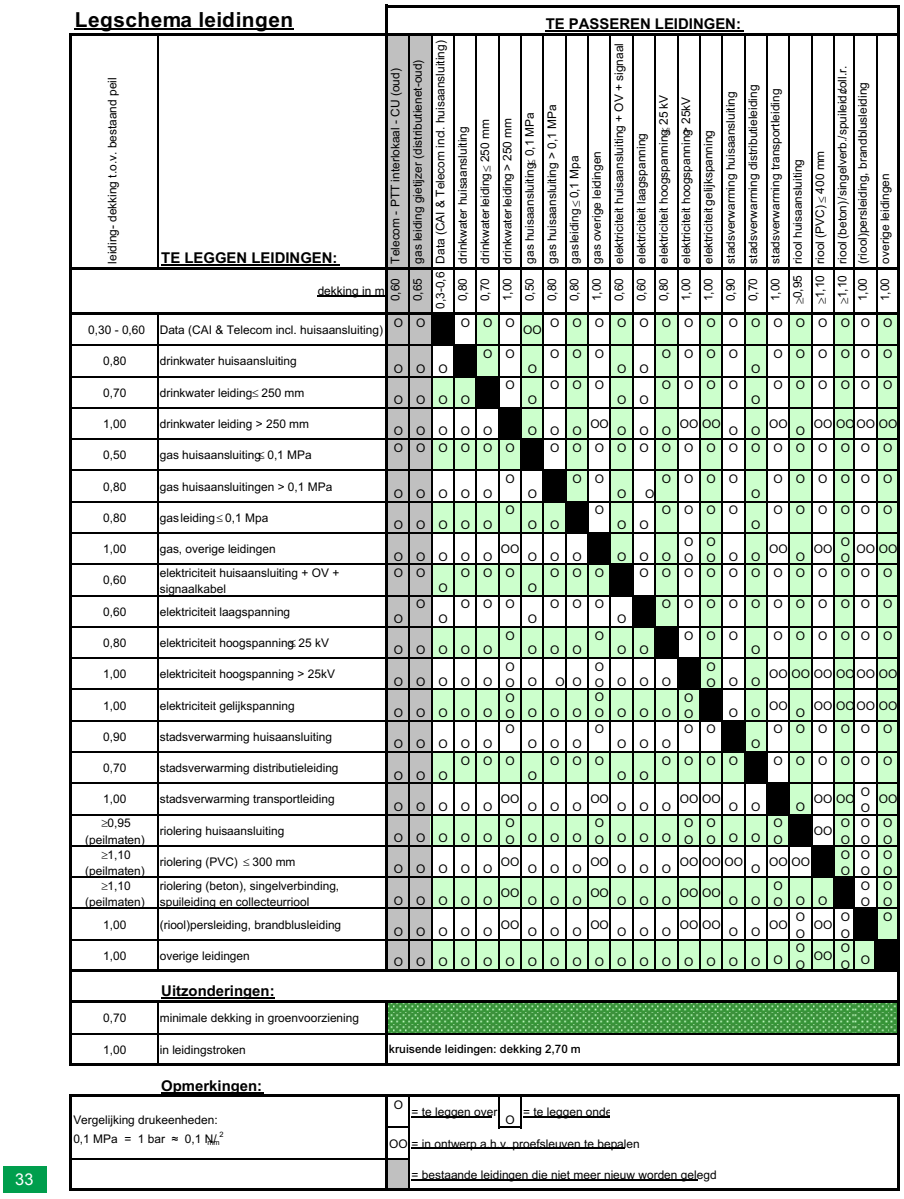

Figure D.5.: 'Legschema' of the municipality of Rotterdam. The left-hand side shows the coverage depth per pipe, the right-hand side shows the vertical position with respect to other pipes. A circle on the upper side of the cell means the pipe must be located above the pipe to be passed. A circle below in the cell means it must pass the other pipe underneath. Two circles in the middle means the location relative to other pipes must be determined in the design (Gemeente Rotterdam, 2022)

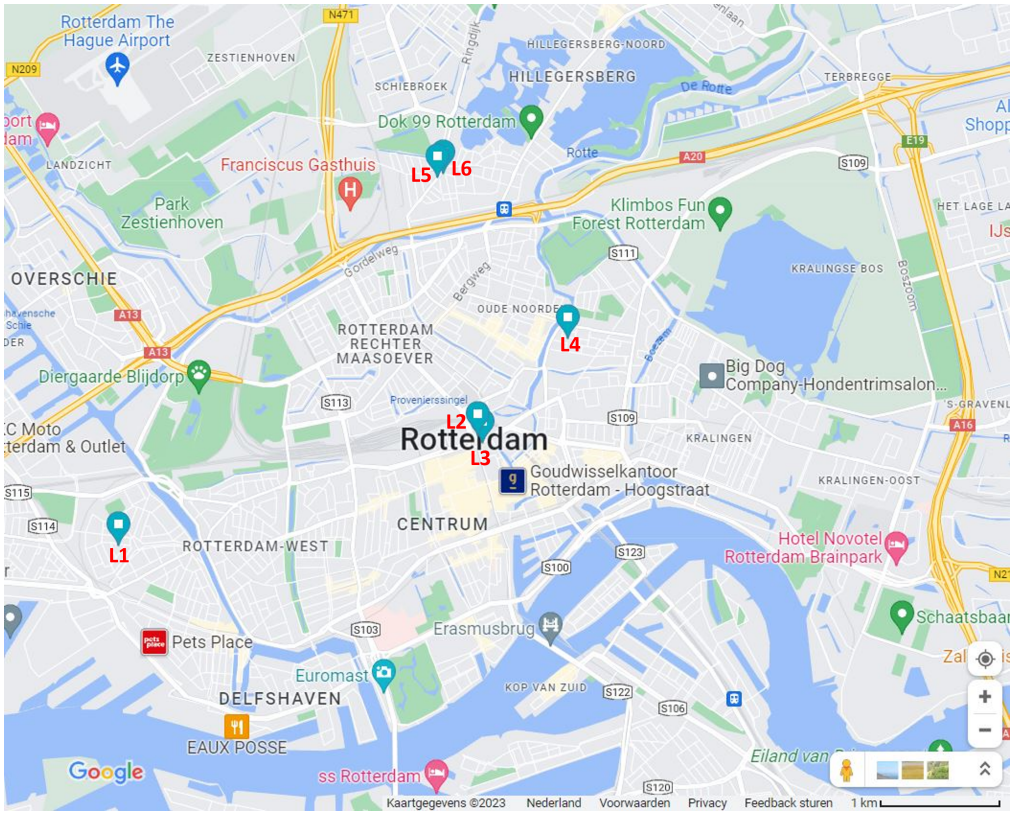

Figure D.6.: The six measurement locations in Rotterdam (Google Maps, 2023).

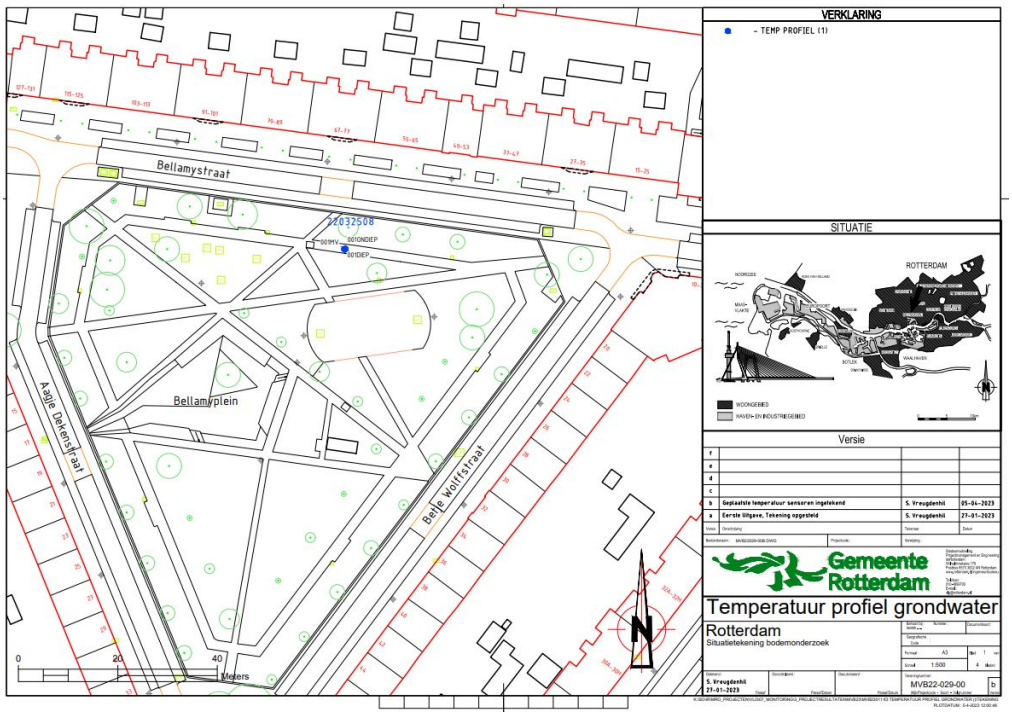

Figure D.7.: Map of location L1.

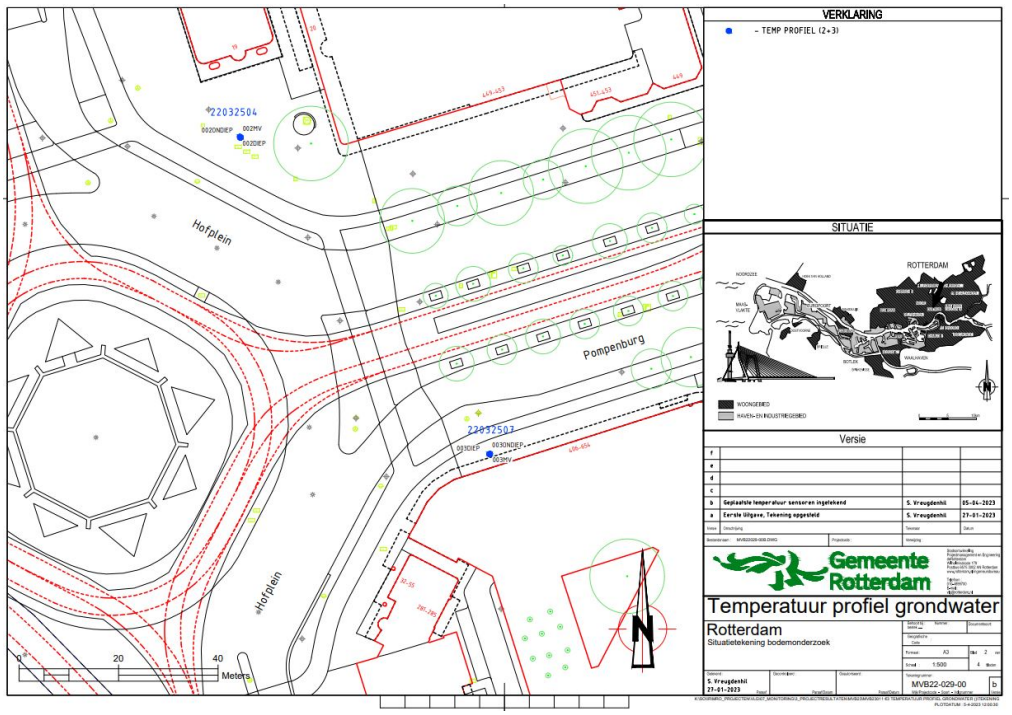

Figure D.8.: Map of location L2 and L3.

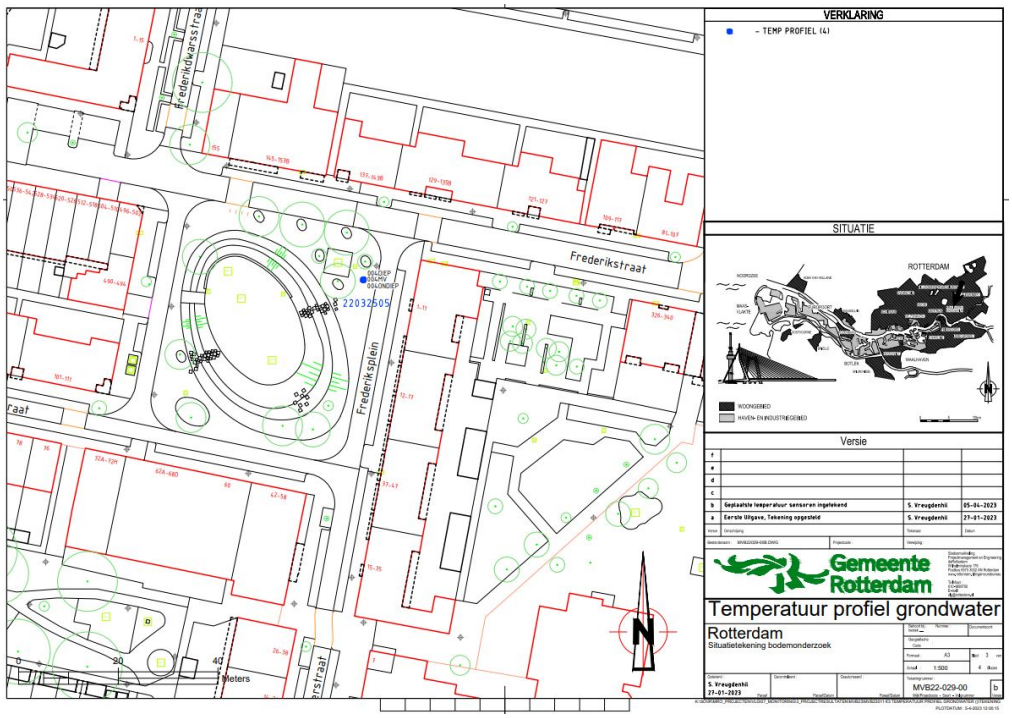

Figure D.9.: Map of location L4.

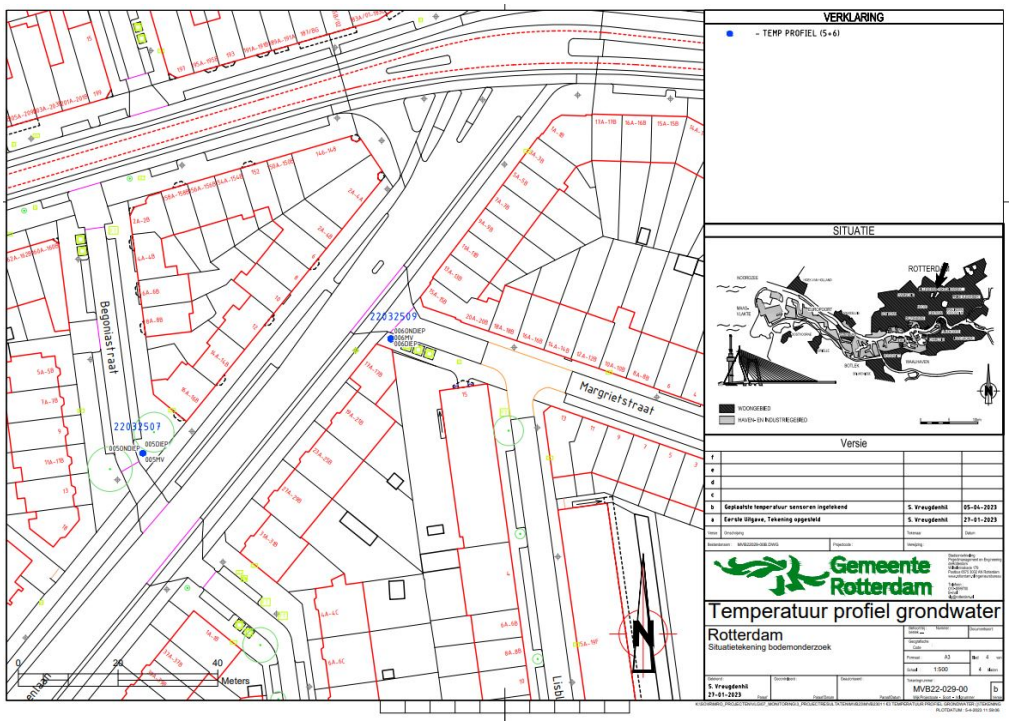

Figure D.10.: Map of location L5 and L6.

(a) L1

(b) L2

(c) L3

Figure D.11.: Measurement locations L1-L3 in Rotterdam.

(a) L4

(b) L5

(c) L6

Figure D.12.: Measurement locations L4-L6 in Rotterdam.

Figure D.13.: Shade map of Hofplein in Rotterdam, June 15 2013 14:00, made in Tygron.

Figure D.14.: Shade map of Hofplein in Rotterdam, August 15 2013 14:00, made in Tygron.

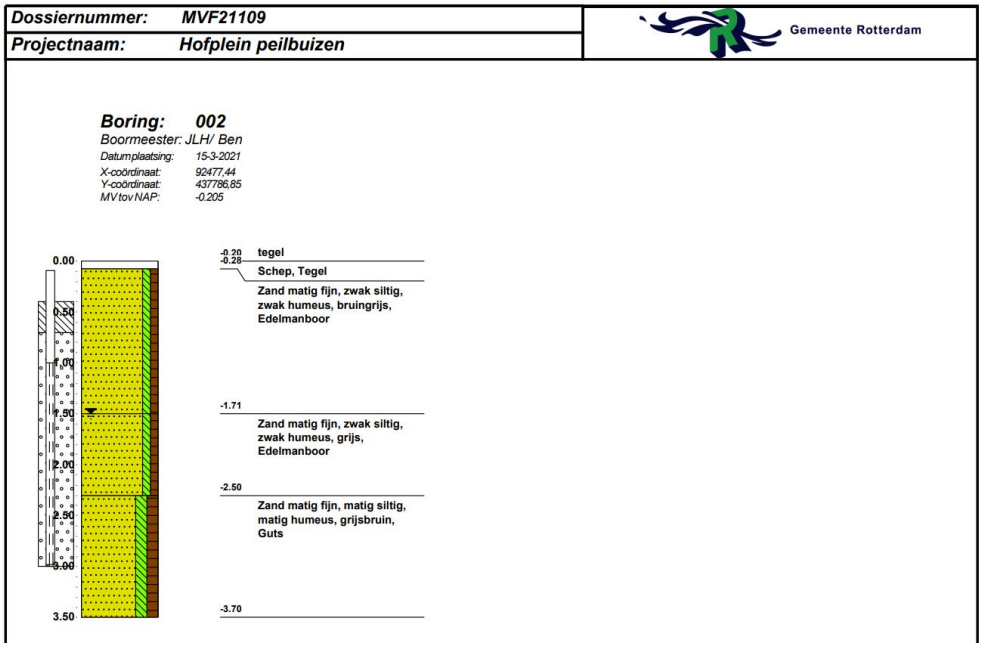

Figure D.15.: Drilling profile at Hofplein, Rotterdam (representing L2 and L3).

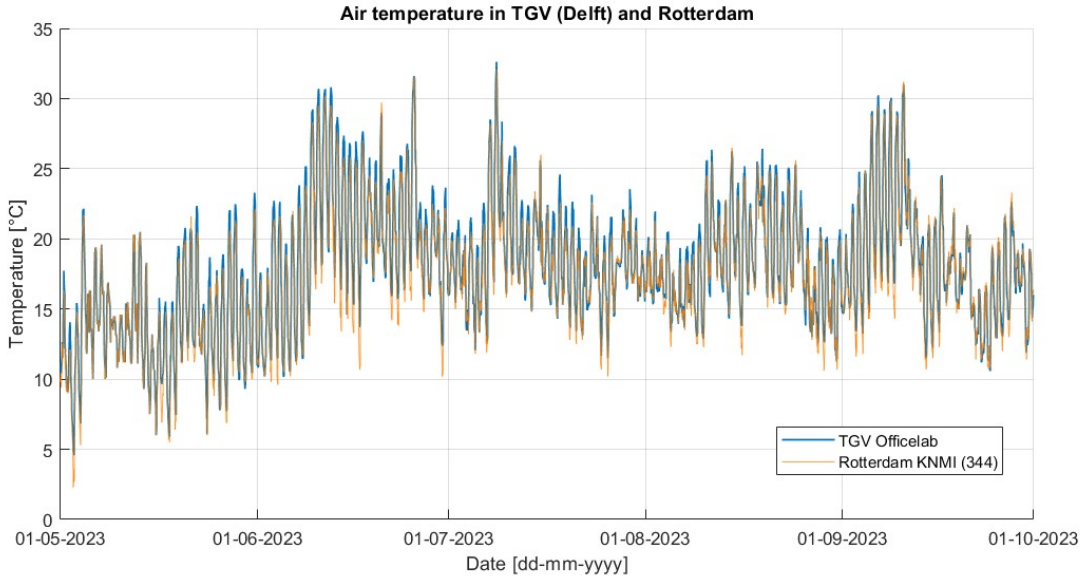

Figure D.16.: Air temperature in TGV (measured at the Officelab) and in Rotterdam (measured at KNMI station 344).

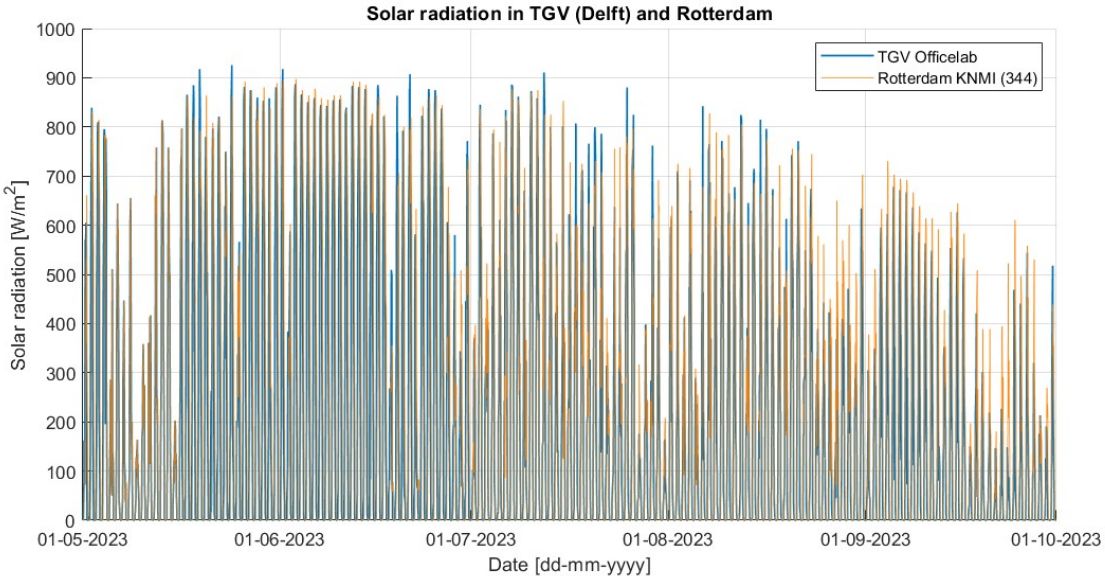

Figure D.17.: Solar radiation in TGV (measured at the Officelab) and in Rotterdam (measured at KNMI station 344).

E. Data (transformation)

E.1. Meteorological data

E.1.1. Rotterdam: KNMI meteorological data

For Rotterdam, the weather data can be extracted from KNMI, station number 344. The coordinates of the location are 4.447 longitudinal (east), 51.962 latitudinal (north), and altitude -4.3 m. The hourly data is available on:
https://www.daggegevens.knmi.nl/klimatologie/uurgegevens (KNMI, 2023b).
On this website, one need to insert the time frame (more than one year to let the model run properly) and start and end hour can remain empty (uneditted) under the section 'period'. Furthermore, under the section 'fields' all fields need to be checked. Lastly, under the section 'weather station' station '344: Rotterdam' needs to be checked. Then, the file can be downloaded as csv file. The period which was used as input for the soil temperature model and therefore subtracted from the KNMI website is December 24 2021 till October 1 2023.

E.1.2. TGV: Officelab meteorological data

In TGV, a Davis Vantage Pro2 weather station is present at the Officelab and at the Co Creation Centre. Since the weather station of the Co Creation Centre does not measure rain, the data from the Officelab was used for this research. The location of the Officelab where the weather station is located is visible on the map in Appendix D.1, Figure D.1.

The data set contains: the date and time [yyyy-mm-ddThh:mm:ss], day rain [mm], outdoor temperature [°C], rain rate [mm/h], wind speed ([m/s] and since June 2 2023 in [km/h]), wind direction [degrees], and solar irradiation [W/m^2]. This data is provided as hourly average: the average of all measurements in a specific hour.

The meteorological data from TGV differs in the parameters it measures and their units compared to the KNMI. As the file has a different format than the KNMI data set, the layout was manually changed in Excel, to align maximally with the KNMI weather data. For example yyyy-mm-ddThh:mm:ss was changed to YYYYMMDD and H and all parameters were set in separate columns next to each other instead of below each other. Also, the units were set equally, where it must be noted that the wind speed in TGV first measured in [m/s] and later in [km/h]. The part of the data that was given in [km/h] was transferred to [m/s] by dividing the value by 3.6. Also, the wind direction was wrongly provided each time the data was retrieved. For each value, 162 degrees needed to be added, where it was controlled that the value remained below 360 degrees.

Other differences are that the KNMI data set contains the value 24 for mid-night, and the set of TGV uses a 0. Besides, the KNMI set assigns this 24 to the previous day, whereas TGV assigns this (0) to the upcoming day. This is particularly necessary to keep in mind when making graphs for a specific day and time in MATLAB®. For instance, to plot August 21 2023, mid-night, the input of the date to retrieve the adequate data differs. For TGV, the weather data of 22-08-2023, 0 hour must be used as input, whereas for KNMI data 21-08-2023, 24 hour must be used.

The data of the Officelab contained a lot of gaps of missing data, for hours or even days. These gaps were all searched for and the gaps were complemented with data of the KNMI, weather station 344 of Rotterdam, since this weather station of the KNMI is located the nearest to TGV. The set also contained outliers, which are values that lie outside the typical range of values in a data set. They were visibly present on graphs via the Grafana website:

https://surfpublic.grafana.net/d/pssXCY8Mk/the-green-village-data-platform?orgId=1
This website contains publicly accessible data of measurements in TGV, but the data cannot be downloaded via this website itself. The data must be requested at the project manager Data & digitalisation of TGV. The dates and hours where the data contained outliers (2022-12-08) showed values of 3276(.)7, so this value was replaced in the whole data set with data of the KNMI for those specific days and times. Temperatures greater than 100 °C were also replaced with data from the KNMI.

The period which was requested to be used as input for the soil temperature model is December 24 2021 till October 1 2023. All together, the file was complemented (in case of gaps) or replaced (in case of outliers) with KNMI data for 1709 hours in total of the total of 15552 hours, so approximately 11 % of the data set. The data from the KNMI is used as originally present in the data set from the KNMI, except for the wind speed. The wind speed is corrected by a factor, because the wind speed in the KNMI file presents higher values since it measures at a higher altitude (10 m) and at an open field. For each hour in from December 2021 till October 2023, the factor wind speed KNMI divided by wind speed of TGV was calculated. This was only performed for wind speeds of TGV equal or above 0.5 m/s, because wind speeds smaller than 0.5 m/s are such low values that they were considered to be not realistic. The average of these factors was 5.88 and this was used to transfer the wind speed from the KNMI when this was used to replace or complement the data from the Officelab of TGV.

E.2. Scripts to transfer meteorological data to input file for the soil temperature model

The input for the soil temperature model is meteorological data. A separate MATLAB® file is available to transfer KNMI data to a proper input file for the soil temperature model. For the data of the Officelab, a similar script was written for this thesis research such that the hourly weather data can be used in the model properly.

KNMI meteorological data
For weather data of Rotterdam, the format in which it is available on the KNMI website is transferred to a proper file which can be used as input in the soil temperature model. Here, only a subset of parameters from the original KNMI file are used. The global radiation is transferred to W/m^2 by multiplying the value (in $J/cm^2/h$) with 10.000/3600. Some other parameters also need to be transferred. The temperature is provided in 0.1°C in the KNMI file, so this data is divided by 10 to get the value in °C. The same is valid for the average wind speed and the precipitation. The output file stores the date [YYYYMMDD], temperature [°C], average wind speed [m/s], cloud cover [in eighths], global radiation [W/m^2], wind direction [degrees: N=360, E=90, S=180, W= 270], relative humidity [%], and precipitation [mm].

Officelab meteorological data
After the data transformation, the meteorological data from the Officelab in TGV still differed in style compared to the one of the KNMI, so a different MATLAB® model was required to transfer the weather data of TGV into a suitable input file for the soil temperature model. The script to transfer KNMI data to a proper input file was used as starter point.

The output file of the script stores almost the same parameters as is stored for the KNMI data, but the cloud cover and relative humidity are not stored, since it was discovered that these parameters are not used in any of the equations in the soil temperature model. This became clear when all equations in the soil temperature model were analysed, as presented in Appendix B. The output file stores the date [YYYYMMDD], temperature [°C], average wind speed [m/s], global radiation [W/m^2], wind direction [degrees: N=360, E=90, S=180, W= 270], and precipitation [mm].

F. Results

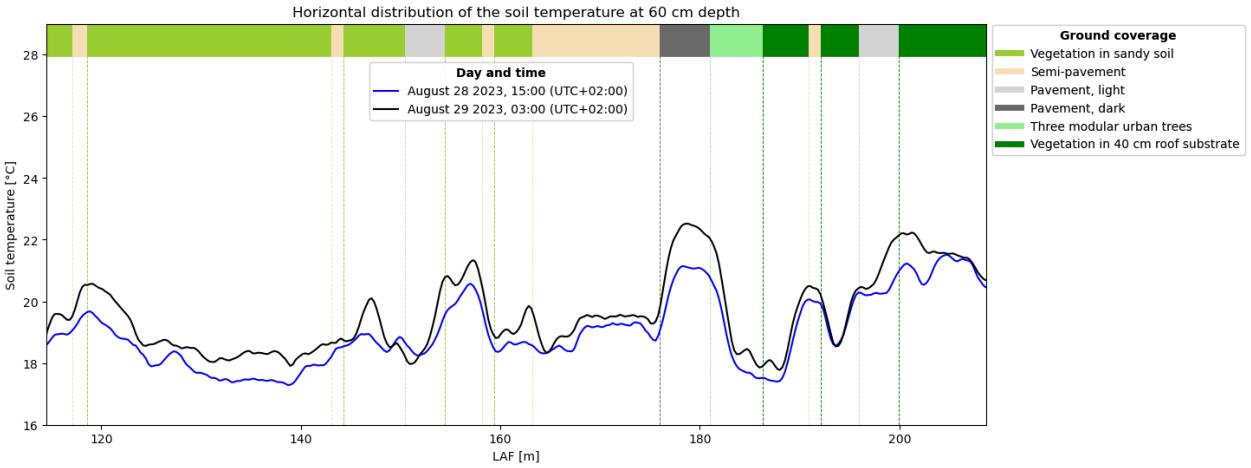

Figure F.1.: Horizontal temperature profile of the HeatSquare in The Green Village, made with DTS at 60 cm depth for August 28 2023, day and night.

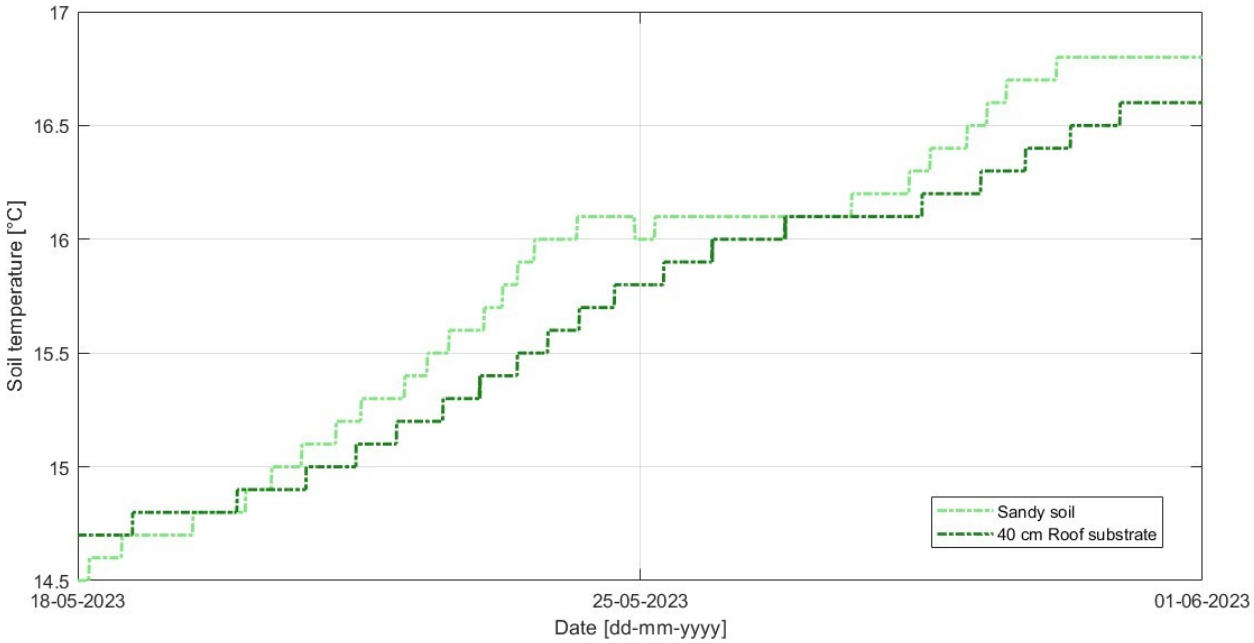

Figure F.2.: The soil temperature at 1 m depth in bare substrate in TGV.

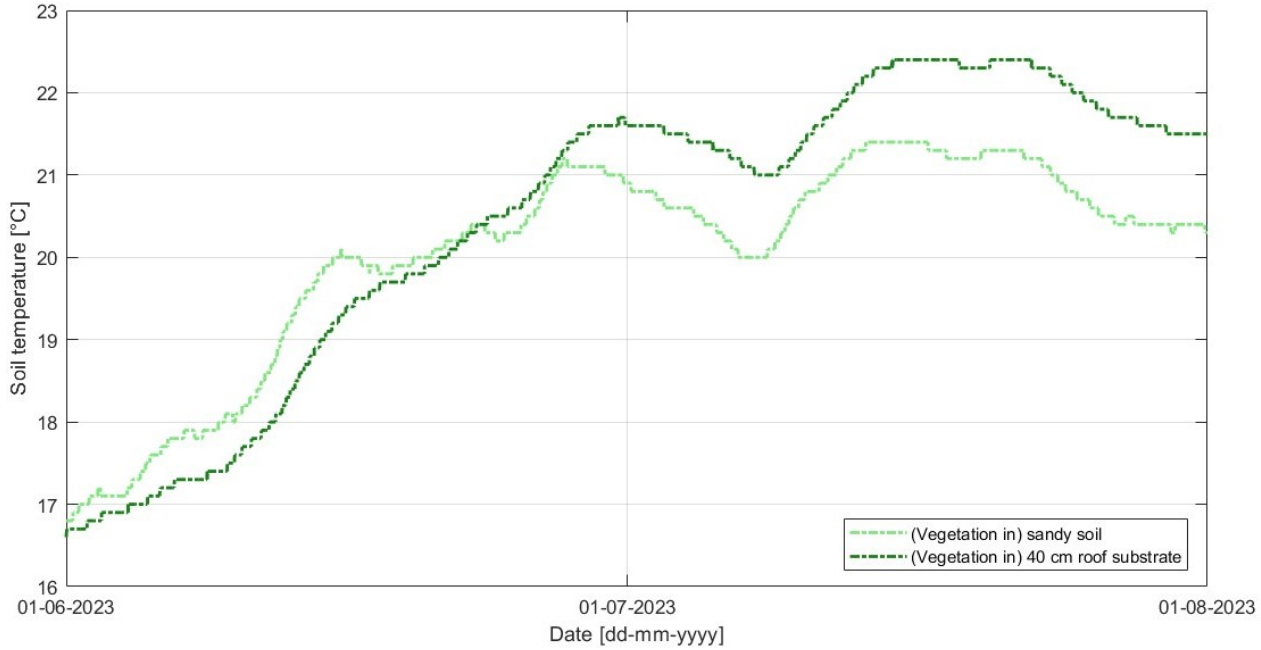

Figure F.3.: The soil temperature at 1 m depth for (vegetation in) sandy soil and 40 cm roof substrate in TGV.

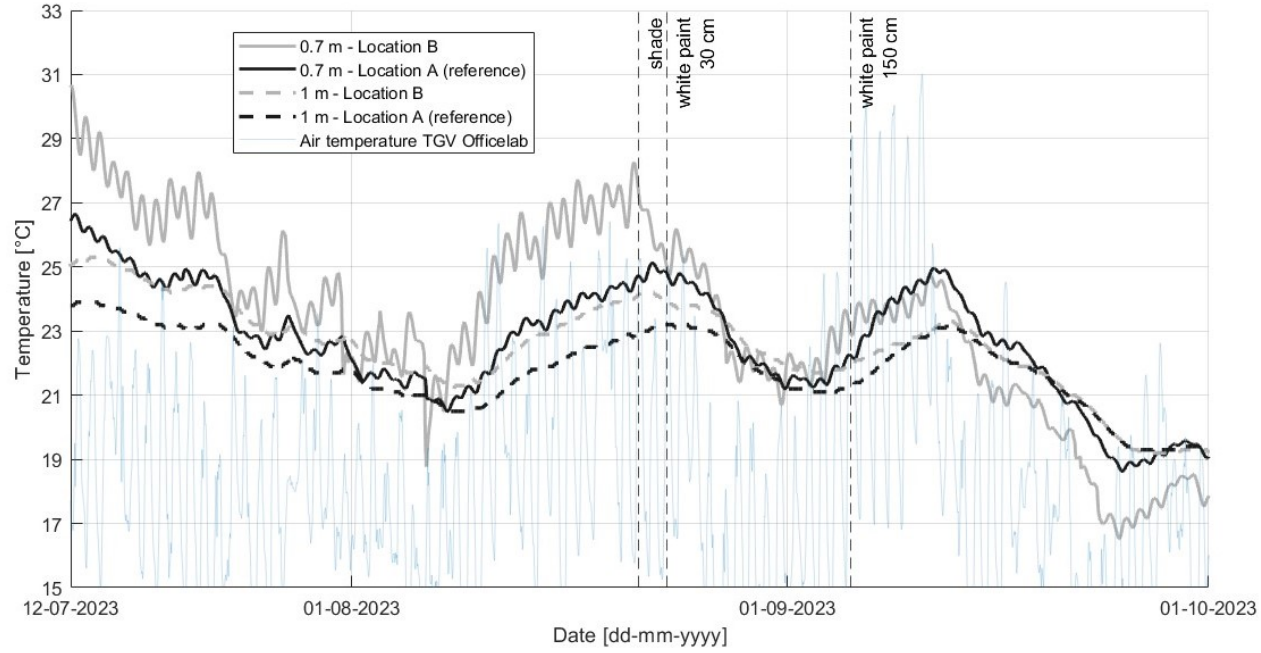

Figure F.4.: The measured soil temperature at 0.7 and 1 m depth below concrete tiles in TGV. Shade was created on August 21 11:00, white paint 30 cm on August 23 11:00, and white paint 150 cm on September 5 12:00. Location A is used as reference: no measures are applied on top of this sensor.

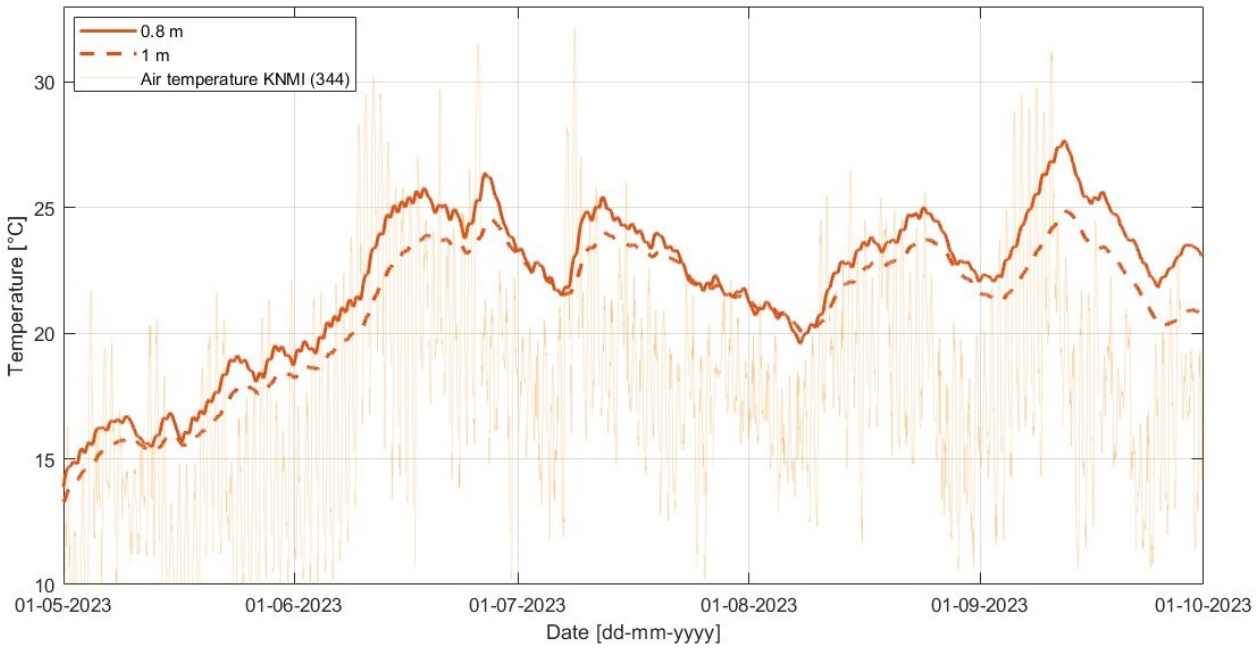

Figure F.5.: The measured mean soil temperature at 0.8 and 1 m depth at location L2 in Rotterdam.

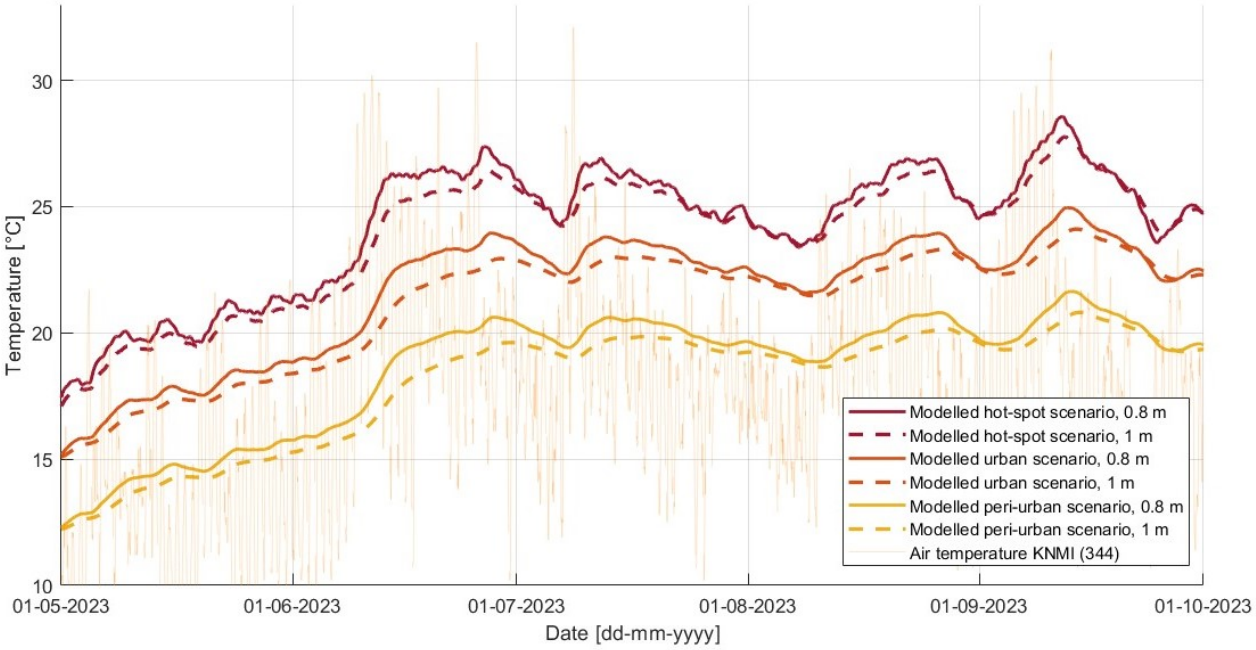

Figure F.6.: The modelled soil temperature at 0.8 and 1 m depth for all three urban types.

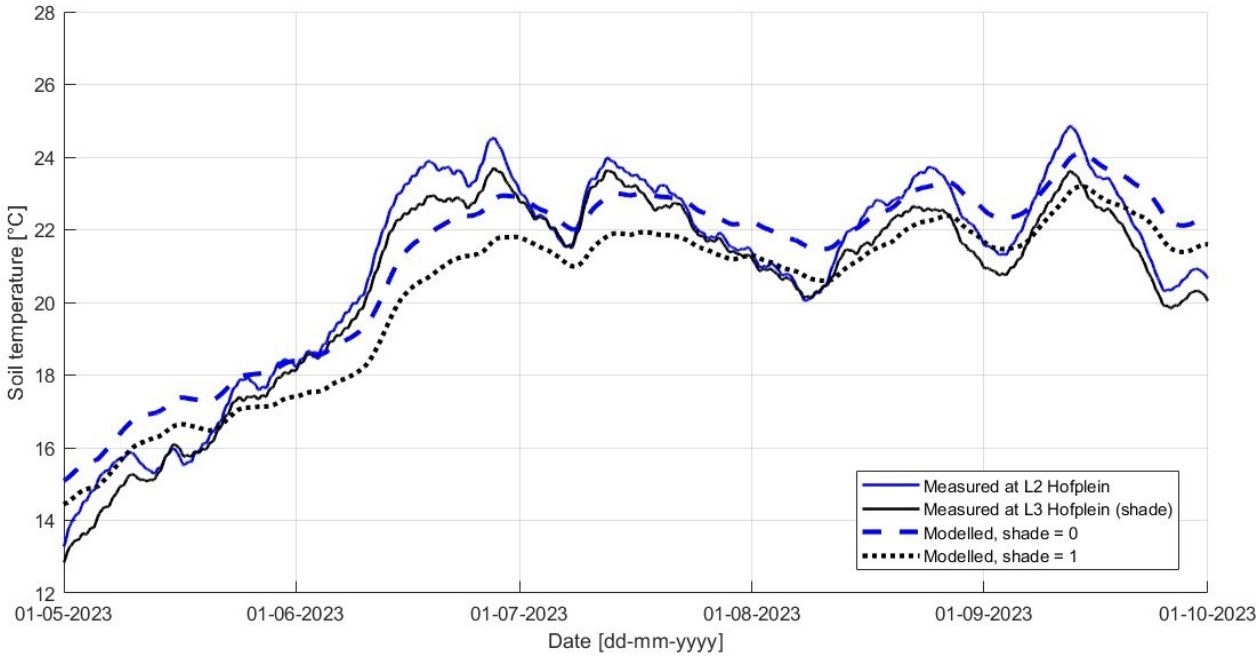

Figure F.7.: The measured and modelled soil temperature at 1 m depth at Hofplein in Rotterdam. The modelled situation is provided both for the urban scenario, with shade=0 or shade=1.

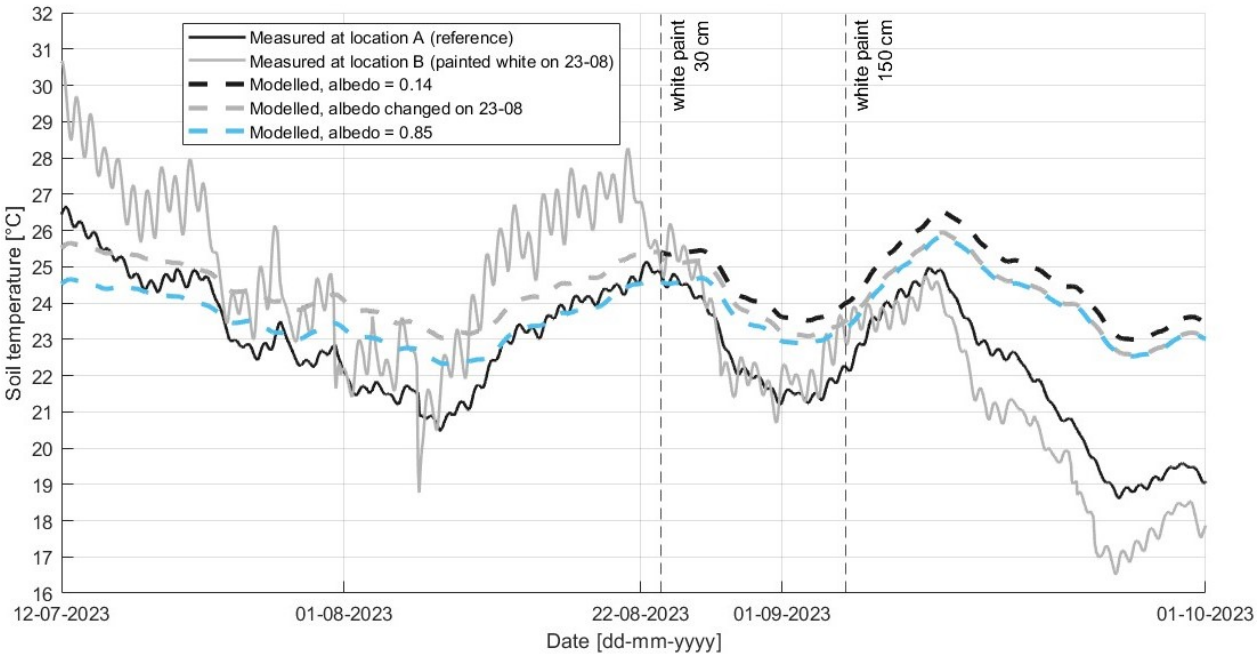

Figure F.8.: For the period 12-07-2023 to 01-10-2023: the measured and modelled soil temperature at 0.7 m depth in TGV, where location B has been painted white. The modelled situation is provided for the urban scenario, with a_{SS}=0.14, a_{SS}=0.85, and for a change in albedo from 0.14 to 0.85 on August 23.

Gemeente
Rotterdam

TU Delft
Delft
University of
Technology